

Distribution of Residence Times of Grains in Sandpile Models.

A Thesis
Submitted to the
Tata Institute of Fundamental Research, Mumbai
For the degree of Doctor of Philosophy
in Physics

by
Punyabrata Pradhan

Department of Theoretical Physics
School of Natural Sciences
Tata Institute of Fundamental Research
Mumbai

July, 2006

Acknowledgments

I am highly grateful to my supervisor, Professor Deepak Dhar, for his guidance throughout the years since I have joined Theoretical Physics group. He provided enormous support in my research with thoughtful suggestions and remarkable patience. Above all these, he influenced me a lot as a person being simple, straightforward and having unbiased critical opinions. I would also like to thank Professor Mustansir Barma as he was always available for discussions. I would like to mention about our small but happy Condensed Matter theory group and its forum, the vibrant “Monday-Meeting”, where Deepak, Mustansir and Kedar all used to spend a lot of time with students. I have really enjoyed it.

It was a nice experience to be there in the theory students’ room. I never got bored there as comments from people on diverse topics always used to circulate in the air (although air didn’t circulate much due to nonfunctional air-condition unit!). I really thank all the students in our theory group as they gave me a nice company and made this long five years journey appear very short. I especially thank Kavita, Arti, Apoorva and Shamik for physics discussions, Ashik for political discussions, and Arghya for his constant support whenever I used to play “Jhalak Dikhla...” amid great opposition from others. My special thanks must go to Anindya (our most wanted “Master-da”!) and Swagato for their unconditional help in all sorts of computer related issues. Many thanks to the people for their critical comments in my synopsis mock-seminar and being present in the synopsis seminar for morale-boosting.

I acknowledge all the staff members of the theory department - Raju, Mr. Pawar, Girish and Mohan - for always being ready to help in all sorts of official matters. I thank Ajay and Deepak Mane for helping in computer matters.

Friends outside the theory group - Biswajit-da, Bipul-da, Kaushik-da, Ritumoni, Jyothsna, Lakshmi...., and my batchmate-cum-friends - Uddipan, Kanchan, Ashutosh, Amala, Anand, Anoop, Apoorva, Deepshikha, Garima, Deepankar, Ajay, Vaibhav....., all made my stay in TIFR really enjoyable one and literally made me feel at home. I had some great moments while going for conferences or schools together with Dada (Apoorva). I would really like to thank Uddipan, Debanjan and Ashik who were the guinea-pigs for all sorts of cooking experiments of mine in the first few years! And Ashutosh, thanks for your hand-churned delicious ice creams and motivating me to go for the movie “Munnabhai MBBS”! That’s a great movie! I am very much grateful to Biswajit-da, Ashutosh and Anindya for extending their helping hands when I was literally ruffled during the period Arti was not well.

I express my deep gratitude to my family members, especially my father, who have always been with me at each and every critical moments I passed through. Finally I would like to mention my wife - Arti has made my life truly a romantic one.

I acknowledge the partial financial support from the Kanwal Rekhi Scholarship

administered by the TIFR Endowment Fund for years 2002-2004.

Declaration

This thesis is a presentation of my original research work. Some part of the work was done in collaboration with Mr. Apoorva Nagar and Prof. Deepak Dhar who are coauthors in my publications. Wherever contributions of non-coauthors are involved, every effort is made to indicate this clearly, with due reference to the literature, and acknowledgment of discussions.

The work was done under the guidance of Professor Deepak Dhar, at the Tata Institute of Fundamental Research.

Punyabrata Pradhan.

In my capacity as supervisor of the candidate's thesis, I certify that the above statements are true to the best of my knowledge.

Prof. Deepak Dhar.

Contents

Acknowledgments	i
Synopsis	ix
0.1 Introduction	ix
0.2 First passage time distribution in random walks	xi
0.3 The distribution of residence times in height type sandpile models . . .	xii
0.3.1 Models	xii
0.3.2 Bak-Tang-Wiesenfeld model in one dimension.	xiii
0.3.3 Generalization to other models and arbitrary dimensions.	xiv
0.4 The distribution of residence times in slope type sandpile models	xvii
0.4.1 Models	xvii
0.4.2 Distribution of residence time T_1 at first site.	xviii
0.4.3 Distribution of total residence time in the pile.	xx
0.4.4 Probability of large deviations in the Oslo rice pile model. . . .	xxi
0.5 Summary	xxii
Publications	xxvii
1 Introduction	1
1.1 The distribution of the residence times and the first passage times in various contexts.	1
1.1.1 Random Walks.	1
1.1.2 Persistence.	3
1.1.3 Diffusion Controlled reaction.	4
1.1.4 Neuron dynamics.	4
1.2 Self-organized criticality (SOC).	5

1.2.1	Models of self-organized criticality and universality classes. . . .	7
1.2.2	Self-organized criticality and $1/f^\alpha$ noise.	11
1.2.3	Self-organized criticality in granular pile and the distribution of residence times of grains in the pile.	14
1.3	Plan of the thesis.	17
2	First passage time distribution in random walks.	19
2.1	Random walk on discrete lattice	20
2.1.1	One dimension	20
2.1.2	Higher dimensions.	22
2.2	Continuum limit: The diffusion equation.	23
2.2.1	One dimension	23
2.2.2	Diffusion in a d -dimension with absorbing boundary.	24
2.2.3	Diffusion inside a right angled isosceles triangle.	25
2.2.4	Diffusion in a circular disc and sphere.	26
2.3	Concluding remarks	27
3	The distribution of residence times in height type sandpile models.	29
3.1	Models	29
3.2	General formalism for calculating the distribution of residence times.	31
3.2.1	The transition matrices.	31
3.2.2	A simple Illustration: $1D$ Bak-Tang-Wiesenfeld model driven at one end.	32
3.3	Analytic results in $1D$ Bak-Tang-Wiesenfeld model: Driving at one end.	37
3.3.1	Small time behaviour in the limit of large system sizes.	37
3.3.2	Scaling function of the distribution of residence times.	41
3.4	Generalization to higher dimensions.	44
3.4.1	Distribution of residence times for isotropic models.	44
3.4.2	Exact solutions in some special cases.	45
3.5	Finite size corrections.	48
3.6	Concluding remarks.	50
4	The distribution of residence times in ricepile models.	51
4.1	Definition of the Models	52

4.1.1	Model-A: The Oslo ricepile model.	53
4.1.2	Model-B : $2d$ generalization of the Oslo model.	53
4.1.3	Model-C : The local limited model.	54
4.1.4	Model-D : Model with non-nearest neighbour transfer of grains.	54
4.2	Relation between residence times at a site and height fluctuations.	56
4.3	Probability of minimum slope configuration in the Oslo ricepile model	59
4.3.1	Explicit calculation of $Prob_L(h_1)$ small L	59
4.3.2	Asymptotic behaviour of $Prob_L(h_1)$ for large L	60
4.3.3	Verification by Monte Carlo simulation.	62
4.4	Residence times in the Oslo ricepile model	74
4.4.1	Distribution of residence times at site 1	74
4.4.2	Total residence times T in the pile.	80
4.5	Generalization to other slope type models	81
4.5.1	Distribution of residence times at site 1 in model-B, C, D.	81
4.5.2	Distribution of total residence times in the pile in model-B, C, D.	85
4.6	Concluding remarks.	86
5	Summary	89
A	Calculation of eigenfunctions of Eq. 3.10	91
B	Finite size corrections	93
B.1	Calculation for $Prob_L(T = 0)$	93
B.2	Calculation for $Prob_L(T = 1)$	94
B.3	Correction in the cumulative distribution	95
	Bibliography	99

List of Figures

0.1	Plot of the coefficient K_L of t/L^2 in the exponential decay of probability of residence times versus lattice size L for the $1d$ BTW model.	xiv
0.2	Motion of three grains starting from $x = 20, 50, 80$ on a one dimensional sandpile of length $L = 100$, where sand grains are added only at the right end.	xv
0.3	Semi log plot of the cumulative distribution $Prob_L(T \geq t)$ as a function of the scaled residence time $t/\langle M \rangle$ for four different cases (1) the $1d$ BTW model, (2) the $1d$ Manna model, (3) the $2d$ BTW model and (4) the $2d$ Manna model. We have chosen $L = 100$ for $1d$ cases and 70×70 cylindrical square lattice for $2d$ cases.	xvi
0.4	Scaling collapse of $Prob_L(T_1 \geq t)$ against the scaling variable $t/L^{0.25}$ for the $1d$ Oslo rice pile model for $L = 20, 25, 35$ and 50	xx
0.5	Scaling collapse of $Prob_L(T \geq t)$ against the scaling variable $t/L^{1.25}$ for the $1d$ Oslo rice pile model for $L = 20, 25, 35$ and 50	xxi
0.6	Logarithm of the probability of the minimum slope configuration (calculated exactly) is plotted versus $L(L+1)(L+2)/6$ for the $1d$ Oslo rice pile model for $L = 1$ to 12	xxiii
1.1	A sketch of the experimental setup of the Oslo experiment taken from the book titled “Self Organized Criticality” by H. J. Jensen (Cambridge Univ. Press, Cambridge, 1998).	14
1.2	Snapshot of ricepile in the Oslo ricepile experiment by Christensen <i>et. al.</i> (Phys. Rev. Lett., 77 , 107, 1996).	15
2.1	A right angled isosceles triangle as the absorbing boundary. The random walker starts at the centre of the triangle [coordinates $(4L/3, 2L/3)$]. . .	25
2.2	The scaling functions $f(\chi)$ of a box and a sphere are plotted against χ . The box and sphere have a ratio of sizes $\frac{2L}{R} = \sqrt{3}$ where L is the linear size of the box and R is the radius of the sphere.	27

3.1	Transfer rule of grains in BTW model on a $2D$ square lattice. Four grains are thrown out from an unstable site and each of the four nearest neighbours gets one grain.	30
3.2	Transfer rule of grains in stochastic Manna model on a $2D$ square lattice. Each of the four grains randomly goes to any one of the four nearest neighbours.	30
3.3	Possible configurations with a marked grain are shown by the asterisk.	34
3.4	Periodic Markov chain in the case of the $1d$ BTW model driven at right end for $L = 4$	36
3.5	K_L has been plotted against lattice size L . K_L has been calculated upto $L = 150$ and extrapolated using a fit to a straight line. Extrapolated value of K_L when L large is 3.668 ± 0.003	37
3.6	The probability distribution of the total residence time T plotted against T for $L = 25, 50, 100, 150$ for the $1d$ BTW model driven at an end.	39
3.7	The plot of scaling function $L^3 Prob_L(T = t)$ against the scaled variable t/L^2 for different lattice sizes for the $1d$ BTW model driven at an end.	40
3.8	Motion of three grains starting from $x = 20, 50, 80$ in the $1d$ BTW sandpile of length $L = 100$ where sand grains are added only at the right end.	41
3.9	Survival probability versus residence time t for the $1d$ BTW model in two cases with grains added only at one or both ends. The theoretical result(full curve) and the simulation result(dotted line) match perfectly. $L = 100$ for both the cases.	43
3.10	Semilog plot of the survival probability of a marked grain as a function of scaled residence time t/M for four different cases: (1) the $1d$ BTW model, (2) the $1d$ Manna model, (3) the $2d$ BTW model, (4) the $2d$ Manna model. We have chosen $L = 100$ in one dimension and 70×70 cylindrical square lattice in two dimensions.	47
3.11	The scaled correction term $L\delta S(t L)$ versus t/L^2 for the $2d$ BTW and Manna model for three different values of $L = 13, 20, 30$. The curve with higher peak is for the Manna model.	48
3.12	Finite size correction for the $1d$ BTW model with grains added everywhere for $L = 40$. Plotted is the scaled deviation of simulation data, $L\delta S(t/L)$, from the simple exponential scaling solution [Eq.(3.21)] and the full curve is the scaled deviation $L\delta S(t/L)$ from theory [Eq.(3.23)].	49
4.1	Rice pile of size $L = 5$ after addition of 100 grains. All grains are numbered by the time they were added to the pile. Minimum slope is denoted by the thick line.	55

4.2	Fluctuation of height at first site with time plotted for the 1d Oslo ricepile model for $L = 20$. The horizontal line is at $h_1 = 33$ which is the most probable height. The first and second vertical lines are at $t = 14$ and $t = 42$ respectively.	57
4.3	Scaling collapse of various probability distributions $Prob_L(\Delta h_1)$ where Δh_1 is the deviation of height at site 1 from its average value, for different system sizes, $L = 100, 200$ and 400 for the 1d Oslo ricepile model.	59
4.4	Logarithm of the probability of occurrence of minimum slope configuration (calculated exactly) is plotted versus $L(L+1)(L+2)/6$ for the 1d Oslo ricepile model for $L = 1$ to 12 .	62
4.5	Schematic diagram illustrating our algorithm. If we start with unstable configuration C_0 , at the next step after toppling the unstable sites, we get a set \mathcal{S} of stable configurations S_1, S_2, S_3 and a set \mathcal{U} of unstable configurations U_1, U_2, U_3, U_4 . The probability of getting any stable configuration is $P(\mathcal{S}) = Prob(S_1) + Prob(S_2) + Prob(S_3)$.	65
4.6	Plot of the probability $Prob(x_{max} < x)$ versus x .	69
4.7	Monte Carlo simulation: Logarithm of probability of the minimum slope configuration plotted against the system size L for the 1d Oslo ricepile model. The data is averaged over 10^3 realizations.	71
4.8	Exact numerical calculation and the Monte Carlo simulation for $L \leq 12$: Logarithm of the probability of the minimum slope configuration is plotted against the system size L for the 1d Oslo ricepile model. The data is averaged over 10^5 realizations.	71
4.9	The frequency distribution of $\log_{10}(Prob. \text{ of } min. \text{ slope})$ taking bin size = 1 and for $L = 20$ for the 1D Oslo ricepile model. The data is averaged over 10^5 initial realizations.	72
4.10	Probability distribution of height at site 1 $Prob_L(h_1 - \langle h_1 \rangle)$ versus $(h_1 - \langle h_1 \rangle)$ is plotted for system sizes $L = 10, 20, 40$ for the 1d Oslo ricepile model. The data is averaged over 10^5 initial realizations.	73
4.11	Scaling collapse: $L^{0.25} Prob_L(h_1 - \langle h_1 \rangle)$ has been plotted against the scaling variable $(h_1 - \langle h_1 \rangle)/L^{0.25}$ for the 1d Oslo ricepile model. The scaling function is highly asymmetric in the tails.	74
4.12	The cumulative probability $Prob_L(T_1 \geq t)$ versus time t for lattice sizes $L = 20, 25, 35$ and 50 for the 1d Oslo ricepile model. A total of 10^9 grains were added.	75
4.13	The cumulative probability $Prob_L(T_1 \geq t)$ versus time t for lattice sizes $L = 100$ and $L = 200$ for the 1d Oslo ricepile model.	76
4.14	The cumulative probability $Prob_L(T_1 \geq t)$ versus time t for lattice size $L = 20$ for the 1d Oslo model.	76

- 4.15 The cumulative probability $Prob_L(T_1 \geq t)$ for residence time at the first site plotted against the scaled residence time $t/L^{0.25}$ for lattice sizes $L = 300, 400$ and 500 for the $1d$ Oslo ricepile model. A total of 10^7 grains were added. The scaling function is fitted with $0.05/(x[\ln x]^{0.5})$. 78
- 4.16 The cumulative probability $Prob_L(T_1 \geq t)$ for residence time at the first site has been plotted against the scaled time $t/L^{0.25}$ for lattice sizes $L = 20, 25, 35$ and 50 for the $1d$ Oslo ricepile model. A total of 10^9 grains were added. The envelop is fitted with $5/(x[\ln x]^{0.75})$ 79
- 4.17 The cumulative probability $Prob_L(T \geq t)$ versus time t for lattice sizes $L = 20, 25, 35$ and 50 for the $1d$ Oslo ricepile model. A total of 5×10^7 grains were added. 81
- 4.18 Scaling collapse of $Prob_L(T \geq t)$ versus scaled residence time $t/L^{1.25}$ for the $1d$ Oslo ricepile model for lattice sizes $L = 20, 25, 35$ and 50 . A total of 5×10^7 grains were added. Scaling function is fitted with $0.26/(x[\ln x]^{0.75})$ 82
- 4.19 The residence time distribution $Prob_L(T_{1,1} \geq t)$ of grains at the corner site versus time t for model-B for lattice sizes $L = 12, 15$ and 20 . A total of 10^6 grains were added. 82
- 4.20 The cumulative probability distribution function $Prob_L(T_{1,1} \geq t)$ versus scaled scaled residence time $t/L^{0.2}$ for model-B for lattice sizes $L = 12, 15$ and 20 . A total of 10^6 grains were added. The envelop formed by the steps is fitted with $2.0/(x[\ln x]^{0.5})$ 83
- 4.21 Model-C for lattice sizes $L = 50, 70$ and 100 . A total of 10^5 grains were added at the first site. **Left panel:** The cumulative probability $Prob_L(T_1 \geq t)$ versus time T_1 . **Right panel:** Scaling collapse of $Prob_L(T_1 \geq t)$. The scaling function is fitted with $0.41/(x[\ln x]^{0.5})$. . . 84
- 4.22 Model-D for lattice sizes $L = 50, 70$ and 100 . A total of 10^4 grains were added at the first site. **Left panel:** The cumulative probability $Prob_L(T_1 \geq t)$ versus time t . **Right panel:** Scaling collapse of $Prob_L(T_1 \geq t)$. The scaling function is fitted with $0.8/(2x[\ln 2x]^{0.5})$. . . 85
- 4.23 Model-B for lattice sizes $L = 12, 15$ and 20 . A total of 10^6 grains were added. **Left panel:** The residence time distribution $Prob_L(T \geq t)$. **Right panel:** Scaling collapse of various $Prob_L(T \geq t)$ versus scaled variable $t/L^{2.0}$. The scaling function is fitted with $0.2/(x[\ln x]^{0.75})$. . . 86
- 4.24 Model-C for lattice sizes $L = 50, 70$ and 100 . A total of 10^6 grains were added. **Left panel:** The distribution function $Prob_L(T \geq t)$ versus time t . **Right panel:** Scaling collapse of $Prob_L(T \geq t)$ versus scaled time $t/L^{1.33}$. The scaling function is fitted with $0.3/(x[\ln(x)]^{0.5})$ 87

- 4.25 Model-D for lattice sizes $L = 50, 70$ and 100 . A total of 10^5 grains were added. **Left panel:** The cumulative probability $Prob_L(T \geq t)$ versus time t . **Right panel:** Scaling collapse of $Prob_L(T \geq t)$ against the scaled variable $t/L^{1.33}$. The scaling function is fitted with $0.63/(2x[\ln(2x)]^{0.55})$.
87
- B.1 The marked grain is added at the site denoted as ‘A’, i.e., at the site $x = 3$ from the left. The site with height zero is at the left but far away from the site where marked grain is added. The star symbol indicates the possible final positions of the marked grain added at ‘A’. 96
- B.2 To generate $N(x_a, x_f)$, we add two numbers diagonally one step above the number $N(x_a, x_f)$. Therefore $N(x_a, x_f) = N(x_a - 1, x_f) + N(x_a, x_f - 1)$. 97

Synopsis

0.1 Introduction

The dynamical behaviour of systems with many particles can be described in terms of their time dependent correlation functions. Two examples of such correlation functions are distributions of residence times (DRT) and first passage times. In general, residence time is defined as the time spent by a particle in a specified region of space. The first passage time is defined as the time taken by a stochastic variable crossing a specified surface in the parameter space for the first time. Residence times and first passage times have been studied extensively, *e.g.*, in the problem of Brownian motion of particles mainly in the context of various transport processes [1], in the persistence problem [2]. Trapping time distribution of a system getting trapped inside a region of phase space has been studied to understand long time tails in correlation functions in Hamiltonian systems with many degrees of freedom [3]. In diffusion controlled reactions, the reaction rates of two molecules are related to the residence times of a molecule inside the reactive range of other molecule [4]. In this thesis I study residence time distribution of grains in sandpile models which are prototype of self-organized criticality (SOC).

The concept of SOC was proposed by Bak, Tang and Wiesenfeld (BTW) to explain abundant fractal structures in nature like self similar mountain ranges, river networks, power law distributed burst like activities in earthquake phenomena etc. BTW introduced a simple model, known in the literature as the BTW sandpile model or Abelian sandpile model (ASM), to illustrate the mechanism of SOC [5]. Sandpile models are threshold activated systems (there is a local relaxation only if a variable crosses some threshold value) which, when driven slowly, organize themselves to a critical non-equilibrium stationary state without any fine tuning of parameters. The long-ranged correlation shows up as fractal structures in space. The long-ranged correlation in time gives rise to $1/f^\alpha$ power spectrum of noise with $\alpha < 2$.

The issue whether avalanche activities in sandpile models show $1/f^\alpha$ noise has attracted a lot of attention since BTW proposed the model. The avalanche activities have different behaviour for two different time scales, the time scale of a toppling event, *i.e.*, correlation among activities within a single avalanche and for the time scales of

slow driving, i.e., correlations among separate avalanches. In the first case, Laurson *et. al* have shown that the power spectrum is $1/f^\alpha$ with $\alpha < 2$ [6]. While in the second case, for some specific one dimensional model [7] it has been shown that long-ranged temporal correlations between avalanches are related to critical avalanche dynamics and give rise to $1/f^{\alpha'}$ noise where exponent α' can be expressed in terms of the standard avalanche exponents of avalanche size distribution.

Although SOC was not seen in experiments on piles of sand [8], piles of long-grain rice have shown evidence of power law distributed avalanches, and provided a good experimental realization of a simple system showing SOC. In the Oslo rice pile experiment [9], Frette *et. al.* studied the transport properties of rice grain by slowly adding rice grains at one end of a pile between two closely spaced parallel rectangular glass plates where grains can leave only at the other end. Coloured tracer grains were added to measure the residence times of grain and distribution of residence times was studied. They estimated the average total residence time of grains in a pile of size L to vary as L^ν with $\nu = 1.5 \pm 0.2$.

There have also been some numerical and analytical studies of these distributions later on. Frette proposed a theoretical model, called the Oslo rice pile model [10], which seems to reproduce the phenomenology of the rice pile experiment well. From numerical simulations of the Oslo model [11], the exponent characterizing the power law decay of the probability density of total residence times at large times was estimated as 2.2 ± 0.1 and exponent ν was estimated to be 1.3 ± 0.1 .

Sandpile models are defined on a lattice and configurations are specified by a height variable which gives the number of grains at each site. There is a threshold condition for toppling at a site and some specified number of grains are transferred to the neighbouring sites after each toppling. Depending on the threshold condition, there are two broad classes in sandpile models, critical height type models and critical slope type models. We call all the slope type models as ricepile models hereafter. We have studied the distribution of residence times (DRT) in various height and slope type models. The residence time t of a grain is the time the grain spends inside the pile. The piles are slowly driven, *i.e.* the time interval between addition of two grains is chosen long enough so that all avalanche activities have died before a new grain is added and this time interval is chosen to be the unit of time in our analysis.

For height type models, we argue that the motion of a grain is diffusive at time-scales

much larger than the interval between successive grain addition and the jump-rates of grains at various sites are space-dependent due to the space dependence of avalanche activity at different sites. We have shown that the DRT, for large residence times and large system sizes, can be expressed in terms of the survival probability of a diffusing particle in a medium with absorbing boundaries and space dependent jump rates. The DRT is of the form $L^{-d}f(t/L^d)$ in d -dimensional pile for system size L and $f(x)$ decays exponentially for large x . However, $f(x)$ is non-universal and depends on how grains are added in the pile.

For slope type models, there is a significant weight at tail of the DRT due to deeply buried grains in the pile. These grains take a long times to come out, the cutoff time scale in the DRT is diverging exponentially with increasing system sizes, and determines the exponent of the power law tail in the DRT. We show that the DRT is a $1/t^2$ power law distribution with a logarithmic correction factor.

0.2 First passage time distribution in random walks

Our first result concerns the problem of first passage time distribution for a random walker in the presence of absorbing boundaries of various geometries. Diffusion is a well studied problem with considerable physical interest. We have studied the simple diffusion of a particle where the particle diffuses in a closed domain of linear size L and gets absorbed when it reaches the boundary. The probability $p(\vec{x}, t)$ that particle being at position \vec{x} at time t satisfies the diffusion equation

$$\frac{1}{D} \frac{\partial p(\vec{x}, t)}{\partial t} = \nabla^2 p(\vec{x}, t) \quad (0.1)$$

Where D is the diffusion constant. We solved this equation with initial condition $p(\vec{x}, 0) = \delta(\vec{x} - \vec{a})$ under the boundary condition $p(\vec{x}, t)|_{boundary} = 0$ in various dimensions where \vec{a} is the centre of the domain. $Prob_L(T \geq t)$ be the probability that the first passage time T of the walker through the boundary being greater than or equal to t is given by $Prob_L(T \geq t) = \int p(\vec{x}, t) d^d \vec{x}$ in d dimensions. We are interested in the probability density $Prob_L(t) = -\frac{\partial}{\partial t} Prob_L(T \geq t)$ which in all cases shows scaling

$$Prob_L(t) = \frac{1}{L^2} f(t/L^2)$$

where t is the first passage time. We obtained explicit form of the scaling function $f(\chi)$, for the following geometries of the boundaries: a box in one dimension, circular,

square and triangular boundaries in two dimensions and cubical box and sphere in three dimensions. In all cases the scaling function can be expressed in terms of the Jacobi Theta functions [12].

For example, in the case of an absorbing boundary of a hypercube of volume $(2L)^d$ in d -dimensions, the scaling function $f(\chi)$ is expressed as

$$f(\chi) = (-1)^d 2 \left(\frac{1}{2\pi}\right)^d \frac{d}{d\chi} (y^d) \quad \text{where } y = \int_{\chi}^{\infty} \frac{\partial \vartheta_3(z, q = e^{-\tilde{\chi}/d})}{\partial z} \Big|_{z=\pi/4} d\tilde{\chi} \quad (0.2)$$

Here $\chi = d\pi^2 Dt/4L^2$ and $\vartheta_3(z, q)$ is the Jacobi theta function of third kind [12]. Similarly in other cases studied, the scaling functions are expressed in terms of theta functions of various kinds. All these results in this section were published in [13].

0.3 The distribution of residence times in height type sandpile models

0.3.1 Models

We have considered two height type models: the deterministic Bak-Tang-Weisenfeld (BTW) model [5] and the stochastic Manna model [14]. Both the models are defined on a d -dimensional hypercubic lattice of volume L^d . The height $h(\vec{x})$ is the number of grains at site \vec{x} . The toppling rule in the BTW model in d -dimension is as follows. If $h(\vec{x}) \geq 2d$ at site \vec{x} , $2d$ grains are thrown out of the site and each of the $2d$ nearest neighbour sites gets one grain. The toppling condition in the Manna model is similar as in the BTW model, but the transfer rule is not deterministic. In this case, $2d$ grains are transferred from a site after each toppling, but each grain is transferred randomly to any one of the nearest neighbours. Grains are added randomly everywhere and leave the pile from the boundary sites. The piles are driven slowly, by adding one grain per unit time. We always topple unstable sites in parallel. The grain added at time n is labeled by the number n .

We have used an important result from queuing theory, known as Little's theorem [15], for the first moment of the DRT in this thesis. From this theorem, it follows that the average residence times of grains inside a pile is equal to the average number of grains inside the pile, *i.e.*,

$$\langle T \rangle = \langle M \rangle \quad (0.3)$$

where T is the residence time of a grain inside the pile and M is the number of grains inside the pile.

This result is quite general and valid for sandpile models, irrespective of whether the toppling rules are height type or slope type.

0.3.2 Bak-Tang-Wiesenfeld model in one dimension.

We have studied the DRT for the BTW model in one dimension where grains are added, say, at the right end ($x = L$) and can leave the system from both the ends. If there are L sites, it can be shown that only $(L + 1)$ configurations occur with non zero probability in the steady state [16]. Among all these steady state configurations, L steady state configurations have a site with zero height and other sites with height 1 and one steady state configuration has all sites with height 1. The time evolution of the sandpile is Markovian and we can construct a transition matrix \mathcal{W} for the Markovian evolution of the system. With one grain marked, the configuration space consists of L^2 configurations. Since this is a Markov process, the DRT must decay exponentially as $\exp(-\lambda_L t)$ for large times t , where λ_L depends on the system size L . We show that for large L , λ_L decays as $1/L^2$. We write $\lambda_L = K_L/L^2$ for any finite L where K_L should tend asymptotically to a constant value for large L . We calculated λ_L exactly numerically by diagonalizing the Markov matrix \mathcal{W} up to $L = 150$ and plotted $K_L = \lambda_L L^2$ versus L in Fig.0.1. We find the asymptotic value of K_L is 3.668 ± 0.003 .

When the residence time T is very small compared to L^2 , and L is large, sand grain almost always gets ejected from the right end. In the large L limit, the DRT is just the distribution of first passage (at $i = 1$) time of a simple unbiased random walker with $2t$ step random walk in an infinite domain and we write

$$Prob_L(T = t) = \frac{2t!}{t!(t+1)!} 2^{-(2t+1)}$$

This expression for $Prob_L(T = t)$ can be approximated as $\frac{1}{2\sqrt{\pi}} t^{-3/2}$ for $t \gg 1$. We assume that the DRT for the 1d BTW model has a scaling form as given below,

$$Prob_L(T = t) = \frac{1}{L^a} f\left(\frac{t}{L^b}\right) \quad (0.4)$$

and we use the first moment condition in Eq.(0.3) and behaviour of the DRT for small t , to deduce values of the exponents, $a = 3$ and $b = 2$. We analytically calculated the exact asymptotic value of K_L for large L . For the 1d BTW case when grains are added

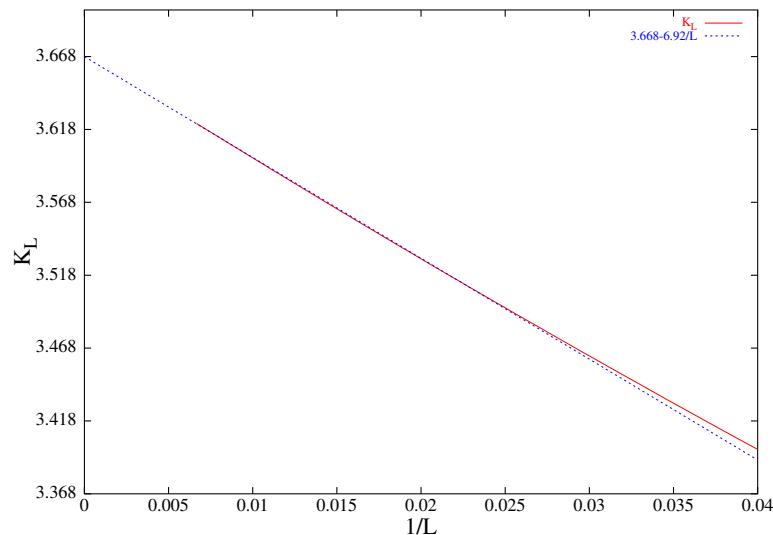


Fig 0.1: Plot of the coefficient K_L of t/L^2 in the exponential decay of probability of residence times versus lattice size L for the 1d BTW model.

at the right most site $x = L$, the probability of toppling at any site x is x/L . Then the probability $P(x, t)$ that a marked grain is at site x at time t can be written in terms of a rate equation where rate of grains jumping out of x to a nearest neighbour site is x/L . The rate equation is

$$\frac{\partial P(x, t)}{\partial t} = \frac{x-1}{L}P(x-1, t) - 2\frac{x}{L}P(x, t) + \frac{x+1}{L}P(x+1, t) \quad (0.5)$$

In the continuum limit, this equation becomes

$$\frac{\partial}{\partial \tau}P(\xi, \tau) = \frac{\partial^2}{\partial \xi^2}[\xi P(\xi, \tau)] \quad (0.6)$$

where $\xi = i/L$, and $\tau = t/L^2$. We have solved the eigenvalue equation $\frac{d^2}{d\xi^2}[\xi\varphi(\xi)] = -\lambda\varphi(\xi)$ with the boundary condition $\varphi(\xi = 1) = 0$. Eigenfunctions are modified Bessel's function of order 1 and we calculated the largest eigenvalue λ_L in terms of the first zero of the modified Bessel's function of order 1. We find that λ_L for large L varies as K/L^2 and $K \approx 3.6705$ (correct upto five significant digits).

0.3.3 Generalization to other models and arbitrary dimensions.

It is straight forward to extend our arguments to any other isotropic height type models where grains are transferred to the nearest neighbour with equal probability and grains

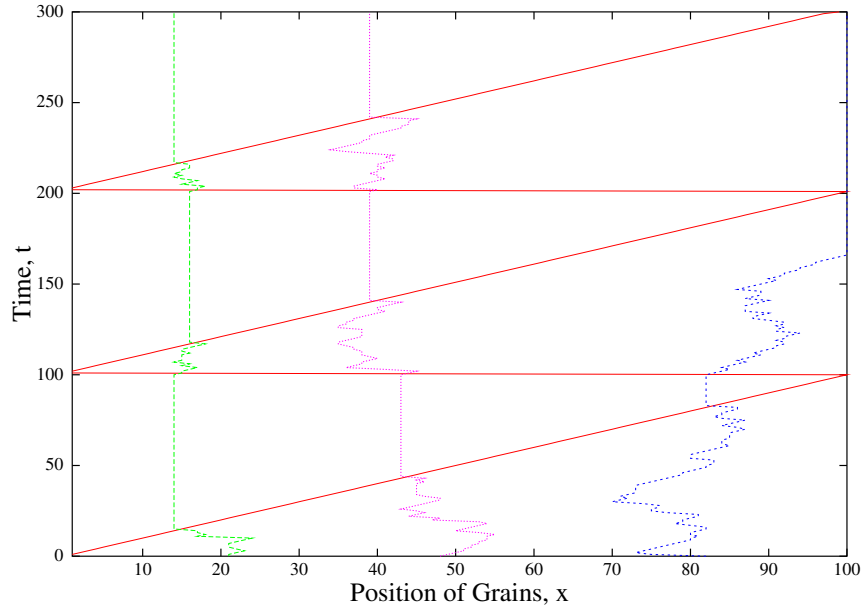


Fig 0.2: Motion of three grains starting from $x = 20, 50, 80$ on a one dimensional sandpile of length $L = 100$, where sand grains are added only at the right end.

can leave the system only from the boundary sites. Although avalanches in sandpile can spread quite far, the typical distance traveled by one marked grain in an avalanche is much smaller than L , linear size of the system. During its motion to the boundary, the marked grain would be involved in a large number of avalanches. At time-scales much larger than unity, the motion is diffusive, with the jump-rate out of different sites being space-dependent because on the average some parts of the lattice have more avalanche activity than others. In the steady state, $n(\vec{x})$, the average number of toppling at \vec{x} per added grain, satisfies the equation (using conservation of sand grains)

$$\nabla^2 n(\vec{x}) = -r(\vec{x}), \quad (0.7)$$

where $r(x)$ is the probability of addition at x and we impose $n(\vec{x}) = 0$ at the boundary.

As the path of the grain is an unbiased random walk, we have $\langle (\Delta \vec{x})^2 \rangle = s$, where s is the average number of jumps the grain makes in this interval. Assuming that $|\Delta \vec{x}| \ll L$, and that $n(\vec{x})$ is a slowly varying function of \vec{x} , we see that s is proportional to $n(\vec{x})\Delta t$, total no of toppling at site x during time interval Δt . For large times t , the probability-density $P(\vec{x}, t)$ satisfies the equation

$$\frac{\partial}{\partial t} P(\vec{x}, t) = \frac{1}{2} K \nabla^2 [n(\vec{x}) P(\vec{x}, t)] \quad (0.8)$$

where K is a constant. The initial condition is given by

$$P(\vec{x}, t = 0) = r(\vec{x}). \quad (0.9)$$

The net current between two sites depends on the difference in the product nP at the two sites, and can be non-zero even if ∇P is zero. We have solved Eq.(0.8) exactly in some special cases as follows.

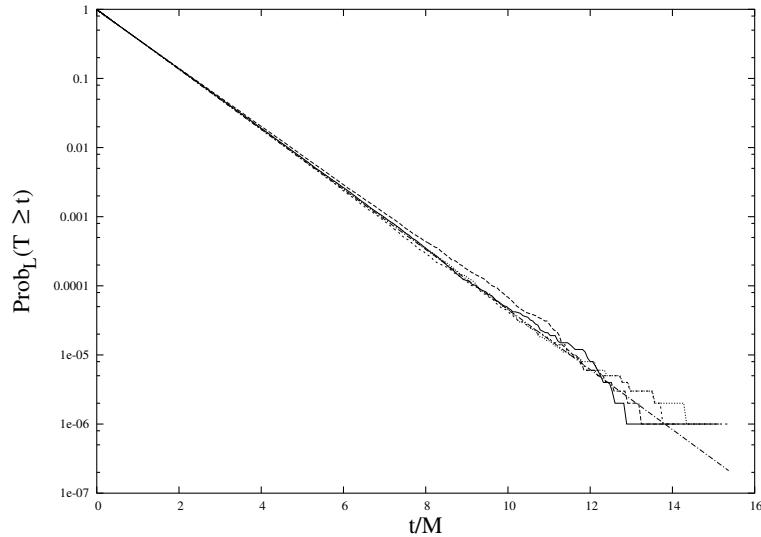


Fig 0.3: Semi log plot of the cumulative distribution $Prob_L(T \geq t)$ as a function of the scaled residence time $t/\langle M \rangle$ for four different cases (1) the 1d BTW model, (2) the 1d Manna model, (3) the 2d BTW model and (4) the 2d Manna model. We have chosen $L = 100$ for 1d cases and 70×70 cylindrical square lattice for 2d cases.

Case-1. When grains are added at both ends with equal probability in 1d models (both the BTW and Manna models) with L sites, *i.e.*, $r(\vec{x}) = \frac{1}{2}\delta(x-1) + \frac{1}{2}\delta(x-L)$, the average number of toppling $n(x)$ at site x is constant, independent of x and Eq.(0.8) becomes a simple diffusion equation. In the case of the 1d BTW model, $n(x) = 1/2$ and $K = 2$, and we have explicitly calculated $Prob(T \geq t)$. It has a scaling form $\frac{1}{L}f(t/L^2)$ and scaling function can be expressed in terms of Jacobi theta function, similar to the results in Sec.2.

$$Prob(T \geq t) = \theta_3(0, \tau) - \theta_3(\pi/2, \tau), \quad (0.10)$$

where $\tau = \pi^2 t / 2L^2$ and $\theta_3(z, \tau)$ is the Jacobi theta function of third kind (putting $q = e^{-\tau}$) [12].

Case-2. When grains are added randomly at any sites in a system with arbitrary shape of the boundary and in an arbitrary dimension, *i.e.*, $r(\vec{x}) = 1/V$ where V is the number of sites in the lattice, the cumulative probability $Prob(T \geq t)$ is interestingly a simple exponential

$$Prob(T \geq t) = \exp(-t/\langle M \rangle). \quad (0.11)$$

We have checked our theoretical results by simulating the BTW and Manna models in both one and two dimensions. In one dimension we have chosen system size $L = 100$ where grains are dissipated at the ends. In two dimensions we have taken a cylindrical 70×70 square lattice and grains are dissipated at the two open boundaries of the cylinder. We have added 10^6 grains in all four cases. The DRT obtained from Eq.(0.11) and simulation have been plotted in Fig.0.3.

Our arguments are valid under the conditions of local conservation of sand grains and isotropy, and are equally applicable to the BTW and Manna models. All these results for height type models were published in [17, 18].

0.4 The distribution of residence times in slope type sandpile models

0.4.1 Models

Here we consider two one dimensional ricepile models, the stochastic Oslo rice pile model [10] and one of the deterministic models defined by Kadanoff *et. al.* [19]. The slope z_i at site i is defined by $z_i = h_i - h_{i+1}$, where h_i is the height at site i and $1 \leq i \leq L$. In Oslo rice pile model, when $z_i > z_c$, one grain is transferred to the right. The threshold value of the slope z_c takes values 1 or 2 with probability q and p (with $p + q = 1$) after each toppling, independent of any history. Grains are added, say, at the left end $i = 1$. In the Kadanoff model, the threshold value of z_c is 2 and after each toppling, two grains are transferred to the right neighbour. In this case, grains are added randomly everywhere. In both the models grains are lost only at the right boundary $i = L$. The piles are driven slowly, by adding one grain per unit time. We always topple unstable sites in parallel. The grain added at time n is labeled by the

number n .

Grains at a particular site are stacked vertically, one above the other. Whenever a grain is added at a site, it sits on top of the stack at the site. When one unstable grain leaves the stack, it is taken from the top of the stack. In Kadanoff model, two grains from the top are thrown out from an unstable site to the right nearest neighbour site. We first take out the topmost grain from the unstable site and put it on the top of the right nearest neighbour stack, and then we take out the second grain from the unstable site and put it on the top of the first grain at the right nearest stack.

The DRT has qualitatively different behaviour for ricepile models. The height of the pile fluctuates between L to $2L$ around some average height αL where α is the average slope ($1 \leq \alpha \leq 2$). The grains which are deeply buried inside the pile take a long time to come out of a site, i.e., until the rare height fluctuation brings the height at the site close to the minimum. We study the distribution of total residence times of grains in the pile as well as the residence time of a grain at a site. We define the residence time T_i at a site i as the time spent by a grain at the site. The average number of grains in the pile is of order L^2 and so the average total residence time is also varies as L^2 , using Eq.(0.3). Similarly, the average residence time $\langle T_i \rangle$ at site i varies as $(L - i)$. The average of total residence times has been incorrectly estimated before as $L^{1.3 \pm 0.1}$ [11, 20].

0.4.2 Distribution of residence time T_1 at first site.

We express the average residence time $\langle T_i \rangle$ at a site i in terms of probability distribution $Prob_L(h_i)$ of height h_i at the site, where L is the system size and p_i is the average frequency of addition at site i per unit time, e.g., $p_1 = 1$ for addition of grains at site 1 and $p_1 = 1/L$ for uniform addition of grains. The average residence time of grains, added when $h_i = h$, can be expressed in terms of $Prob_L(h_i)$ as given below.

$$\langle T_i \rangle_h = \frac{Prob_L(h_i > h)}{p_i Prob_L(h_i = h)} \quad (0.12)$$

The behaviour of all T_i 's are qualitatively similar for i not too close to the right edge and we study distribution of residence time T_1 only at site 1. We define $Prob_L(T_1 \geq t | h_1)$ be the conditional probability that a grain stays at site 1 for time greater than t , given that it was added when the height was h_1 . $Prob_L(h_1)$ is the probability that height at site 1 was h_1 when the grain was added. So we have, summing over all possible values

of h_1 ,

$$Prob_L(T_1 \geq t) = \sum_{h_1=L}^{2L} Prob_L(h_1) Prob_L(T_1 \geq t|h_1).$$

Approximating $Prob_L(T_1 > t|h_1)$ by a simple exponential and using Eq.(0.12), we write, for large t ,

$$Prob_L(T_1 \geq t) \simeq \sum_{h_1=L}^{2L} Prob_L(h_1) e^{-tp_1 Prob_L(h_1)} \quad (0.13)$$

In the steady state, the average value of h_1 varies as L , and the width σ_{h_1} varies as L^{ω_1} , where exponent $\omega_1 < 1$. For large L , the probability distribution of h_1 has a scaling form $Prob_L(h_1) = L^{-\omega_1} g(\frac{h_1 - \bar{h}}{L^{\omega_1}})$ and the scaling function $g(x)$ varies as $\exp(-|x|^\alpha)$ for $|x| \gg 1$, with $\alpha > 1$. For large L and t , the terms, which contribute to $Prob_L(T_1 \geq t)$ in Eq. (0.13), correspond to the values of h_1 for which $h_1 \ll \bar{h}_1$. Substituting the scaling form of $Prob_L(h)$ in Eq (0.13) and converting the summation into an integral, we show that,

$$Prob_L(T_1 \geq \tau L^{\omega_1}) \sim 1/[\tau(\ln \tau)^{\frac{\alpha-1}{\alpha}}] \quad (0.14)$$

When grains are added randomly everywhere in the pile, e.g., in the Kadanoff model, the average residence time $\langle T_1 \rangle_{h_1}$ of a grain added at height h_1 varies as $L/[Prob_L(h_1)]$ [see Eq. (0.12)]. Now there is an extra $1/L$ factor inside the exponential in the Eq. (0.13) and the scaling variable $\tau = t/L^{\omega_1}$ in Eq. (0.14) is replaced by $\tau = t/L^{1+\omega_1}$.

Simulation: We have checked our theoretical arguments by simulating the Oslo rice pile model. The qualitative behaviour of distributions $Prob_L(T_i \geq t)$ for $i = 1$ in this model can be seen in the simulation results shown in Fig.0.4 We have done our simulations for $p = q = \frac{1}{2}$, and different system sizes, $L = 20, 25, 35$ and 50 . We averaged the data for a total 10^9 grains which were added in the pile for each L . Fig.0.4 shows the plot of $Prob_L(T_1 \geq t)$ versus scaled time $t/L^{0.25}$ for different values of L . Interestingly, various curves for different L have steps like structures and the curves for different values of L cross each other many times. The existence of several steps, whose positions and logarithmic widths are different for different L 's, implies that simple finite size scaling cannot hold in this case. However, our scaling theory correctly describes the envelop function of the staircase. In Kadanoff model We don't see any steps like structure. The cumulative probability is smooth and monotonic function of L for a

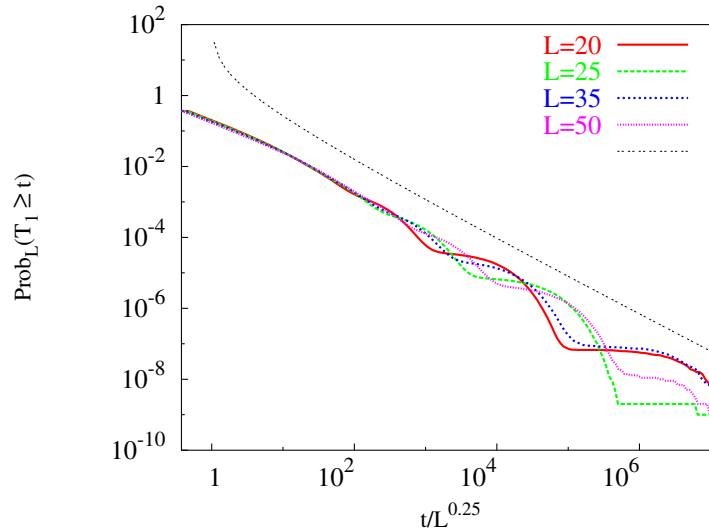


Fig 0.4: Scaling collapse of $Prob_L(T_1 \geq t)$ against the scaling variable $t/L^{0.25}$ for the $1d$ Oslo rice pile model for $L = 20, 25, 35$ and 50 .

fixed t , and has a simple scaling form. Various $Prob_L(T_1 \geq t)$ for different values of L collapse to a single curve when plotted versus $t/L^{1.33}$.

In an earlier work, Boguna and Corral [20], and Carreras *et. al.* [21] used a continuous-time random walk model of the motion of grains, with long trapping times and a power-law distribution of step sizes, to explain the anomalous diffusion of tracer grains. The exponent of the power law distribution of trapping times used in their analysis was not equal to 2 and was incorrect as shown in this thesis. They did not consider the logarithmic correction factor in the distribution of trapping times and hence overestimated the exponent.

0.4.3 Distribution of total residence time in the pile.

Similarly, from the results for the distribution of T_1 , We can expect the behaviour of the cumulative distribution $Prob_L(T \geq t)$ to be a scaling function of t/L^ω , where the exponent ω is different from ω_1 defined earlier. So we write

$$Prob_L(T \geq t) = f\left(\frac{t}{L^\omega}\right) \quad (0.15)$$

where the scaling function $f(x)$ varies as $1/[x(\ln x)^\delta]$ for large x , and the exponent δ would also be different from δ_1 defined earlier. Using the condition that the mean

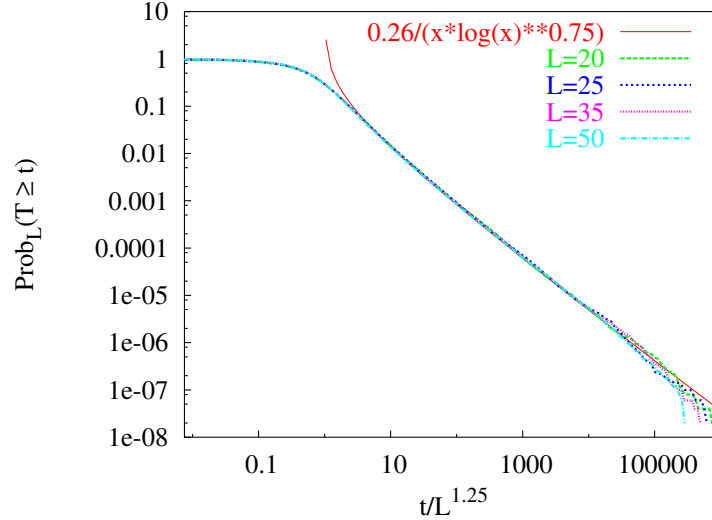


Fig 0.5: Scaling collapse of $Prob_L(T \geq t)$ against the scaling variable $t/L^{1.25}$ for the $1d$ Oslo rice pile model for $L = 20, 25, 35$ and 50 .

residence time in the pile is equal to the mean active mass in the pile, and hence scales as L^2 , can be used to determine δ in terms of ω and γ by integrating $Prob_L(T \geq t)$ over t up to the cut-off time scale $\exp(\kappa L^\gamma)$. Now we get,

$$\delta = 1 - (2 - \omega)/\gamma \quad (0.16)$$

Simulation: For Oslo rice pile, we have plotted $Prob_L(T \geq t)$ versus scaled variable t/L^ω in Fig.0.5 where $\omega \approx 1.25$. We get the value of δ approximately equal to 0.75 from Eq. (0.16), assuming $\gamma = 3$. The fit is seen to be very good. In the numerical analysis of Christensen *et al.* [11], no logarithmic factor was used, and the data was fitted with a larger effective exponent, *i.e.*, $1/t^{1.22}$ decay. We can expect a similar behaviour in Kadanoff model. Various $Prob_L(T \geq t)$ for different system sizes collapse to a single curve when plotted versus $t/L^{1.33}$ in Kadanoff model.

0.4.4 Probability of large deviations in the Oslo rice pile model.

The function $Prob_L(h_1)$ can be exactly calculated numerically for small L using the operator algebra satisfied by addition operators [22]. We denote any stable configuration by specifying slope values at all sites from $i = 1$ to $i = L$, *e.g.*, $|122\dots 21\rangle$. Whenever slope z_i becomes 2 after additions or toppling at site i , we denote such slope by $\bar{2}$, *i.e.*,

$|\dots\bar{2}\dots\rangle$. The overbar denotes that the site is unstable and may topple with probability q . Using these two toppling rules repeatedly and the Abelian property of the $1d$ Oslo rice pile model, we can relax any unstable configurations.

The probability of maximum slope configuration (i.e., when $h_1 = 2L$) is p^L . That this probability varies as exponentially with L is incorporated in the scaling hypothesis by assuming that the scaling function $g(x)$ of distribution of height h_1 varies as $\exp(-ax^{\frac{1}{1-\omega_1}})$ for $x \gg 1$ where a is a constant.

For small q , the probability of the minimum configuration is $\mathcal{O}(q^{m_L})$ where we conjecture m_L to be exactly $L(L+1)(L+2)/6$. The coefficient of q^{m_L} in the probability is harder to compute explicitly for large L . For sufficiently small q , the probability of the minimum height configuration in the $1d$ Oslo model varies as $\exp[-\kappa(q)L^3]$, where $\kappa(q)$ is a q -dependent function. Then, as there is no change in the behaviour of the Oslo rice pile expected as a function of q , this behaviour should persist for all non-zero q . For the scaling function, this would imply that $g(x)$ varies as $\exp[-\kappa(q)|x|^{\frac{3}{1-\omega_1}}]$ for $x \ll -1$. The probability of the minimum slope can be written in a general form as given below.

$$Prob(\text{slope} = 1) \sim \exp[-\kappa(q).L^3] \quad (0.17)$$

where $\kappa(0) = \infty$ and $\kappa(1) = 0$. We have calculated, $Prob_L(\text{slope} = 1)$, i.e., the probability of the minimum slope configuration, exactly numerically for $q = 0.50, 0.60, 0.75$ for $L = 1$ to 12 and the logarithm of $Prob_L(\text{slope} = 1)$ has been plotted versus $L(L+1)(L+2)/6$ in Fig.0.6.

All these results for critical slope type models have been published in [23].

0.5 Summary

1. We have studied the first passage time distribution of a particle obeying simple diffusion equation with absorbing boundary. We explicitly calculated the scaling function, for the following geometries of the boundaries - a box in one dimension, circular, square and triangular boundaries in two dimensions and cubical box and sphere in three dimensions.

2. The DRT of sand grains in height type models, in the scaling limit, can be ex-

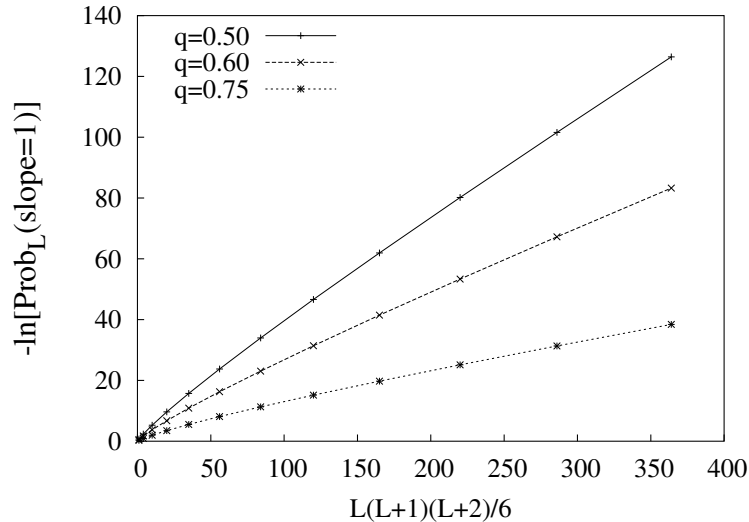


Fig 0.6: Logarithm of the probability of the minimum slope configuration (calculated exactly) is plotted versus $L(L+1)(L+2)/6$ for the 1d Oslo rice pile model for $L = 1$ to 12.

pressed in terms of the survival probability of a single diffusing particle in a medium with absorbing boundaries and space-dependent jump rates. This is valid under the conditions of local conservation of sand grains, transfer of fixed number of grains at each toppling and isotropy, and are equally applicable to deterministic and stochastic models.

3. For height type models, the DRT has scaling form $L^{-d}f(t/L^d)$. The scaling function $f(x)$ is non-universal, and depends on the probability distribution according to which grains are added at different sites. However, the DRT does not have any long time tail and $f(x)$ decays exponentially for $x \gg 1$.

4. For ricepile models, the tail in the DRT at a site, and the DRT of grains inside a pile, are dominated by the grains that get deeply buried in the pile. We show that, for a pile of size L , the probabilities that the residence time at a site or the total residence time is greater than t , both decay as $1/t(\ln t)^x$ for $L^\omega \ll t \ll \exp(L^\gamma)$ where γ is an exponent ≥ 1 , and values of x and ω in the two cases are different. This power law tail is independent of details of the toppling rules, and of the dimensionality of the systems.

5. In the Oslo rice pile model we find that the probability that the residence time

T_i at a site i being greater than or equal to t , is a non-monotonic function of L for a fixed t and does not obey simple scaling. We show that the probability of minimum slope configuration in the steady state, for large L , varies as $\exp(-\kappa L^3)$ where κ is a constant.

Bibliography

- [1] R. Metzler and J Klafter, Phys. Rep. **339**, 1-77 (2000). R. Metzler and J Klafter, J. Phys. A: Math Gen., **37**, R161 (2004).
- [2] S. N Majumdar, Cur. Sci., **77**, 370 (1999).
- [3] Y. Y. Yamaguchi and T. Konishi, Prog. Theo. Phys., **99**, 139 (1998).
- [4] G. Wilemski and M. Fixman, J. Chemical Phys., **58**, 4009 (1972).
- [5] P. Bak, C. Tang, and K. Wiesenfeld, Phys. Rev. Lett. **59**, 381 (1987); Phys. Rev. A **38**, 364 (1988).
- [6] L. Laurson, M. J. Alava and S. Zapperi, J. Stat. Mech.: Theo. and Expt., L11001 (2005).
- [7] J. Davidsen and M. Paczuski, Phys. Rev. E, **66**, 050101(R) (2002).
- [8] H. M. Jaeger, C. Liu and S. R. Nagel, Phys. Rev. Letts., **62**, 40 (1989).
- [9] V. Frette, K. Christensen, A. Malthe-Sorensen, J. Feder and T. Jossang and P. Meakin, Nature (London) **379**, 49 (1996).
- [10] V. Frette, Phys. Rev. Lett. **70**, 2762 (1993).
- [11] K. Christensen, A. Corral, V. Frette, J. Feder, and T. Jossang, Phys. Rev. Lett., **77**, 107 (1996).
- [12] M. Abramowitz and I. A. Stegun, *Hand Book of Mathematical Functions*, (Dover Publications, Inc., New York, 1972).

For convenience we give definition of $\vartheta_3(z, q)$ here: $\vartheta_3(z, q) = 1 + 2 \sum_{n=1}^{\infty} q^{n^2} \cos 2nz$ ($|q| < 1$).

-
- [13] A. Nagar and P. Pradhan, *Physica A*, **320**, 141, (2003).
- [14] S. S. Manna, *J. Phys. A: Math. and Gen.*, **24**, L363, 1991.
- [15] J. D. C. Little, *Operations Research*, **9**, 383, 1961.
- [16] P. Ruelle and S. Sen, *J. Phys. A: Math. Gen.*, **25**, L1257, 1992.
- [17] P. Pradhan and A. Nagar, *Proceedings of National Conference on Nonlinear Systems and Dynamics (NCNSD-2003)*, **97**, (2003). Cond-mat/0403769.
- [18] D. Dhar and P. Pradhan, *Journal of Statistical Mechanics: Theory and Experiment*, **P05003** (2004).
- [19] L. P. Kadanoff, S. R. Nagel, L. Wu, and S. Zhou, *Phys. Rev. A*, **39**, 6524, 1989.
- [20] M. Boguna and A. Corral, *Phys. Rev. Letts.*, **78**, 4950, 1997.
- [21] B. A. Carreras, V. E. Lynch, D. E. Newman and G. M. Zaslavsky, *Phys. Rev. E*, **60**, 4770, 1999.
- [22] D. Dhar, *Physica A*, **340**, 535 (2004).
- [23] P. Pradhan and D. Dhar, *Phys. Rev. E* **73**, 021303 (2006).

Publications

- *Probability distribution of residence times of grains in models of rice piles*, Punyabrata Pradhan and Deepak Dhar, Phys. Rev. E **73**, 021303 (2006).
- *Probability Distribution of Residence Times of Grains in Sandpile Models*, Deepak Dhar and Punyabrata Pradhan, Journal of Statistical Mechanics: Theory and Experiment, **P05003** (2004).
- *Sampling rare fluctuations of height in the Oslo ricepile model*, Punyabrata Pradhan and Deepak Dhar, (Submitted to Journal of Physics: A, Cond-mat/0608144).
- *First passage time distribution in random walks with absorbing boundaries*, Apoorva Nagar and Punyabrata Pradhan, Physica A, Vol. **320**, 141, (2003).
- *Residence Time Distribution of Sand Grains in the 1-Dimensional Abelian Sandpile Model*, Punyabrata Pradhan and Apoorva Nagar, Proceedings of National conference on nonlinear systems and dynamics (NCNSD-2003), **97**, (2003). Cond-mat/0403769.

Introduction

The dynamical behaviour of systems with many particles can be described in terms of their time dependent correlation functions. Two examples of such correlation functions are distribution of residence times (DRT) and of first passage times (DFPT). In general, residence time is defined as the time spent by a particle in a specified region of space. The first passage time is defined as the time taken by a stochastic variable crossing a specified surface in the parameter space for the first time. For granular piles, where once grains are thrown out of the system cannot come back again, these two quantities first passage time of a grain to the boundary of the pile and residence time of a grain inside the pile are basically same. The distributions of the residence times and the first passage times have been studied extensively in the literature. We start with a brief overview of the literature.

1.1 The distribution of the residence times and the first passage times in various contexts.

1.1.1 Random Walks.

For example, in the problem of continuous time random walks (CTRW's), especially in the context of various transport processes [1], the distribution of first passage times (DFPT) is of particular interest. The DFPT has been calculated for a simple unbiased random walker as well as a random walker with long waiting times and long jumps (Levy flight). For example, the classic Polya problem which is as follows. We consider a simple unbiased random walker starting from a point $x = x_0$ in one dimension when mean waiting time and mean square jump length both are finite. It can be shown that the DFPT to origin is given by $F(t) \sim \frac{x_0}{\sqrt{Dt^3}} \exp(-\frac{x_0^2}{4Dt})$ where $F(t)dt$ is the probability for the particle to arrive at the origin $x = 0$ in the time interval t to $t + dt$. It's

asymptotic functional form in long time limit has $3/2$ power law tail, $F(t) \sim t^{-3/2}$ [2, 3]. In a finite domain of size L , the DFPT has an exponential tail. In the next chapter we exactly calculate the DFPT of random walkers moving inside domains of various shapes in various dimensions where random walker gets absorbed whenever it hits the boundaries. Two other interesting cases are when probability distribution of waiting time τ between two successive jumps is a power law $\tau^{-(1+\alpha)}$ for large τ with $0 < \alpha < 1$ (root mean square displacement of the particle $\langle x^2 \rangle \sim t^\alpha$ upto time t) or when probability distribution of jump length a is a power law $a^{-(1+\mu)}$ with $0 < \mu < 2$ (standard deviation of jump length $\langle a^2 \rangle = \infty$). In the first case when mean waiting time diverges but the mean jump length is finite, the DFPT to origin starting from $x = x_0$ in one dimension has been shown to vary as $F(t) \sim x_0 t^{-(1+\alpha/2)}$ using method of images [4]. Interestingly in the case of long jumps, long time behaviour of the DFPT to the origin is same $3/2$ power law as in the simple unbiased Brownian motion, i.e., $F(t) \sim t^{-3/2}$ [5, 6, 7], although a naive guess (however wrong) would be a faster decay than by $t^{-3/2}$ due to the much quicker exploration of space by the particle [8, 9, 10].

Other two similar quantities of wide interest are local residence time T_x at a neighbourhood of a point x and the residence time T_D inside a sub-domain D of the region [11]. If $X(t)$ is the position of a random walker at time t , the local residence time at a point x upto time t is defined as $T_x(t) = \int_0^t \delta[X(t') - x] dt'$ and the residence time $T_D(t)$ upto time t is defined as $\int_D T_x(t) dx$. For example in the case of a simple unbiased random walker, the distribution of residence time $T_D(t)$ of the walker in positive x -axis upto time t is given by $\frac{1}{\pi \sqrt{T_D(t-T_D)}}$. The cumulative probability that the residence time is less than or equal to T_D is famous Levy arcsine law $\frac{2}{\pi} \sin^{-1}(\sqrt{T_D/t})$ [2]. The distribution of residence times has recently attracted particular attention in disordered systems [12]. In the systems with quenched impurities, one injects a tracer particle which tends to get stuck to the impurity sites, while diffusing around, until they are unstuck by thermal fluctuations. The concentration of impurity sites can be inferred from the local residence time spent by the tracer at that point.

Other than the Brownian motion, the DFPT has been studied for various other stochastic processes in many other problem, e.g., persistence problem, diffusion limited aggregation, problem of neuron dynamics, etc which will be discussed briefly in next sections.

1.1.2 Persistence.

The persistence problem have attracted a lot of attention in non-equilibrium systems [13]. Persistence is defined as the probability of a fluctuating quantity being above (or below) a level at least upto time t once it is above that level. The probability decays as $t^{-\theta}$ for large time t where the exponent θ is defined to be persistence exponent. For example in the case of simple unbiased random walk in one dimension, this probability is just the survival probability of the walker at least upto time t , with an absorbing boundary at the origin, and it is the cumulative DFPT, i.e., $\int_t^\infty F(t')dt'$ which varies as $t^{-1/2}$ for large time t . So the persistence exponent in this case is $\theta = 1/2$. For other stochastic processes, the calculation of the persistence exponent is quite difficult, and only in some cases analytical answers are known.

Some non-stationary stochastic processes can be transformed to a stationary Gaussian process. Therefore the much simpler case where the stochastic process $\Phi(t)$ is stationary and Gaussian, and hence fully characterized only by two point correlation function $\langle \Phi(t)\Phi(t') \rangle = f(t-t')$, has been studied for long time [14]. It has been shown that if the two point correlation function $f(t)$ falls faster than $1/t$, then the persistence probability falls as a simple exponential $\exp(-\alpha t)$ for large t where α is a constant [13]. For a special case where stochastic process is stationary Gaussian Markov process, the correlation function is purely exponential, i.e., $f(t) = \exp(-\lambda t)$ where λ is a constant and in this case the persistence probability is exactly given by $\frac{2}{\pi} \sin^{-1}[\exp(-\lambda t)]$ [14]. For large t , this probability goes as $\exp(-\lambda t)$.

For a non-Markov and non-stationary process, for example, if we consider $\Phi(t)$ where $\Phi(t)$ satisfies a Langevin equation $\frac{d^2\Phi(t)}{dt^2} = \eta(t)$ and η is a delta correlated Gaussian noise, the persistence probability goes as $t^{-1/4}$ [15]. In more complicated cases, the stochastic process $\Phi(x, t)$ may be a function of space variable x and time variable t , both. For example, if $\Phi(x, t)$ satisfies the diffusion equation $\frac{\partial\Phi(x, t)}{\partial t} = \nabla^2\Phi(x, t)$ where initial condition $\Phi(x, t)$ is a Gaussian random variable, the persistence exponent θ is non-trivial and has been numerically calculated to be $\theta \approx 0.1207, 0.1875, 0.2380$ in one, two and three dimensions respectively [13].

1.1.3 Diffusion Controlled reaction.

There are a variety of problems in chemical physics and biophysics where one is interested in the average time required for a biochemical particle (equivalently rate of reaction), diffusing under an influence of a potential, to reach a target. For example, the rates of biochemical reactions involving two molecular partners are determined by the diffusive process which lead to the necessary encounter of the reactants. Another problem that has been studied is the diffusion controlled inter-chain reaction of a polymer with two reactive groups attached at two ends [16, 17]. The reaction occurs with a certain rate whenever two ends of the polymer chain are sufficiently close, and one likes to know the average time needed for two ends to collide for the first time. So in a diffusion controlled reaction, reaction rates of two molecules are related to the passage of a molecule into the reactive range of other molecule.

The average reaction time τ can be calculated from the survival probability $S(t)$ at least upto time t , i.e., $\tau = \int_0^\infty S(t)dt$ [3, 18]. The motion of the particle diffusing in a potential $U(x)$ is governed by a Fokker-Planck equation $\frac{\partial p(x,t)}{\partial t} = j(x,t)$ where $p(x,t)dx$ is the probability of finding the particle between x and $x + dx$ at time t and $j(x,t) = D(x)[\frac{\partial p}{\partial x} + \beta \frac{\partial U(x)}{\partial x}]$ is the flux at position x at time t . Here $D(x)$ is the space dependent diffusion constant. The boundary condition one may impose $j(r = a, t) = \kappa p(r = a, t)$ ("radiation" boundary condition) or Smoluchowski boundary condition $p(r = a, t) = 0$. One prevents particle to go out of the system, and imposes reflecting boundary condition at $x = R$, $j(x = R, t) = 0$. In the case of radiation boundary condition particle can reach $x = a$ many times before getting absorbed, but in the second case of Smoluchowski boundary condition, particle gets absorbed once it is reached (hence corresponds to first passage time).

1.1.4 Neuron dynamics.

A neuron is a fundamental unit of a nervous system. A neuron generates a series of voltage spikes, i.e., intermittent bursts. The train of voltage spikes are detected to post synaptic neuron so that brain generates a particular sensory information from the input. The distribution of time interval between these voltage spikes has long been studied in the literature [19, 20]. Still we do not understand exactly how a stimulus (such as odour, image or sound) is represented within the nervous systems as a distributed set of voltage spikes. However, no doubt, a major component of sensory information is

transmitted to brain uses a code which is based on the time interval of neuron firing, i.e., inter voltage-spike time duration [21, 22]. Considerable effort has been made to understand the inter spike interval (ISI) distribution as this provides basic information about underlying neurophysical processes. The mechanism behind these voltage spikes is that the polarization level in a neuron changes by a small amount due to excitatory and inhibitory voltage inputs [3]. When the polarization level in the neuron first exceed a specific threshold value, the neuron emits a voltage spike and again returns to the reference level. So the time interval between these voltage spikes is the first passage time for the polarization to reach a certain value.

There is a simple model for the neuron dynamics which is called the integrate-and-fire model [23]. Although the model does not incorporate many complexities of real neuron behaviour, it does provide a starting point for understanding basic features of ISI distribution. In the model excitatory and inhibitory inputs occur at rate α_E and α_I respectively. These inputs causes the polarization increase or decrease by, say, a_E and a_I . In the continuum limit the evolution of the polarization is approximated by a diffusion equation with a bias velocity $v = \alpha_E a_E - \alpha_I a_I$ and a diffusion constant $D = \sqrt{\alpha_E a_E^2 + \alpha_I a_I^2}$. The neuron will fire if polarization reaches the threshold value x_0 . Clearly the ISI distribution is nothing but the first passage time distribution of a biased diffusing particle which starts from position x_0 and gets absorbed at the origin. So the ISI distribution is given by the simple formula $\frac{x_0}{\sqrt{4\pi Dt^3}} e^{-(x_0-vt)^2/4Dt}$. To get more physical features, various other stochastic process, e.g., Ornstein-Uhlenbeck process [20], or a periodically varying threshold [24], etc have been used instead of the simple biased diffusion of integrate-and-fire model.

Now we will discuss how the time dependent properties have been formulated in terms of residence time distribution of grains in sandpile models of self-organized criticality. We shall briefly discuss about the self-organized criticality in the next section.

1.2 Self-organized criticality (SOC).

We start with a short recapitulation of the basic ideas of SOC. The concept of SOC was proposed by Bak, Tang and Wiesenfeld (BTW) [25] to explain abundant fractal structures in nature like self similar mountain ranges, river network, power law distributed burst like activity in earthquake phenomena and rainfall, ubiquitous $1/f^\alpha$ flicker noise etc.

For example in the case of mountain ranges, the irregular height profile can be characterized by mean square height difference Δh between two points separated by a distance r which varies as, $\langle(\Delta h)^2\rangle \sim r^\alpha$. The average is taken over spatial points separated by distance r . The exponent α does not seem to depend on a particular mountain.

River networks are formed in a time scale of hundred of thousands of years and have a fractal spatial structure. If drainage area of a stream has an area A as we go down a distance l along the stream in the network, the area has simple power law relation with the distance l as $A \sim l^y$. This law is known as Hack's law [26].

Phenomena of earthquakes is due to the slow but steady motion of tectonic plates (a few centimeter per year) which makes earth's crust. Due to the convection current in magma (the molten region inside the earth crust), these plates move and consequently stress develops along the fault line of two plates. When the stress is greater than frictional force between two plates, energy due to the stress developed between plates is released and there is an earthquake [27]. It has been known empirically that the amount of energy E released in an earthquake event is power law distributed and this is known as Gutenberg-Richter law [28]. Here power law distribution means that there is no characteristic scale in the underlying physical phenomena.

Rainfall related quantities have been studied since a long time [29], and recently, high resolution data have been recorded [30] and rain rate was measured. If one defines an event of rainfall as a sequence of successive nonzero rain rate, the event size M is defined to be $M = \sum_t q(t)\Delta t$ where $\Delta t = 1$ minute, $q(t)$ is the rate of rainfall [31], i.e., an event size is just the total amount of water released in a container in a particular event of rainfall. The probability $Prob(M \geq y)$ that the total amount of rainfall M in a rainfall event is greater than y is a power law, i.e., $Prob(M \geq y) \sim y^{-0.36}$ [31]. So rainfall events also do not have any characteristic scale.

Flicker noise is characterized by long-ranged temporal correlation and the power spectrum $S(f)$ of the noise signal varies with frequency f as $1/f^\alpha$ for low frequency where $0 < \alpha < 2$. The flicker noise has been observed in various seemingly disconnected context such as in the light from quasars, intensity of sunspot, voltage fluctuation in a current carrying resistor, sand flow in hour glass etc [25]. Although occurrence of the flicker noise is ubiquitous in nature, there is no unifying mechanism for it.

Bak, Tang and Wiesenfeld introduced a simple model, called the BTW sandpile

model (also known as the Abelian sandpile model), which illustrates the mechanism of SOC [25]. Sandpile models are threshold activated systems (there is local relaxation only if a variable crosses some threshold value) which, when driven slowly, organize themselves to a critical non-equilibrium stationary state without any fine tuning of parameters. The long-ranged correlation shows up as fractal structures in space. The long-ranged correlation in time gives rise to $1/f^\alpha$ power spectrum of noise with $\alpha < 2$. One of the main motivation of BTW in introducing the concept of SOC was to explain the $1/f^\alpha$ flicker noise. BTW argued that emergence of the self-organized critical state gives a connection between the $1/f^\alpha$ power spectrum and the fractal spatial structure of the critical system. Study of time dependent properties of various sandpile models have gone into two different directions, one is the study of power spectrum of avalanche activity in sandpile models and other is study of the residence time distribution of grains in sandpile models. In subsequent sections we shall first discuss about various SOC models and then the temporal properties of these models [32, 33, 34].

1.2.1 Models of self-organized criticality and universality classes.

Sandpile models are defined on a lattice and configurations are specified by a height variable which gives the number of grains at each site. There is a threshold condition for toppling at a site and some specified number of grains are transferred to the neighbouring sites after each toppling. Depending on the threshold condition, there are two broad classes in sandpile models, critical height type models and critical slope type models. We call all the slope type models as ricepile models hereafter. The piles are slowly driven, *i.e.* the time interval between addition of two grains is chosen long enough so that all avalanche activity has died before a new grain is added and this time interval is measured to be one unit of time in our analysis. Grains can leave the pile when there is toppling at the boundary sites. Once a grain is out of the pile, it cannot again come back inside the pile.

Historically, perhaps because of their relation to the earthquake phenomena, studies of sandpile have generally focused on distribution of avalanche sizes which may be measured by total number of toppling events after addition of a grain. In the critical steady state the avalanche size distribution has a power law scaling form $s^{-\gamma_s} f(s/L^{D_s})$ where s is the size of a particular avalanche and γ_s, D_s are two positive exponents. The cutoff scale L^{D_s} is due to the finite size of the system and the power law distribution

extends upto infinity in the limit of infinite system size. The long-ranged spatial correlation in the critical state is characterized by this power law with the exponent γ_s . Other quantities of interest are diameter and area of the region affected by the avalanche activity. These also have power law distribution with another set of exponents in the steady state. The long-ranged temporal correlation is measured by distribution of lifetime of an avalanche activity τ which is also a power law and has a finite size scaling form $\tau^{-\gamma_\tau} f(\tau/L^{D_\tau})$. So we see that in the critical state various quantities are power law distributed and therefore there is no characteristic scale in the system. Below we describe various sandpile models and discuss various universality classes in sandpile models.

Height type sandpile models.

In height height type sandpile models, toppling condition at each site depends on the height, i.e., number of grains, at that site. If height crosses a threshold value, a fixed number of grains are distributed to the neighbouring sites.

The BTW model: The BTW model is defined in a finite d -dimensional lattice and there is a variable called height variable $h(\vec{x})$, at a lattice point \vec{x} . The height $h(\vec{x})$ is number of sand grains at site \vec{x} . The time evolution is very simple, when $h(\vec{x}) \geq 2d$ the site becomes unstable and there is a toppling event, i.e., all $2d$ grains are thrown out of the site and each of the $2d$ neighbouring site gets one grain. The boundary is open, and grains are lost when there is a toppling at the boundary sites. Once toppling starts at a site after addition of a grain, topplings go on till all the sites are stable. Given more than one unstable sites, it does not matter which way one topples the unstable sites. The final stable configuration is independent of the order of toppling the unstable sites (this is called the Abelian property of the BTW sandpile) [35]. The BTW model has been studied extensively both numerically and analytically. Values of the standard avalanche exponents in two dimensions are as follows: $\gamma_s \approx 1.22$ and $\gamma_\tau \approx 1.32$ [36]. For the recent result see the review [32, 33, 34].

Models with stochastic toppling rules: Manna defined a model with stochastic toppling rules [37]. There are variations of the Manna model, but now onwards we shall call all models with similar rules as Manna models. For example, one of such stochastic models is Manna four state model which is defined in a finite d -dimensional

lattice. The height $h(\vec{x})$ is number of sand grains at site \vec{x} . The time evolution in Manna model is not deterministic as in the BTW model. The toppling rules are as follows: whenever $h(\vec{x}) \geq 2d$, the site becomes unstable and each of the $2d$ grains are transferred randomly to any of the neighbour, independent of each other. This model also has an Abelian property, i.e., the final stable configuration reached from a given unstable configuration is independent of the order of toppling the unstable sites [34]. Grains are added randomly everywhere and grains are lost at the boundary. Values of the standard avalanche exponents in two dimensions are as follows: $\gamma_s \approx 1.28$ and $\gamma_\tau \approx 1.47$ [38]. However the original stochastic model defined by Manna [37] does not have the Abelian property and there is hard core interaction between grains, i.e., there can be only one grain at each site. But the exponents are same as in the case four state model. For recent results see [34].

Zhang model: In this model, there is a continuous real variable $E(\vec{x})$ defined at each site \vec{x} of a d -dimensional lattice and the energy $E(\vec{x})$ can take values upto a threshold E_c . The threshold value E_c is chosen to be 1 [39]. The system is driven by increasing energy at a randomly chosen site \vec{x} by an amount δ . If the energy at a site $E(\vec{x}) \geq 1$, the site becomes unstable. Then it relaxes by transferring the full amount of energy equally to each of its $2d$ nearest neighbours and resetting its own energy to zero. Energy can be lost through the open boundary. This model is not Abelian, unstable sites are updated in parallel. Although energy at any site can take continuous values upto 1, interestingly energy distribution at a site has $2d$ distinct peaks in d -dimensions. For example in two dimensions, the distribution is peaked around four values $E \approx 0.02, 0.34, 0.66$ and 0.98 . Using local energy conservation and the isotropy in energy transfer rule, the distribution of a few quantities have been predicted [39]. For example, the probability distribution of area a of an avalanche cluster has been argued to have a power law distribution $a^{-\gamma_a}$ with $\gamma_a = 2 - 2/d$ in any arbitrary dimension d . The lifetime τ of an avalanche activity is related to linear size of the avalanche cluster r as $\tau \sim r^{\gamma_{\tau r}}$ where $\gamma_{\tau r} = (d + 2)/3$ for $d \leq 4$. Although the exponents match with the values from numerical simulations within the error bar, it is not clear why the arguments given by Zhang do not also work for other isotropic models like the BTW or the Manna models.

The Directed BTW model: The directed version of the BTW model can be defined on a d -dimensional lattice [40]. For simplicity we consider two dimensional case.

Generalization to higher dimensions is straightforward. The two dimensional square lattice is oriented in $(1, 1)$ direction so that edge of the system is at angle of 45° to any bond of the lattice. One can assume periodic boundary in one direction (cylindrical shape). Grains are added randomly at any site on the top edge and grain can leave the pile at the bottom. If $h(\vec{x}) > 1$, there is toppling and two grain are transferred, one grain to each of the two downward nearest neighbours. This model is also Abelian like its isotropic version. This model has been solved exactly by Dhar and Ramaswamy [40]. The distribution of avalanche size s has power law form $s^{-\gamma_s}$ with $\gamma_s = 4/3$. The distribution of lifetime τ is also power law $\tau^{-\gamma_\tau}$ where $\gamma_\tau = 3/2$. The values of γ_s and γ_τ for $d > 3$ are $3/2$ and 2 respectively. The relation between avalanche size s and lifetime τ is given as $s \sim t^{3/2}$ in $d = 2$ and as $s \sim t^2$ in $d \geq 3$ [40]. For $d = 3$, there are logarithmic corrections to the power laws in the distributions of s and τ . For example distribution of lifetime τ varies as $(\ln \tau)/\tau^2$ in $d = 3$ [40].

Slope type sandpile models.

In slope type sandpile models, toppling condition at each site depends on the slope value which is suitably defined from the height variable. If slope crosses a threshold value, a fixed number of grains are distributed to the neighbouring sites.

KNLZ models: Kadanoff *et. al.* have studied several slope type models both in one and two dimensions to investigate different scaling properties and the question of universality classes in SOC [41]. They have particularly studied distribution of two quantities, i.e., number of grains that drop off the edge in one avalanche and avalanche size. These $1D$ models have nontrivial scaling structure unlike the one dimensional BTW model. They do not appear to have a simple finite size scaling form, and a multi-fractal analysis is much better in collapsing data for various system sizes. However in the case of $2D$ models, simple finite size scaling works quite well.

In finite size analysis one assumes that in the regime $X, L \gg 1$ the distribution function $P(X, L)$ has a scaling form $L^{-\beta}g(X/L^\alpha)$ where X is either drop number or avalanche size and α, β are two positive exponents. But more generally the exponent β is different in different length scales, i.e., if X is of order L^α , then $P(X, L)$ is of order L^β . So β is a function of α , i.e., $\beta = f(\alpha)$. Now in this case $P(X, L)$ has a general form $P(X, L) \sim \int d\alpha \mu(\alpha) L^{-f(\alpha)} g(x/L^\alpha)$ where $\mu(\alpha)$ is some function of α . Therefore when the simple scaling assumption does not work, one uses a multi-fractal form as

$\ln[P(X, L)]/\ln(L/L_0) = f[\ln(X/X_0)/\ln(L/L_0)]$ where X_0 and L_0 are two suitable constants such that one gets a good fit. The quantity $\ln(X/X_0)/\ln(L/L_0)$ is called α and the fit is called $f - \alpha$ representation [41]. When $g(x)$ is a simple power law, $df/d\alpha$ equals the usual scaling exponent γ_x previously discussed for various critical models. Universality is determined by the scaling exponents α and β in the case of simple power law scaling, other wise they are determined by the functional form of $f(\alpha)$ [41].

Oslo ricepile model: The Oslo ricepile model is a stochastic model defined by Frette *et. al.* [42, 43]. The precise details of the toppling rules will be given later in section 4.1.1.

The question of universality classes in SOC models is well debated in the literature. It was first discussed by Kadanoff *et. al.* [41]. They concluded, depending on of various toppling criteria (height type or slope type) and other symmetry properties (such as isotropy or directedness), there exists several universality classes. They have shown that several one dimensional slope type models have nontrivial multi-scaling structure, unlike the trivial one dimensional BTW model, and on the basis of the multi-scaling form of the distribution function (i.e., $f - \alpha$ representation), there are several universality classes exist also in one dimension. Later on many authors [45, 46] have discussed about universality classes in height type isotropic models. Even though BTW, Manna and Zhang models have different toppling rules, all these three models were supposed to be in the same universality class. Pietronero *et. al.* developed a RG scheme [47] and argued that BTW and Manna models are in the same universality class. Biham *et. al.* have shown from extensive numerical simulation that BTW, Manna and Zhang models have different exponents of various power law distributions and hence belong to three different universality classes [45].

1.2.2 Self-organized criticality and $1/f^\alpha$ noise.

The issue whether avalanche activity in sandpile models shows $1/f^\alpha$ noise has attracted a lot of attention since BTW proposed the model. In this subsection, we will review the recent literature which explores whether sandpile models show $1/f^\alpha$ noise or not. Here one should note that the avalanche activity have different behaviour for two different time scales, the time scale of a toppling event, i.e., correlation among activity within a single avalanche and for the time scales of slow driving, i.e., correlations among

separate avalanches. We discuss about these two cases separately below.

In the time scale of an toppling, it has long been debated whether avalanche activity in the BTW model shows $1/f^\alpha$ power spectrum. Initial simulations pointed that there is long-ranged temporal correlation in the avalanche activity, but the power spectrum has $1/f^2$ behaviour at low frequency [48, 49], not $1/f^\alpha$ with non-trivial $\alpha < 2$. Recently, Laurson *et. al* have done a more detailed numerical analysis and shown that the power spectrum is indeed $1/f^\alpha$ with a nontrivial exponent $\alpha < 2$ [51].

The basis of their analysis is as follows. Let us represent time series of the noise signal for a avalanche of size s by $y(t|s)$. So the power spectrum $S(f|s)$ is $|\tilde{y}(f|s)|^2$ where $\tilde{y}(f|s)$ is the Fourier transform of the signal, i.e., $\tilde{y}(f|s) = \int y(t|s)e^{ift} dt$. Clearly $\tilde{y}(f = 0|s) \sim s$ which is the avalanche size s . The power spectrum $S(f|s)$ has a scaling form $S(f|s) = s^2 g(f^{\gamma_{st}} s)$ where γ_{st} is an exponent. The exponent γ_{st} relates a particular avalanche size s to its life time τ as $s \sim \tau^{\gamma_{st}}$. The scaling function $g(x)$ varies as $1/x$ for large x [50, 51]. Now the form of power spectrum $S(f)$ of the actual signal $y(t)$, which is random superposition of signal $y(t|s)$, can be obtained after averaging over various avalanche sizes s . So the total power spectrum is given by $S(f) = \int P(s)S(f|s)ds$ where $P(s)$ is the probability distribution of s . Now putting $P(s) \sim s^{-\gamma_s}$, we get $S(f)$ to be $f^{-\gamma_{st}(3-\tau)} \int^{s^* f^{\gamma_{st}}} x^{2-\gamma_s} g(x)dx$ where s^* is upper cut-off of avalanche size. Since $g(x) \sim 1/x$, the integral varies as $1/f^{\gamma_{st}}$ and hence $\alpha = \gamma_{st}$. Kertesz *et. al.* [48] and Jensen *et. al.* [49] have taken wrong form of $g(x) \sim 1/x^2$ and got $S(f) = 1/f^2$.

Laurson *et. al.* have found the exponent in the power spectrum to be $\alpha \approx 1.59$ for the two dimensional BTW model and $\alpha \approx 1.77$ for the two dimensional Manna two state model. The exponent α is expected to be 2 in dimensions greater than 3 [51].

In the second case, there is no long-ranged correlation found from the simulation in the avalanche activity in the time scale of addition of grain in BTW or Manna model [51]. However for some specific one dimensional models, $1/f^\alpha$ power spectra were found in the mass fluctuation of the pile. None of these two models have simple power law scaling form of the probability distribution $P(s)$ of avalanche size s , i.e., $P(s) = s^{-\gamma_s} f(s/L^{D_s})$, however the avalanche size distributions are broad and have diverging first moment in the limit of large system sizes. For example, the BTW models were studied for quasi one dimensional geometries (on a ladder, etc.) by some authors [52, 53]. They analytically found that the power spectrum of total mass fluctuation of

the pile has the $1/f^\alpha$ form with $\alpha = 1$.

Davidson *et. al.* [54] have studied another one dimensional model called stick-slip model introduced by de Souza Viera [55] which evolves towards a critical steady state upon slow driving. They have considered a one dimensional system of finite size where a continuous variable f_i at site i . The variable f_i represents force at the respective site. If $f_i \geq f_c$, relaxation occurs with conservative redistribution of force from this site to its nearest neighbours. The time signal they have considered the total force in the system, i.e., $y(t) = \sum_i f_i(t)$. They found from the numerical simulation that this signal has non-trivial long-range correlation $1/f^\alpha$ with $\alpha \approx 1.38$. Power spectrum $S(f)$ has a scaling form $S(f) = f^{-\alpha} g(fL^\beta)$. L^β is the cutoff time scale beyond which the signal gets completely decorrelated. And this decorrelation occurs after all sites have relaxed at least once and this probability is of the order $L^{-D_s(\gamma_s-1)}$ where the probability distribution of avalanches has a scaling form $s^{-\gamma_s} f(s/L^{D_s})$. So we get the exponent $\beta = D_s(\gamma_s - 1)$. The first moment relation, $\langle s \rangle \sim L$ [55], implies $D_s(2 - \gamma_s) = 1$ and using it we obtain $\beta = (\gamma_s - 1)/(2 - \gamma_s)$. This model is conjectured to be in the universality class of interface depinning with interface pulled at one end [56]. The standard deviation $\sigma^2 = \langle (y - \bar{y})^2 \rangle$ (i.e., $\sigma^2 = \int S(f) df$) has been shown to have the scaling of $L^{2(D_s-2)}$. Now σ^2 has a scaling $\sigma^2 \sim L^{\beta(\alpha-1)}$ which can be obtained from the scaling form of the $S(f)$. Comparing these two scaling relation, one gets $\beta(\alpha - 1) = 2(D_s - 2)$. One gets value of $\alpha = (3D_s - 5)/(D_s - 1) = (5\gamma_s - 7)/(\gamma_s - 1)$. So the critical avalanche dynamics and long-ranged temporal correlations between avalanches are strongly related and produce $1/f^\alpha$ noise and the exponent α , which is equal to $(5\gamma_s - 7)/(\gamma_s - 1)$, can be expressed in terms of standard (static) exponent γ_s for single avalanche size distribution.

Recently Baies *et. al.* have studied one of the sandpile models, local limited model defined by Kadanaoff *et. al.*, where position of the site, at which a grain is added, changes according to a random walk, i.e., the site $i(t)$ where grain is added at time t is chosen randomly between two neighbours of the site where grain has been added at the previous step $i(t - 1)$. The spatial correlation in grain addition is translated into intermittent avalanche activity where the power spectrum of avalanche size time series has $1/f$ power law spectrum and power law distribution of waiting times between two successive avalanche activity. Previously Sanchez *et. al.* [57] have studied running sandpile [58] with correlation in external driving. They also found broad power law distribution of waiting times between two successive avalanche activity. However,

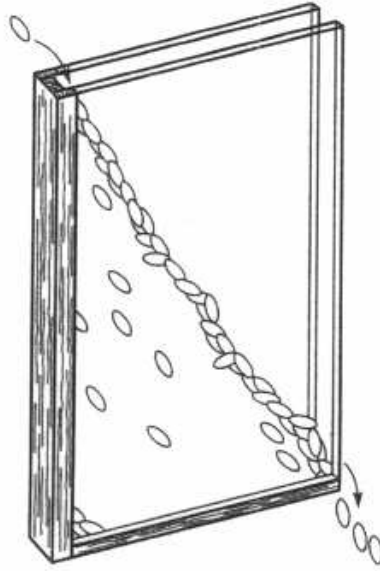


Fig 1.1: A sketch of the experimental setup of the Oslo experiment taken from the book titled “Self Organized Criticality” by H. J. Jensen (Cambridge Univ. Press, Cambridge, 1998).

without the correlation in external driving, they found the waiting time distribution is a simple exponential.

1.2.3 Self-organized criticality in granular pile and the distribution of residence times of grains in the pile.

Although SOC was not seen in experiments on piles of sand [59], piles of long-grain rice have shown evidence of power law distributed avalanches and provided a good experimental realization of a simple system showing SOC. In the Oslo rice pile experiment [60], Frette *et. al.* studied the transport properties of rice grain by slowly adding rice grains at one end of a pile between two closely spaced parallel rectangular glass plates (100 cm \times 120 cm) where grains can leave only at the other end. See Fig. 1.1 and Fig. 1.2. The separation between the two plates was such that almost three layers of rice grain are possible. Coloured tracer grains were added (20 grains/min) when the pile reached the stationary state and the residence times of grains were measured. They

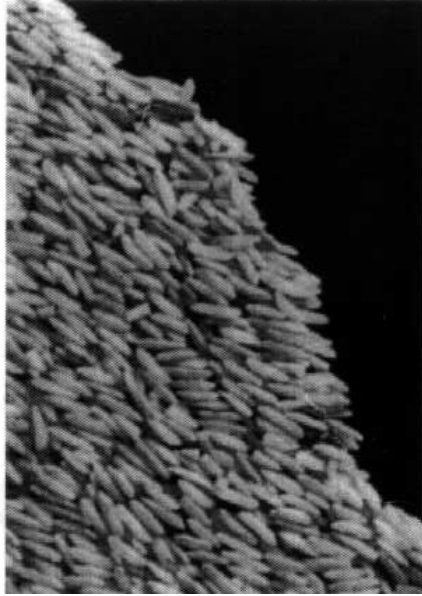


Fig 1.2: Snapshot of ricepile in the Oslo ricepile experiment by Christensen *et. al.* (Phys. Rev. Lett., **77**, 107, 1996).

studied distribution of residence times. The probability distribution function $P_L(T)$ of the residence time T was determined for various system sizes L and the fitting the data to a scaling form $P_L(T) = L^{-\nu}F(T/L^\nu)$ was done with $\nu = 1.5 \pm 0.2$. They obtained that the scaling function $F(x)$ has the following form: $F(x)$ is constant for $x < 1$ and $F(x) \sim x^{-\alpha}$ where α was found to be 2.4 ± 0.2 by fitting the data to a power law. The average total residence time of grains in a pile of size L was estimated to be $\langle T \rangle \sim L^\nu$ from the scaling form of the probability distribution function.

There have also been some numerical and analytical studies of these distributions later on. Frette proposed a theoretical model, called the Oslo rice pile model [61], which seems to reproduce the phenomenology of the rice pile experiment well. From numerical simulations of the Oslo model [62], the exponent characterizing the power law decay of the probability density of total residence times at large times was estimated as $\alpha = 2.2 \pm 0.1$ and exponent ν was estimated to be 1.3 ± 0.1 . However we show in this thesis that the mean residence time varies as L^2 and argue that the form of the scaling function $F(x)$ is actually $1/[x^2(\ln x)^\delta]$ for large x where δ is a positive exponent.

Boguna *et. al.* [63] argued that the dynamics of the Oslo model and the Oslo ricepile experiment can be explained in terms continuous time random walk (CTRW) with Levy flight and long tailed trapping time for the grain. The trapping time distribution was

taken to be $\psi(t) \sim 1/t^{2+\beta}$ where $\psi(t)dt$ is the probability of a grain being trapped at some site for time t to $t + dt$ and the exponent $0 < \beta \leq 1$. The jump length distribution $\phi(l)$ varies as $\phi(l) \sim 1/l^{2+\gamma}$ with $0 < \gamma \leq 1$ where $\phi(l)dl$ is the probability of jump length of l to $l + dl$ during an avalanche. For these distributions, mean waiting time and mean jump length both are finite, but second moment of both the quantities are infinite. The long time behaviour of the residence time distribution $P_L(T)$ has a long tail $P_L(T) \sim 1/T^{2+\beta}$ independent of jump length distribution and it implies that $2 + \beta = \alpha$ where the exponent α has been defined in the previous paragraphs. Small time behaviour of the distribution is $P_L(T) \sim 1/L^{1+\gamma}$ which independent of the residence time T . Assuming a scaling form of $P_L(T) = L^{-\nu}F(T/L^\nu)$, it was shown that $\beta = \gamma$ and $1 + \gamma = \nu$.

A similar analysis has been done by Carreras *et. al.* in the context of plasma transport where some of the phenomena observed in plasma, confined in a magnetic field, have long-ranged space and time correlations. Various data analysis of electromagnetic fluctuation have suggested that the dynamics is governed by SOC mechanism [64] and the transport of charged particles in the plasma is governed by avalanche like activity. They have explained the transport of particles in plasma using a cellular automata based on a simple sandpile model, called running sandpile [41, 58]. The authors have studied the underlying transport properties of grains in the pile by following the motion of a tracer grain in running sandpile [65] where transport is super-diffusive. They were interested in the ensemble average of various moments of displacement of the tracer grain $\langle [|x(t) - x(0)|]^n \rangle$ where $x(t)$ is the position of the tracer grain at time t . They analyzed the behaviour of moments $\langle [x(t) - x(0)]^n \rangle \sim t^{n\nu(n)}$ for $0 < n < 1$ and found that the exponent $\nu(n) \approx 0.74$ for fractional n [65]. They have modeled the motion of grains using the following fractional Fokker-Planck equation $(A|q|^\gamma - Bu^\beta)P(q, u) = Bu^{\beta-1}$ ($0 < \gamma, \beta \leq 1$) where $P(x, t)dx$ is the probability of finding the particle between x and $x + dx$ at time t and $P(q, u) = 1/2\pi \int_0^\infty \int_{-\infty}^\infty dt dx P(x, t) e^{-iqx} e^{-ut}$, i.e., Laplace-Fourier Transform of $P(x, t)$. The exponents γ and β are related to the exponents of the power law jump length distribution $\phi(l)$ and trapping time distribution $\psi(t)$ as $\phi(l) \sim 1/l^{1+\gamma}$ and $\psi(t) \sim 1/t^{1+\beta}$. The behaviour of moments is $\langle |x(t) - x(0)|^n \rangle \sim t^{n\beta/\gamma}$ for large t and therefore the exponent ν defined earlier is equal to β/γ . The values of γ and β were found directly from the simulation and, putting these in, one finds $\nu \approx 0.68$ which agree within error bar with the value of ν found from the direct simulation.

1.3 Plan of the thesis.

The thesis is organized as follows. In chapter 2, we calculate the first passage time distribution in simple, unbiased random walks in presence of absorbing boundaries of various shapes. We have solved diffusion equation with absorbing boundary condition and obtained explicit solutions for the following geometries of the boundaries - a box in 1 dimension, circular, square and triangular boundaries in 2 dimensions and cubical box and sphere in 3 dimensions. The distribution in all cases shows scaling and the scaling function have been expressed in terms of the Jacobi Theta functions.

In chapter 3, we have studied the distribution of residence times (DRT) of grains in height type sandpile models. First we describe general formalism for calculating the residence time distribution of grains in sandpile models in terms of transition matrices. We illustrate this by numerically calculating the DRT in the one dimensional BTW model driven by adding grains at one end. Then we discuss analytically the small time behaviour of the distribution for the 1D BTW model driven at an end and also derive the continuum equation describing motion of the grains in the hydrodynamic limit for the same model. We generalize our theoretical argument to higher dimensions and other isotropic height type models. We have argued that the motion of a grain is diffusive at time-scales much larger than the interval between successive grain addition and the jump-rates of grains at various sites are space-dependent due to the space dependence of avalanche activity at different sites. We have shown that the DRT, for large residence times and large system sizes, can be expressed in terms of the survival probability of a diffusing particle in medium with absorbing boundaries and space dependent jump rates. We have exactly solved the DRT in some special cases. The DRT is of the form $L^{-d}f(t/L^d)$ in d -dimensional pile for system size L and $f(x)$ has been shown to decay exponentially for large x . In our analysis, the small time behaviour of the DRT has not been taken care of well due to boundary avalanches. We study the finite size corrections in the DRT and for the one dimensional BTW model driven at an end we exactly calculate the leading order correction due to the finite system size L , i.e., correction of order $\mathcal{O}(1/L)$.

In chapter 4, we have studied the DRT at a site and in the pile for slope type sandpile models. We have defined various slope type models for which we have done Monte Carlo simulation to check our theoretical arguments. First we discuss relation between the residence times at a site and the height fluctuation of the pile. The DRT in slope type

models are qualitatively different than the DRT in height type sandpiles. For slope type models, there is a significant weight at tail of the DRT due to the deeply buried grains in the pile. These grains take a long times to come out, the cutoff time scale in the DRT is diverging exponentially with increasing system sizes. We show that this determines the exponent of the power law tail in the DRT. To calculate the probability of occurrence of minimum height of the pile, we have considered the one dimensional Oslo ricepile model. This model is more tractable analytically because some simplifications occur due to its Abelian property. We exactly calculated the probability of minimum slope configuration of the Oslo pile for smaller system sizes both analytically and numerically. In the limit of system size L being large, we have argued that for stochastic ricepile models in d dimensions the probability of the minimum slope configuration varies as $\exp(-\kappa L^{d+2})$. We verify this prediction numerically. The probability of the minimum slope for large L is so small that one cannot calculate it using a simple Monte Carlo simulation. The probability of large deviations in height fluctuation of the pile was studied by Monte Carlo simulation using importance sampling to sample the rare events with probabilities, say, of order $\mathcal{O}(10^{-100})$. Then we study the DRT in the pile which is just sum of residence times at various sites. We have shown that the DRT, both at a site and in the pile, have same $1/t^2$ power law behaviour. We also point out that the a $1/t^2$ power law tail of the DRT' have a logarithmic correction factor which is different for the residence time at a site and the total residence times in the pile.

In chapter 5, we summarize our results with some concluding remarks.

First passage time distribution in random walks.

In this chapter we calculate the first passage time distribution for a random walker in the presence of absorbing boundaries of various geometries. This is a well studied problem [2, 3, 66] with considerable physical interest. For example there is classic Polya's problem, i.e., distribution of first passage time to origin for a simple random walker in an infinite domain [2]. The first passage time distribution of a random walker in one dimension with two absorbing barriers at two ends can be calculated using repeated reflection principle [2, 3, 66]. The distribution of time between successive voltage spikes in the modeling of neuron dynamics [3] or the distribution of avalanche sizes in the modeling of sandpiles (Linear Avalanche Model) [67] can be mapped on to a first passage time distribution problem. In the later chapters we shall see that the residence time distribution of grains in the height type sandpile models can be reduced to a problem of diffusing particle in a medium where jump rates are space dependent and in some special cases motion of the grains are described by the simple diffusion equation with absorbing boundary conditions.

The problem we consider is of a random walker performing a simple, unbiased random walk (equal probability of going in all directions) with absorbing boundaries of various geometries in 1, 2 and 3 dimensions. We calculate $P^*(t|L)$, the first passage time distribution, where $P^*(t|L)dt$ is the probability of the walker being absorbed at the boundary of size L between a time interval, from time t to $t + dt$. This distribution shows a scaling form $P^*(t|L) = \frac{1}{L^a} f(\frac{\beta t}{L^b})$ where β is an arbitrary constant and it is easy to see from the scale transformation of the diffusion equation that the values of both a and b are 2. The scaling function $f(\chi)$ decays exponentially for large χ , we fix the arbitrary constant β by requiring that $\lim_{\chi \rightarrow \infty} f(\chi) \exp(\chi)$ tends to a nonzero finite constant. We have derived the explicit form of the function $f(\chi)$ for various geometries

of the boundaries and expressed it in terms of the Jacobi theta functions.

Though a lot of work has been done in the general area of the first passage time distribution [2, 3, 66, 68, 69], we did not find any earlier published result for the explicit form of the scaling function.

2.1 Random walk on discrete lattice

2.1.1 One dimension

We first studied the discrete random walk case in one dimension, where a walker starting from the origin, at each step, performs a random walk of unit step size with equal probability of going in either direction. Let $P(x, N)$ be the probability of the walker being found at the point x at the N -th step it satisfies the Master equation

$$P(x, N + 1) = \frac{1}{2}P(x - 1, N) + \frac{1}{2}P(x + 1, N) \quad (2.1)$$

where $x = 0, \pm 1, \pm 2, \dots, \pm L$ and $N = 0, 1, 2, \dots, \infty$.

We consider absorbing boundaries at $x = \pm L$, i.e., once the random walker reaches at the site $x = \pm L$, it is absorbed or annihilated and it cannot come back to the site $x = \pm(L - 1)$. Then $P(x, N)$ at $x = \pm(L - 1)$ satisfies the equation

$$\begin{aligned} P(-L + 1, N + 1) &= \frac{1}{2}P(-L + 2, N) \\ P(L - 1, N + 1) &= \frac{1}{2}P(L - 2, N) \end{aligned} \quad (2.2)$$

which implies that the boundary condition is $P(x = \pm L, N) = 0$. Since the walker starts from the centre, the initial condition is $P(x, 0) = \delta_{x,0}$. Expressing $P(x, N)$ in Fourier sine-series, we have

$$P(x, N) = \sum_{n=1}^{2L-1} a_n(N) \sin \frac{n\pi(x + L)}{2L} \quad (2.3)$$

We solve the recursion relation for $a_n(N)$ by substituting Eq. (2.3) into Eq. (2.1) as given below.

$$a_n(N + 1) = a_n(N) \cos\left(\frac{n\pi}{2L}\right) \quad (2.4)$$

We obtain the Fourier co-efficients $a_n(0)$ from the initial condition. Since the initial distribution $P(x, 0)$ is an even function of x , the solution $P(x, N)$ for the symmetric

random walk at any time N in Eq. (2.3) has the sine modes for which n is odd. The final solution is

$$P(x, N) = \sum_{m=1}^L (-1)^{m+1} \frac{1}{L} \cos^N \left(\frac{(2m-1)\pi}{2L} \right) \sin \frac{(2m-1)\pi(x+L)}{2L} \quad (2.5)$$

The survival probability, $S(N|L)$ is given by $\sum_{x=-(L-1)}^{L-1} P(x, N)$ which is the probability of the walker not being absorbed up to the N -th step. So the probability $P^*(N|L)$ of being absorbed at the N -th step is simply $S(N-1|L) - S(N|L)$ and is given by

$$P^*(N|L) = \sum_{m=1}^L (-1)^{m+1} \frac{1}{L} \cos^{N-1} \frac{(2m-1)\pi}{2L} \left[2 \sin^2 \frac{(2m-1)\pi}{4L} \right] \\ \times \sum_{x=-(L-1)}^{L-1} \sin \frac{(2m-1)\pi(x+L)}{2L} \quad (2.6)$$

Doing the sum over x in the above equation we get the final expression for the probability density $P^*(N|L)$ which is given below.

$$P^*(N|L) = \sum_{m=1}^L (-1)^{m+1} \frac{1}{L} \cos^{N-1} \frac{(2m-1)\pi}{2L} \sin \frac{(2m-1)\pi}{4L} \\ \times \left[\cos \frac{(2m-1)\pi}{4L} - \cos \frac{(2m-1)\pi(4L-1)}{4L} \right] \quad (2.7)$$

In the limit $N \rightarrow \infty$ $L \rightarrow \infty$, we get

$$P^*(N|L) = \sum_{m=1}^{\infty} (-1)^{m+1} \frac{(2m-1)\pi}{2L^2} \exp \left[-\frac{(2m-1)^2 \pi^2}{8L^2} N \right] \quad (2.8)$$

The scaling function $f(\chi)$ is defined as

$$\lim_{N, L \rightarrow \infty} \text{Prob}(aL^2 \leq N\beta \leq bL^2) \rightarrow \int_a^b f(\chi) d\chi \quad (\chi = \beta N/L^2) \quad (2.9)$$

where $\text{Prob}(aL^2 \leq N\beta \leq bL^2) \equiv$ the probability of the walker being absorbed between $N = aL^2/\beta$ and $N = bL^2/\beta$. So, for the box in 1-dimension the function $f(\chi)$ is as follows,

$$f_{1\text{box}}(\chi) = -\frac{1}{\pi^2} \frac{\partial \vartheta_3(z, q = e^{-\chi})}{\partial z} \Big|_{z=\pi/4} \quad (2.10)$$

where $\vartheta_3(z, q)$ is the Jacobi theta function [70], defined by

$$\vartheta_3(z, q) = 1 + 2 \sum_{n=1}^{\infty} q^{n^2} \cos 2nz \quad (\text{for } |q| < 1) \quad (2.11)$$

2.1.2 Higher dimensions.

Now we consider a random walker in higher dimensional lattice. The positions of random walker is specified by \vec{x} in the d -dimensional lattice. The probability of being present at site $\vec{x} \equiv \{x_1, x_2, \dots, x_d\}$ at $N + 1$ -th step satisfies following difference equation,

$$P(\vec{x}, N + 1) = \frac{1}{2d} \sum_{\vec{a}} P(\vec{x} + \vec{a}, N) \quad (2.12)$$

where \vec{a} denotes the nearest neighbour lattice sites of \vec{x} . The random walker starts from the centre. Once it escapes through the surface at $x_i = L$, it cannot again come back to the domain surrounded by the absorbing boundaries.

For example we consider a random walker in 2-dimensions, starting at the centre, of an absorbing square boundary. In the discrete case, the equation for the probability of being present at site (x, y) at $N + 1$ -th step is given by

$$P(x, y, N + 1) = \frac{1}{4}P(x - 1, y, N) + \frac{1}{4}P(x + 1, y, N) + \frac{1}{4}P(x, y - 1, N) + \frac{1}{4}P(x, y + 1, N) \quad (2.13)$$

where $x, y = 0, \pm 1, \pm 2, \dots, \pm L$ and $N = 0, 1, 2, \dots, \infty$.

We impose boundary conditions $P(x, \pm L, N) = 0$, $P(\pm L, y, N) = 0$ which implies once particle is out of the boundary it cannot come back inside again. We impose initial condition $P(x, y, 0) = \delta_{x,0}\delta_{y,0}$.

The solution of Eq.(13) is

$$P(x, y, N) = \sum_{m_1, m_2} (-1)^{m_1+m_2} \frac{2}{(2L)^2} \left[\cos \frac{(m'_1 + m'_2)\pi}{4L} \cos \frac{(m'_1 - m'_2)\pi}{4L} \right]^N \times \sin \frac{m'_1\pi(x + L)}{2L} \sin \frac{m'_2\pi(y + L)}{2L} \quad (2.14)$$

where $m'_1 = (2m_1 - 1)$, $m'_2 = (2m_2 - 1)$.

Working as in the 1-dimensional case and taking the large N, L limit we obtain $P^*(N|L)$, the probability of the walker being absorbed at N -th step,
 $= S(N - 1|L) - S(N|L)$

$$= \sum_{m_1=1}^{\infty} \sum_{m_2=1}^{\infty} (-1)^{m_1+m_2} \frac{m_1'^2 + m_2'^2}{m_1' m_2'} \frac{1}{L^2} \exp\left[-\frac{(m_1'^2 + m_2'^2)\pi^2 N}{16L^2}\right] \quad \text{as } N, L \rightarrow \infty \quad (2.15)$$

where $S(N|L)$ is the probability of the walker surviving upto time t . Here $\beta = \frac{\pi^2}{8}$ and the scaling function is given by

$$f_{2box}(\chi) = \frac{1}{2\pi^2} \frac{\partial \vartheta_3(z, q = e^{-\chi/2})}{\partial z} \Big|_{z=\pi/4} \int_{\chi}^{\infty} \frac{\partial \vartheta_3(z, q = e^{-\chi/2})}{\partial z} \Big|_{z=\pi/4} d\chi \quad (2.16)$$

This can be easily generalized to the d -dimensional lattice and in the next section we solve the first passage time distribution problem in the continuum limit inside a d -dimensional box.

2.2 Continuum limit: The diffusion equation.

2.2.1 One dimension

First let us go over to the continuum case in one dimension. Let us denote the lattice spacing by a and the waiting time of the random walker at any lattice point is τ . Now the difference equation, Eq 2.1, can be rewritten as

$$P(x, t + \tau) - P(x, t) = \frac{1}{2} [P(x + a, t) - 2P(x, t) + P(x - a, t)] \quad (2.17)$$

In the continuum limit, $a \rightarrow 0$ and $\tau \rightarrow 0$, using the Taylor expansion we write,

$$P(x, t + \tau) = P(x, t) + \tau \frac{\partial P(x, t)}{\partial t}$$

$$P(x \pm a, t) = P(x, t) \pm a \frac{\partial P(x, t)}{\partial x} + \frac{a^2}{2} \frac{\partial^2 P(x, t)}{\partial x^2}. \quad (2.18)$$

We substitute these in Eq 2.17 and considering only lowest order terms in a and τ we see that $P(x, t)$ satisfies the diffusion equation

$$\frac{1}{D} \frac{\partial P(x, t)}{\partial t} = \frac{\partial^2 P(x, t)}{\partial x^2} \quad (2.19)$$

Where D is the diffusion constant defined by,

$$D = \lim_{a \rightarrow 0, \tau \rightarrow 0} \frac{a^2}{2\tau}$$

It should be noted that the continuum limit is taken in such a way that D is finite.

We solved this equation under the boundary condition $P(\pm L, t) = 0$ and initial condition $P(x, 0) = \delta(x)$. Expressing $P(x, t)$ in the Fourier-sine series and using the initial condition, we get the solution of the Eq.(9) as

$$P(x, t) = \sum_n (-1)^{n+1} \frac{1}{L} \sin \frac{(2n-1)\pi(x+L)}{2L} \exp[-(2n-1)^2 \omega^2 t] , \quad \omega^2 = \frac{\pi^2 D}{4L^2} \quad (2.20)$$

Let $S(L, t)$ be the probability of the walker being absorbed after time t and given by

$$S(L, t) = \int_{-L}^L P(x, t) dx \quad (2.21)$$

We are interested in the probability of the walker being absorbed between time t and $t + \Delta t$ which is $P^*(t|L) = -(\partial S/\partial t) \Delta t$. Therefore,

$$P^*(t|L) = \sum_{n=1}^{\infty} (-1)^{n+1} \frac{D(2n-1)\pi}{L^2} \exp\left[-\frac{(2n-1)^2\pi^2 D}{4L^2} t\right] \quad (2.22)$$

which gives us the same equation as Eq.(5) and the scaling function $f(\chi)$ is also the same function as in Eq.(7). The results for the first passage time distribution in the one dimension can be easily generalized to d dimension as discussed next.

2.2.2 Diffusion in a d -dimension with absorbing boundary.

We obtain the diffusion equation in the d - dimensions, in a similar fashion as in $1D$,

$$\frac{1}{D} \frac{\partial P(\vec{x}, t)}{\partial t} = \vec{\nabla}^2 P(\vec{x}, t) \quad (2.23)$$

where $\vec{x} \equiv (x_1, x_2, \dots, x_d)$, a d -tuple. It is easy to see that all the results obtained previously can be generalized if we consider the problem with an absorbing boundary of a hypercube of volume $(2L)^d$ in d -dimensions with the boundary condition that the P vanishes at the boundary of the hypercube and the initial condition $P(\vec{x}, 0) = \delta^d(\vec{x})$. The eigenfunctions which satisfy the boundary condition are as given below.

$$u_{n_1, n_2, \dots, n_d} = \sin \frac{n_1\pi(x_1 + L)}{2L} \sin \frac{n_2\pi(x_2 + L)}{2L} \times \dots \times \sin \frac{n_d\pi(x_d + L)}{2L}$$

where $n_1, n_2, \dots, n_d = 1, 2, \dots, \infty$. Expanding $P(\vec{x}, t)$ in terms of the eigenfunctions as before and using the initial condition, we can solve Eq. (2.23). The scaling function in this case can be expressed in terms of Jacobi's theta function as

$$f_{dbox}(\chi) = (-1)^d 2 \left(\frac{1}{2\pi}\right)^d \frac{d}{d\chi} (y^d) \quad (2.24)$$

where $y = \int_{\chi}^{\infty} \frac{\partial \vartheta_3(z, q=e^{-\tilde{\chi}/d})}{\partial z} \Big|_{z=\pi/4} d\tilde{\chi}$ and $\beta = \frac{\pi^2 D d}{4}$.

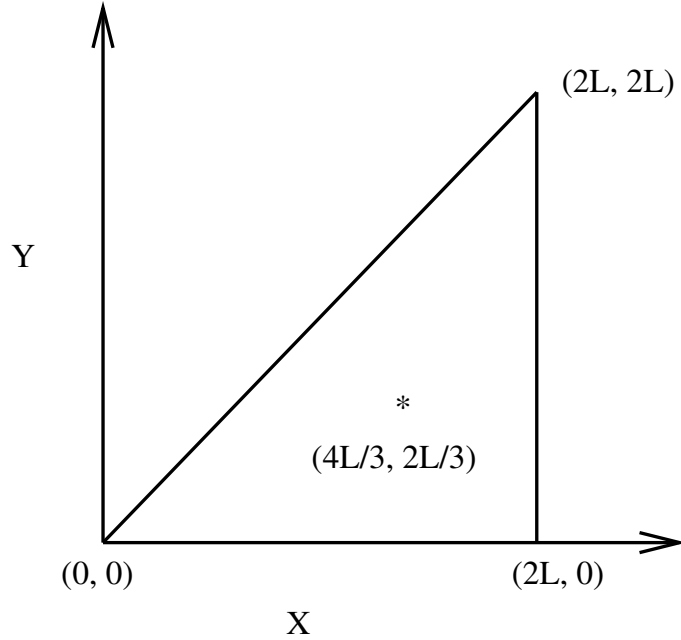


Fig 2.1: A right angled isosceles triangle as the absorbing boundary. The random walker starts at the centre of the triangle [coordinates $(4L/3, 2L/3)$].

2.2.3 Diffusion inside a right angled isosceles triangle.

Let us consider a right angled isosceles triangle as the absorbing boundary as shown in Fig. 2.1. The random walker starts at the centre of the triangle (coordinates $(4L/3, 2L/3)$ in the figure).

Boundary conditions: $p(x = 2L, y, t) = 0, p(x, y = 0, t) = 0, p(x, y, t)|_{x=y} = 0$

Initial condition: $p(x, y, 0) = \delta(x - \frac{4}{3}L)\delta(y - \frac{2}{3}L)$

The eigenfunctions are as follows

$$\psi_{n_1, n_2}(x, y) = \sin \frac{n_1 \pi x}{2L} \sin \frac{n_2 \pi y}{2L} - \sin \frac{n_2 \pi x}{2L} \sin \frac{n_1 \pi y}{2L} \quad (2.25)$$

where $n_1, n_2 = 1, 2, \dots, \infty$ and $n_1 > n_2$. We can again expand the solution in terms of these eigenfunctions and obtain $p(x, y, t)$ to be

$$p(x, y, t) = \sum_{n_1 > n_2} \frac{1}{2L^2} \left[\sin \frac{2n_1 \pi}{3} \sin \frac{n_2 \pi}{3} - \sin \frac{2n_2 \pi}{3} \sin \frac{n_1 \pi}{3} \right] \psi_{n_1, n_2}(x, y) \exp[-\omega^2(n_1^2 + n_2^2)t] \quad (2.26)$$

where $\omega^2 = \frac{\pi^2 D}{4L^2}$. Now defining $S(L, t) = \int_0^L dx \int_{y=0}^{y=x} p(x, y, t) dy$, we get $P^*(t|L)$ which is equal to $-\frac{\partial S}{\partial t}$ as given below.

$$P^*(t|L) = \sum_{n_2=1}^{\infty} \sum_{n_1=1}^{\infty} [(-1)^{n_1+n_2+1} \sin \frac{2n_1\pi}{3} \sin \frac{2n_2\pi}{3} + \sin \frac{2n_2\pi}{3} \sin \frac{2n_1\pi}{3}] \frac{(n_1^2 + n_2^2)D}{4n_1n_2L^2} \exp[-\omega^2(n_1^2 + n_2^2)t] \quad (2.27)$$

and the scaling function is

$$f_{triangle}(\chi) = -\frac{1}{32\pi^2} \frac{d}{d\chi} [\tilde{y}^2 + y^2] \quad (2.28)$$

where $\tilde{y} = \int_{\chi}^{\infty} \frac{\partial \vartheta_4(z, q=e^{-\tilde{\chi}/2})}{\partial z} \Big|_{z=\pi/3} d\tilde{\chi}$ and $y = \int_{\chi}^{\infty} \frac{\partial \vartheta_3(z, q=e^{-\tilde{\chi}/2})}{\partial z} \Big|_{z=\pi/3} d\tilde{\chi}$. Here $\beta = \pi^2 D/2$ and $\chi = \frac{\beta t}{L^2}$, and ϑ_4 is the Jacobi's theta function [70] defined by

$$\vartheta_4(z, q) = 1 + 2 \sum_{n=1}^{\infty} (-1)^n q^{n^2} \cos 2nz \quad (\text{for } |q| < 1) \quad (2.29)$$

2.2.4 Diffusion in a circular disc and sphere.

We can also consider a circular absorbing boundary of radius R with the walker starting at the origin. In this case the first passage time probability can be expressed in terms of Bessel's functions (the eigenfunctions of the problem) as

$$P^*(t|R) = \sum_{n=1}^{\infty} \frac{Dx_n}{J_1(x_n)R^2} \exp[-\omega_n^2 t] \quad (2.30)$$

Where D is the diffusion constant, $J_1(x)$ is the first order Bessel's function, x_n are the zeroes of the zero-th order Bessel's function $J_0(x)$ and $\omega_n = \frac{x_n \sqrt{D}}{R}$. In this case we could not find a known function which can express the scaling function into a simple form.

Lastly, we calculate the probability distribution in the case of an absorbing spherical shell of radius R . We solve the differential equation in spherical-polar co-ordinate system.

Boundary condition: $p(r = R, \theta, \phi, t) = 0$

Initial condition: $p(r, \theta, \phi, t = 0) = \delta(r)$

The eigenfunctions in this case are given by the spherical harmonics and the spherical Bessel's functions as $Y_m^l(\theta, \phi) j_l(\alpha r)$. The symmetry of the problem demands $m = 0$ and

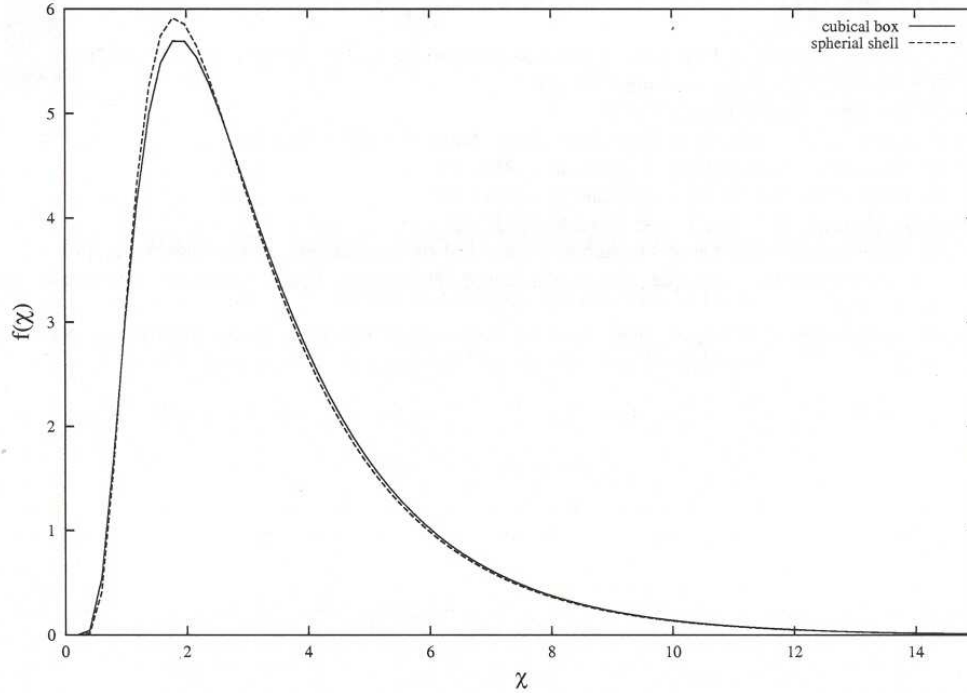


Fig 2.2: The scaling functions $f(\chi)$ of a box and a sphere are plotted against χ . The box and sphere have a ratio of sizes $\frac{2L}{R} = \sqrt{3}$ where L is the linear size of the box and R is the radius of the sphere.

$l = 0$. Thus only $j_0(\alpha r)$ which is $\frac{1}{r} \sin \alpha r$ contributes to the radial function. Expanding $p(r, \theta, \phi, t)$ in terms of the eigenfunctions and proceeding as before, we get

$$P^*(t|R) = \sum_{n=1}^{\infty} (-1)^{n+1} \frac{2n^2 \pi^2 D}{R^2} \exp\left[-\frac{n^2 \pi^2 D t}{R^2}\right] \quad (2.31)$$

which gives the scaling function as

$$f_{sphere}(\chi) = \frac{1}{16} \frac{\partial^2 \vartheta_3(z, q = e^{-\chi})}{\partial z^2} \Big|_{z=\pi/4} \quad (\beta = \pi^2 D \text{ and } \chi = \beta t/R^2) \quad (2.32)$$

where the theta function mentioned above is defined in the Eq(8).

2.3 Concluding remarks

Let us compare the scaling functions of a sphere and a cube

$$f_{3dbox}(\chi) = c'_1 \exp(-\chi) + c'_2 \exp(-2\chi) + c'_3 \exp(-3\chi) + \dots \quad (2.33)$$

$$f_{sphere}(\chi) = c_1'' \exp(-\chi) + c_2'' \exp(-4\chi) + c_3'' \exp(-9\chi) + \dots \quad (2.34)$$

For large time t , only the first terms are the dominant ones and we can drop the higher order terms. Demanding the equality of the argument of exponentials in the first term, we get the condition on the sizes of the cube and sphere as $\frac{2L}{R} = \sqrt{3}$. The ratio of the co-efficients comes out to be $\frac{c_1'}{c_1''} = \frac{32}{\pi^3} \approx 1.032$. The series expansion clearly shows that the two functions are not same and the near equality of the co-efficients of the first order term suggests that the functions should look very similar for large t . This can easily be seen in Fig. 2.2 where we have plotted the scaling functions of a box and a sphere having a ratio of sizes $\frac{2L}{R} = \sqrt{3}$. The dependence on shape of the eigenvalues of a differential equation is an important problem and has been studied very well. M. Kac posed the problem as “can one hear the shape of the drum” [71, 72].

To summarize, in this chapter, we have obtained the explicit form of the scaling function for first passage time distribution of a random walker moving inside absorbing boundaries of various geometries and expressed it in terms of the Jacobi theta functions.

The distribution of residence times in height type sandpile models.

In the previous chapter we have calculated the first passage time distribution for a simple random walker inside a closed domain in presence of the absorbing boundaries of various shapes. Let us now consider the distribution of residence times of grains in height type sandpile models. The residence time of a grain is the time spent by the grain inside the pile. As in the case of a simple random walker considered in the previous chapter, in the case of sandpile also the residence times of grains are just the first passage times of grains to the boundary of the pile.

We argue that the problem of determining the distribution of residence times (DRT) of grains in the height type sandpile models can be reduced to that of finding the probability distribution of hitting time of a single diffusing particle to the boundary, diffusing in a medium with site-dependent jump rates. In the scaling limit of large system sizes, DRT becomes a function of a single scaling variable t/L^b , where t is the residence time, L is the linear size of the system, and b is some exponent. This function is non-universal, and is a complicated function of the spatial distribution of added grains used to drive the pile to its steady state. We determine this function explicitly for 1-dimensional sandpile when grains are added randomly only at the ends. When grains are added with equal probability everywhere, we prove that the exact scaling function of the DRT is a simple exponential. This result is independent of dimension, and of the shape of the pile.

3.1 Models

We have considered two height type sandpile models: the deterministic Bak-Tang-Weisenfeld (BTW) model [25] and the stochastic Manna model [74]. Both the models

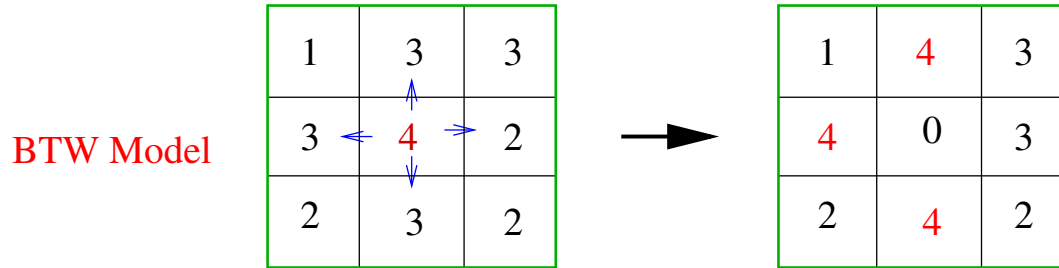


Fig 3.1: Transfer rule of grains in BTW model on a $2D$ square lattice. Four grains are thrown out from an unstable site and each of the four nearest neighbours gets one grain.

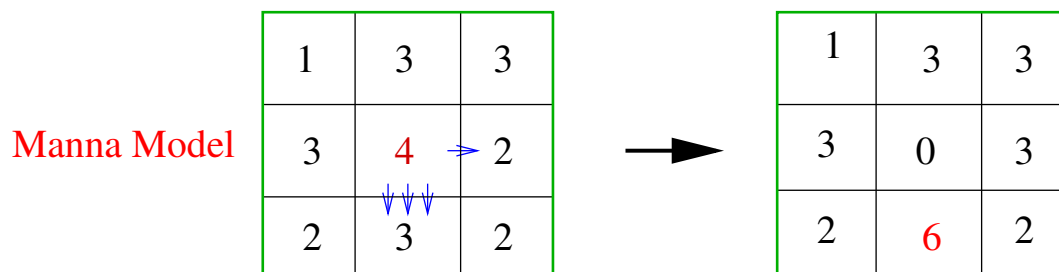


Fig 3.2: Transfer rule of grains in stochastic Manna model on a $2D$ square lattice. Each of the four grains randomly goes to any one of the four nearest neighbours.

are defined on a d -dimensional hypercubic lattice of volume L^d . The height $h(\vec{x})$ is the number of grains at site \vec{x} . The toppling rules of these two models have been given earlier in section 1.2.1. In Fig. 3.1 and Fig. 3.2 we have shown schematically the transfer rules of grains for these models on a two dimensional square lattice.

Grains are added randomly everywhere and leave the pile from the boundary sites. The piles are driven slowly, by adding one grain per unit time. We always topple unstable sites in parallel. If we want to study DRT in sandpile models, we have to mark the grains. The grain added at time n is labeled by the number n . However, with marked gains, the model is not Abelian. This is because toppling at two adjacent unstable sites in different order no longer give the same result. For a full specification of the rules governing the motion of grains in the model, we have to define precisely in which order the unstable sites are toppled, and how the grains are transferred under toppling. We choose the parallel update scheme: make a list of all sites which are unstable at a time t , choose at random two grains from each of these sites (if there are only two grains, both are selected), and randomly assign one of them to go the

left neighbour, and the other to the right. All these grains which are to be moved are then added to their destined sites, at the same time. This constitutes a single micro step of evolution. Then we construct the new list of unstable sites for the next micro time-step, and repeat.

The constant time elapsed between two successive additions of grains (P micro-steps) will be called a meso-time step. We measure the residence time in units of meso-steps. We mark all grains by the meso-time step when they were added to the pile. Then, if the grain numbered T_{in} (added at meso-step T_{in}) gets out of the system at meso-step T_{out} , we will say that its residence time is $T_{out} - T_{in}$.

3.2 General formalism for calculating the distribution of residence times.

3.2.1 The transition matrices.

Any configuration of sandpile is specified by the value of height at each site. In the steady state, total number of configurations occur is, say, N . These steady state configurations are called recurrent configurations. Now let us consider configurations of the sandpile after we add a marked grain. In the presence of the marked grain, any configuration is specified not only by specifying the height at each site, we also have to specify the site where the marked grain is located. So corresponding to a recurrent configuration a , there are, say, n_a number of sites where the mark grain can stay (obviously the marked grain cannot stay at the site with height zero). There are total \mathcal{N} configurations with all possible positions of the marked grain, i.e., $\mathcal{N} = \sum_{a=1}^N n_a$. These \mathcal{N} number of configurations constitute the vector space and we define transition probabilities $\mathcal{W}_{i,j}$ which is the probability of transition from j -th configuration to i -th configuration per unit time. Now the probability $P_i(t)$ that i -th configuration occur at time step t in the steady state satisfy the evolution equation given below.

$$P_i(t+1) = \sum_{j=1}^{\mathcal{N}} \mathcal{W}_{i,j} P_j(t) \quad (3.1)$$

all elements of the transition matrix \mathcal{W} are positive and the sum of elements in any column of \mathcal{W} cannot be greater than 1, i.e., $\sum_{i=1}^{\mathcal{N}} \mathcal{W}_{i,j} \leq 1$ for all j . But it should be noted that $\sum_{i=1}^{\mathcal{N}} \mathcal{W}_{i,j} < 1$ for some j , and therefore there is no steady state of this

Markov chain, i.e., all the eigenmodes of time evolution operator \mathcal{W} decays exponentially with time. Now we define $Prob_L(T \geq t)$ is the probability that the marked grain is inside the pile of size L at least up to time t , i.e., probability of residence time T of the marked grain is greater than or equal to t . So we get

$$Prob_L(T \geq t) = \sum_{i=1}^{\mathcal{N}} P_i(t). \quad (3.2)$$

Once we construct the transition matrix \mathcal{W} , it is possible to calculate the cumulative probability distribution $Prob_L(T \geq t)$ by exactly diagonalizing the matrix \mathcal{W} . But in general, calculating all the elements of the transition matrix \mathcal{W} is tedious for large L , even for 1D BTW model where grains are added randomly everywhere. In the next section we discuss a simple case where we can construct \mathcal{W} and describe the large time behaviour of $Prob_L(T \geq t)$ for arbitrary L .

3.2.2 A simple Illustration: 1D Bak-Tang-Wiesenfeld model driven at one end.

As an illustrative example, let us consider the problem in the simplest setting: the BTW model [25] on a line of L sites, labeled by integers 1 to L . At each site i we have a non-negative integer height variable h_i . The site is stable if $h_i \leq h_c$ where we choose $h_c = 1$. If $h_i \geq 2$, the site is said to be unstable, and relaxes by toppling. In this process, h_i decreases by 2, and h_{i-1} and h_{i+1} increase by 1. The pile is driven by adding grains at the right end and grains may be lost whenever there is toppling at any of the ends.

The long-time behaviour under the deterministic evolution is that after an initial transient period, it falls into a cycle of period $L + 1$. The stable configurations of the pile that belong to the cycle are L configurations having all, except one site, with height 1, and one configuration with all $h_i = 1$.

If we start with the state with all $h_i = 1$, adding a particle at $i = L$ gives a stable configuration with $h_1 = 0$. Adding a particle again, we get the recurrent configuration in which $h_2 = 0$. For each new added grain, the position of the zero shifts one step to the right, till after L steps it is at $i = L$. Then adding another grain, the zero disappears. We choose to say that in this case the zero is at $i = 0$. The number of toppling to get the next stable configuration is also periodic with the same period : $L \rightarrow L - 1 \rightarrow (L - 2) \dots 1 \rightarrow 0 \rightarrow L$.

From our definition, it follows that the probabilities of different paths taken by a grain are exactly that of an unbiased random walker on the line. This is because when a grain moves under toppling, it is equally likely to take a step to the right, or to the left. So, for example, the average number of steps a grain takes before it leaves the pile is equal to the average number of steps a random walker would take from that starting point. However, the time between two jumps of the grain is random, and has very non-trivial correlations with times of previous jumps, and also with jump times of other particles. This is what makes this problem nontrivial.

To calculate the DRT for the linear chain of L sites, we consider adding a marked grain into the pile. All other grains are unmarked, and indistinguishable from each other. Then, stable configurations of the pile are L^2 in number. Configuration in which the site a has height 0, and the marked grain is at site b will be denoted by $\mathcal{C}_{a,b}$. All sites other than a and b are occupied by unmarked grains. For each value of a , $1 \leq a \leq L$, then there are $L - 1$ possible configurations corresponding to different values of b . For the recurrent configuration with all $h_i = 1$, we define $a = 0$, and in this case there are L possible positions of b . Thus there are in total L^2 possible stable configurations of the pile.

Now we study the behaviour of the function $Prob_L(T = t)$ when $t \gg L^2$. Since time evolution of states of the system is a Markov process, there is exponential decay of probabilities of states for large value of time, due to the presence of the absorbing boundaries. So the probability distribution $Prob_L(T = t)$ must decay as $\exp(-K_L t/L^2)$ for very large T . For large L , the coefficient, K_L , tends to a constant K and scaling function $f(x)$ must go as $\exp(-Kx)$ for large x . We define K as a limit given below,

$$K = - \lim_{L \rightarrow \infty} \left[\lim_{t \rightarrow \infty} \frac{L^2 \ln Prob_L(T = t)}{t} \right]$$

We numerically calculate values of K_L 's for various finite lattice sizes by defining transition probability matrices for the system going from one recurrent configuration to another. We need to distinguish between different recurrent configurations, with a specified position of site with height zero, according to different positions of the marked grain. Configurations with same position of the marked grain can be distinguishable with respect to the position of the site with height zero. Obviously the marked grain can be at any site except the site where height is zero.

As an illustrative example, we indicate how to construct such transition matrices for $L = 4$. When the site with zero height is at the end, i.e., at $i = 4$, three distinguishable

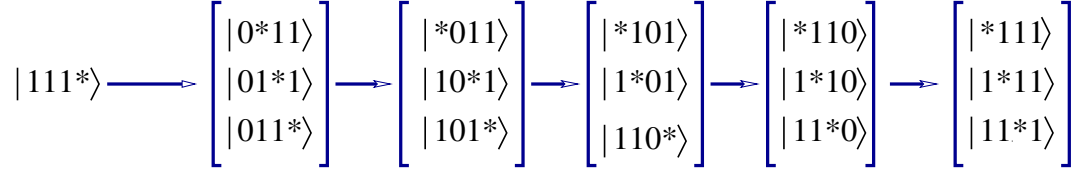


Fig 3.3: Possible configurations with a marked grain are shown by the asterisk.

configurations are represented respectively as $|^*110\rangle$, $|1^*10\rangle$, $|11^*0\rangle$ where asterisk denotes the position of marked grain, “1” denotes the site with height one and “0” denotes the site with height zero. If we keep on adding sand at the right end of the one dimensional chain, the transitions will occur from one state to another. In this case transitions will be from

$$\begin{aligned} \{1110\} &\rightarrow \{1111\} \rightarrow \{0111\} \rightarrow \{1011\} \\ &\rightarrow \{1101\} \rightarrow \{1110\} \end{aligned}$$

(same initial states after $L + 1 = 5$ time steps).

Here marked grain can be at any one of the sites with height 1. The all possible states are shown below.

We represent basis states for a particular configuration $\mathcal{C}_{Y_0,j}$ as $|Y_0,j\rangle$ where j denotes the position of marked particle and Y_0 denotes the index of the site with height zero. Since marked grain cannot stay at the site with height zero, there are $L - 1$ basis states for a particular configuration (i.e. for a fixed Y_0). Y_0 can take value from 0 to L . $Y_0 = 0$ means that all sites are with height 1. Whenever we add sand grain at the right end, there is transition from any of the basis states with some value of Y_0 to any of the basis states with $Y_0 + 1$ (i.e., $\mathcal{C}_{Y_0,j} \rightarrow \mathcal{C}_{Y_0+1,i}$). i and j denote the position of marked sand grain. Now we define the transition matrix element $\mathcal{T}_{Y_0}(i|j)$ as the transition probability from the j -th state to i -th state where Y_0 denotes that the transition occurs from the configuration with height zero at Y_0 -th site to the configuration with height zero at $(Y_0 + 1)$ -th site. The transition matrices \mathcal{T}_1 , \mathcal{T}_2 , \mathcal{T}_3 , \mathcal{T}_4 and \mathcal{T}_0 for $L = 4$ are written below explicitly.

$$\mathcal{T}_1 = \begin{bmatrix} \frac{1}{2} & (\frac{1}{2})^2 & (\frac{1}{2})^3 \\ \frac{1}{2} & (\frac{1}{2})^2 & (\frac{1}{2})^2 \\ 0 & \frac{1}{2} & (\frac{1}{2})^2 \end{bmatrix} \quad \mathcal{T}_2 = \begin{bmatrix} 1 & 0 & 0 \\ 0 & \frac{1}{2} & (\frac{1}{2})^2 \\ 0 & \frac{1}{2} & (\frac{1}{2})^2 \end{bmatrix}$$

$$\mathcal{T}_3 = \begin{bmatrix} 1 & 0 & 0 \\ 0 & 1 & 0 \\ 0 & 0 & \frac{1}{2} \end{bmatrix} \qquad \mathcal{T}_4 = \begin{bmatrix} 1 & 0 & 0 \\ 0 & 1 & 0 \\ 0 & 0 & 1 \end{bmatrix}$$

$$\mathcal{T}_0 = \begin{bmatrix} \frac{1}{2} & (\frac{1}{2})^2 & (\frac{1}{2})^3 \\ 0 & \frac{1}{2} & (\frac{1}{2})^2 \\ 0 & 0 & \frac{1}{2} \end{bmatrix}$$

The full time evolution operator \mathcal{W} mentioned in Eq.3.1 in this case can be written in terms of a matrix containing distinct blocks as given below.

$$\mathcal{W} = \begin{bmatrix} 0 & \mathcal{T}_1 & 0 & 0 & 0 \\ 0 & 0 & \mathcal{T}_2 & 0 & 0 \\ 0 & 0 & 0 & \mathcal{T}_3 & 0 \\ 0 & 0 & 0 & 0 & \mathcal{T}_4 \\ \mathcal{T}_0 & 0 & 0 & 0 & 0 \end{bmatrix}$$

This operator acts on $L(L-1) + L - 1 = (L^2 - 1)$ dimensional vector space [i.e., $\mathcal{N} = (L^2 - 1)$ in Eq.3.1] considering all possible configurations (see in Fig.3.3) with marked grain in the steady state of the $1d$ BTW model on lattice of size L . In this case however, we did not consider the configuration with marked grain at $x = L$ and heights are 1 everywhere (first configuration in Fig. 3.3), in our vector space, as this particular configuration is transient and does not appear in the subsequent time steps.

The transition matrix $\mathcal{T}^{(L)} = \prod_{Y_0=0}^L \mathcal{T}_{Y_0}$ gives back the initial configuration after the period of time $L + 1$. The superscript in $\mathcal{T}^{(L)}$ is denoting that the marked grain is added when the initial configuration is with $Y_0 = L$. In general, if the grain is added with the initial configuration where position of the site with height zero is at $i = Y_0$, the transition matrix will be $\mathcal{T}^{(Y_0)} = \mathcal{T}_{Y_0-1} \mathcal{T}_{Y_0-2} \dots \mathcal{T}_{L-1} \mathcal{T}_L \mathcal{T}_0 \dots \mathcal{T}_{Y_0-1} \mathcal{T}_{Y_0}$. The different values of Y_0 in transition matrices correspond to the addition of sand grains to the configurations with different sites with height zero. The matrix \mathcal{W}^{L+1} is block diagonal and blocks are basically $\mathcal{T}^{(Y_0)}$,s for different values of Y_0 . For $L = 4$ it is written below explicitly.

$$\mathcal{W}^{L+1} = \begin{bmatrix} \mathcal{T}^{(4)} & 0 & 0 & 0 & 0 \\ 0 & \mathcal{T}^{(3)} & 0 & 0 & 0 \\ 0 & 0 & \mathcal{T}^{(2)} & 0 & 0 \\ 0 & 0 & 0 & \mathcal{T}^{(1)} & 0 \\ 0 & 0 & 0 & 0 & \mathcal{T}^{(0)} \end{bmatrix}$$

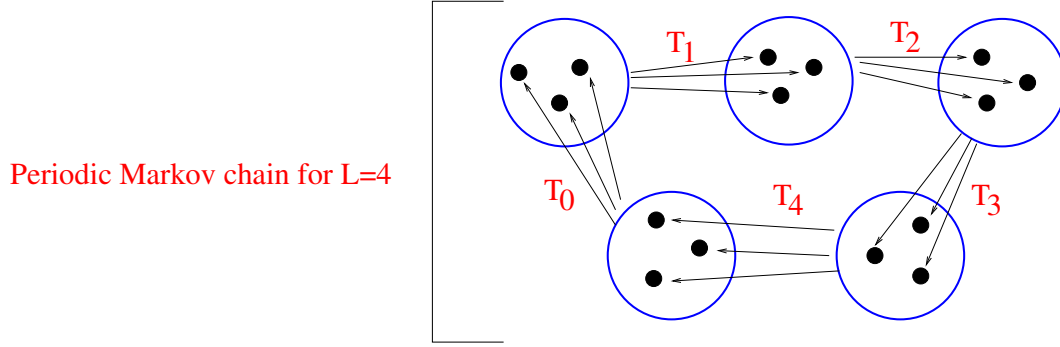


Fig 3.4: Periodic Markov chain in the case of the 1d BTW model driven at right end for $L = 4$.

To find out the coefficient K_L in the exponential decay of the distribution of residence time, we diagonalize any matrix $\mathcal{T}^{(Y_0)}$, say $\mathcal{T}^{(L)}$, and take the largest eigenvalue, λ_{max} . We diagonalize any one matrix of the different transition matrices because the eigen values for the different transition matrices, $\mathcal{T}^{(Y_0)}$ s (we get various $\mathcal{T}^{(Y_0)}$ s just with cyclic permutation of matrices $\mathcal{T}_0, \mathcal{T}_2, \mathcal{T}_3, \dots, \mathcal{T}_L$ etc.) are same. We diagonalize the matrix $\mathcal{T}^{(Y_0)}$ using following algorithm. We take any column vector $|X\rangle$ and operate $\mathcal{T}^{(Y_0)}$ on the column vector N times, i.e., we get $|X_N\rangle = (\mathcal{T}^{(Y_0)})^N |X\rangle$. When N is very large, the quantity $[\frac{\langle X|X_N\rangle}{\langle X|X\rangle}]^{1/N}$ converges to the largest eigenvalue λ_{max} of $\mathcal{T}^{(Y_0)}$.

$$\lambda_{max} = \lim_{N \rightarrow \infty} \left[\frac{\langle X | (\mathcal{T}^{(Y_0)})^N | X \rangle}{\langle X | X \rangle} \right]^{1/N}$$

For large value of time $t (\gg L^2)$, the cumulative distribution of residence time decays exponentially as given below.

$$Prob_L(T \geq t) \sim (\lambda_{max})^{t/(L+1)} \quad (3.3)$$

i.e., $Prob_L(T \geq t)$ varies as $\exp(\frac{t}{L+1} \ln \lambda_{max})$ for $t \gg 1$. The coefficient K_L is then given by as below.

$$K_L = -\frac{L^2}{L+1} \ln \lambda_{max} \quad (3.4)$$

In the Fig. 3.5 we have plotted K_L against the number of sites in the 1-dimensional lattice, L . It shows that K_L saturates to the value of K . So the coefficient is independent of lattice size L for large value of L .

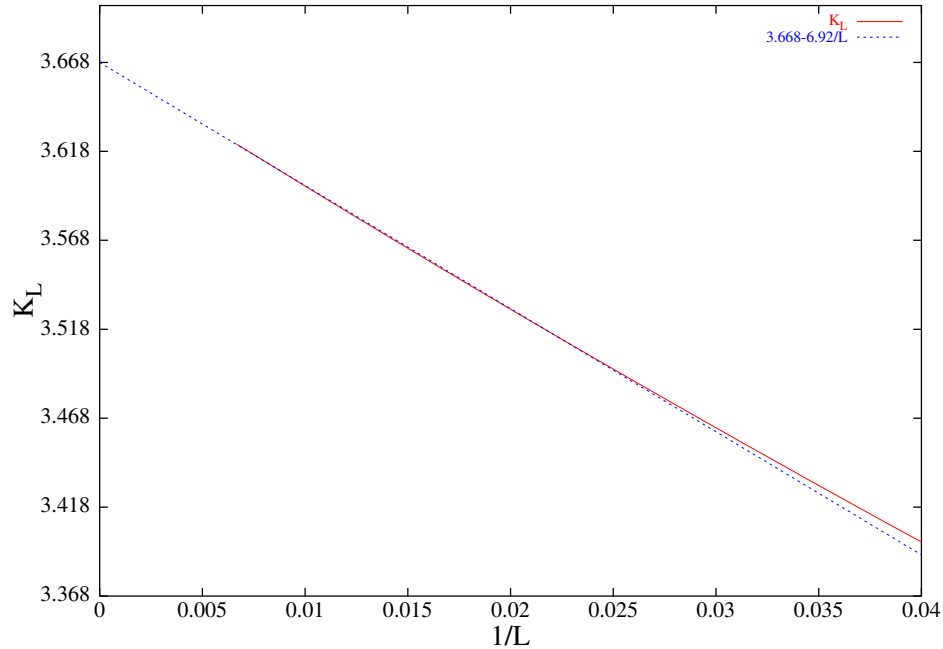


Fig 3.5: K_L has been plotted against lattice size L . K_L has been calculated upto $L = 150$ and extrapolated using a fit to a straight line. Extrapolated value of K_L when L large is 3.668 ± 0.003 .

3.3 Analytic results in 1D Bak-Tang-Wiesenfeld model: Driving at one end.

3.3.1 Small time behaviour in the limit of large system sizes.

When the residence time T is very small compared to L , sand grains almost always get ejected from the right end and do not go to the left of the site $i = L - T$ (except for the case when $h_i = 1$ at all sites at time $T = t$ and grain might be ejected from the left end, but the probability of this happening is exponentially small). It's very unlikely that the marked sand grain meets the site with height zero (the probability $\leq \frac{t}{(L+1)}$ which goes to zero for large value of L). In the limit of L large compared to the residence time t , the residence time distribution is well approximated by the distribution of the first passage (at $i = 1$) time of a simple unbiased random walker with $2t$ steps random walk. So, for $T \ll L$, We can exactly calculate the residence time distribution [2]

$$Prob_L(T = t) = \frac{2t!}{t!(t+1)!} 2^{-(2t+1)}$$

where $Prob_L(T = t)$ is the probability that the marked sand grain gets ejected from the system immediately after time t . Using Stirling approximation to the above expression,

we get the function $Prob_L(T = t)$ equals $\frac{1}{2\sqrt{\pi}} \frac{1}{t^{3/2}}$ for $1 \ll t \ll L$. Now we can extend our result whenever $t \ll L^2$. The argument is as follows. After time steps $T \sim L^\alpha$ where $\alpha < 2$, the standard deviation of the position of the marked sand grain goes as $L^{\alpha/2}$. So the probability that the marked grain will meet the site with height zero goes as $L^{\alpha/2-1}$ which will tend to zero in the large L limit. Therefore for any $1 \ll t \ll L^2$, the limiting probability distribution $Prob_L(T = t)$ is proportional to $t^{-3/2}$, the first passage (at $i = 1$) time distribution of a simple unbiased random walker with $2t$ steps random walk. For the large value of t the distribution function decays exponentially like $\exp(-K_L t/L^2)$, as shown in the previous section, where K_L tends to a constant value for large L .

Even though we don't know the full distribution function $Prob_L(T = t)$, we can find out the first moment of the residence time distribution easily, using an important result in queuing theory, known as Little's theorem [75]. We give a proof here. We define mass of the sandpile as the total number of particles in the pile (i.e., $\sum_{i=1}^{i=L} h_i$). It's easy to see that mean residence time $\langle T \rangle = \langle \text{Total mass of the pile} \rangle$. To prove this, let us define an indicator function $\eta_{n,T}$ as given below.

$$\eta_{n,t} = 1 \quad \text{if the sand grain, added at time } n, \text{ is in the system}$$

$$\text{at time } t, \text{ otherwise } \eta_{n,t} = 0.$$

The mean residence time can be written as

$$\begin{aligned} \langle T \rangle &= \lim_{\mathcal{N}, \mathcal{T} \rightarrow \infty} \frac{1}{\mathcal{N}} \sum_{n=1}^{\mathcal{N}} \sum_{t=1}^{\mathcal{T}} \eta_{n,t} = \frac{1}{\mathcal{N}} \sum_{t=1}^{\mathcal{T}} \sum_{n=1}^{\mathcal{N}} \eta_{n,t} \\ &= \frac{1}{\mathcal{N}} \sum_{t=1}^{\mathcal{T}} (\text{Total mass of the pile at time } t) \\ &= \langle \text{Total mass of the pile} \rangle \end{aligned}$$

The average of the total mass in the pile is $[\frac{L}{L+1}(L-1) + \frac{1}{L+1}L]$ which goes as L for large L .

We find out the scaling form of the function $Prob_L(T = t)$ using the mean residence time and the previous limiting distribution. The scaling function $f(x)$ is defined as

$$f(x)dx = \lim_{L \rightarrow \infty} L^{a-b} Prob_L(xL^b \leq t \leq (x+dx)L^b)$$

So the form of the distribution function $Prob_L(T = t)$ is $\frac{1}{L^a} f(\frac{t}{L^b})$. Since $Prob_L(T = t)$ varies as $t^{-3/2}$ for $1 \ll t \ll L$, $f(x)$ must go as $x^{-3/2}$ for very small value of x and

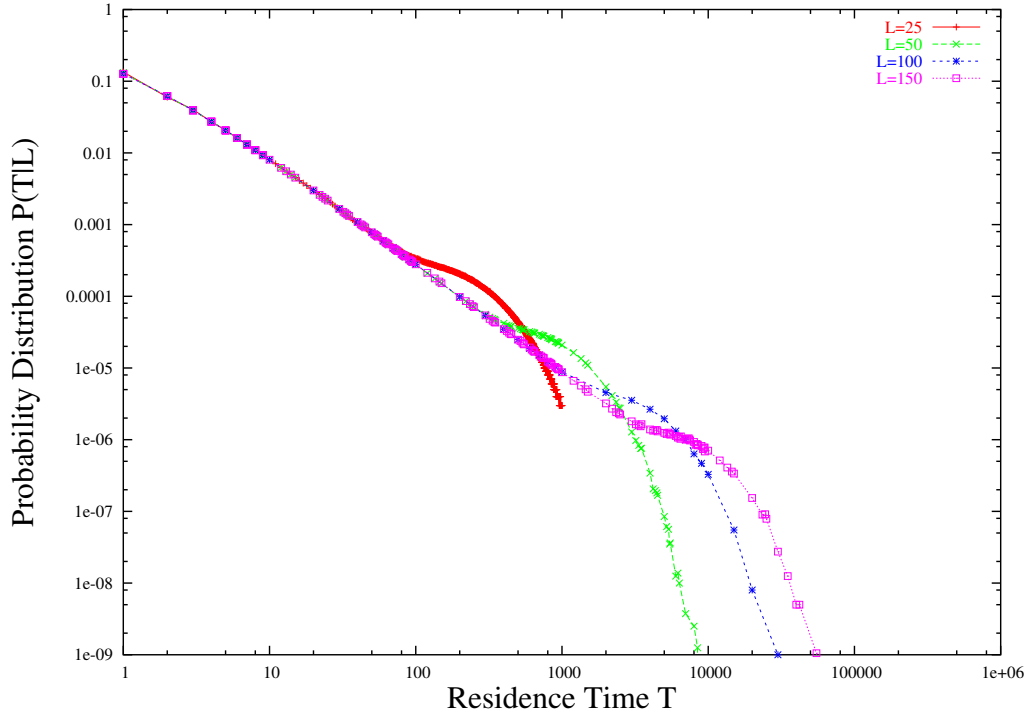


Fig 3.6: The probability distribution of the total residence time T plotted against T for $L = 25, 50, 100, 150$ for the 1d BTW model driven at an end.

therefore $\frac{1}{L^a} f(\frac{t}{L^b})$ goes as $L^{(3b/2-a)} t^{-3/2}$. As $Prob_L(T = t)$ is independent of L for $1 \ll t \ll L$, we get $a/b = 3/2$. Even though the scaling function $f(x)$ is divergent as x tends to zero, we can normalize $Prob_L(T = t)$ without any problem, since x has lower cutoff $\frac{1}{L^b}$. As $f(x)$ goes as $x^{-3/2}$, the normalization integral is

$$L^{b-a} \int_{1/L^b}^{\infty} f(x) dx \sim L^{3b/2-a}$$

which is independent of L as $a/b = 3/2$. The mean residence time $\langle T \rangle$ is given by

$$\int_0^{\infty} \frac{1}{L^{3b/2}} f(t/L^b) t dt \sim L^{b/2}$$

As there is no divergence in the integrand, we can put the lower limit in the integration zero. Since $\langle T \rangle \sim L$, we find $b = 2$ and therefore can write the scaling form of the $Prob_L(T = t)$ as $t^{-3/2} \tilde{f}(\frac{t}{L^2})$ for large L . In Fig.1. probability distributions, $Prob_L(T = t)$, of residence time of sand grains are plotted for different lattice sizes $L = 25, 50, 100, 150$. In Fig.2. $Prob_L(T = t)$ for various system sizes collapse to a single curve when we plot $L^3 Prob_L(T = t)$ against t/L^2 .

We can easily extend results to the case when $h_c = 2$ under the toppling rules that whenever the height at any site is greater than $h_c = 2$, the site becomes unstable and

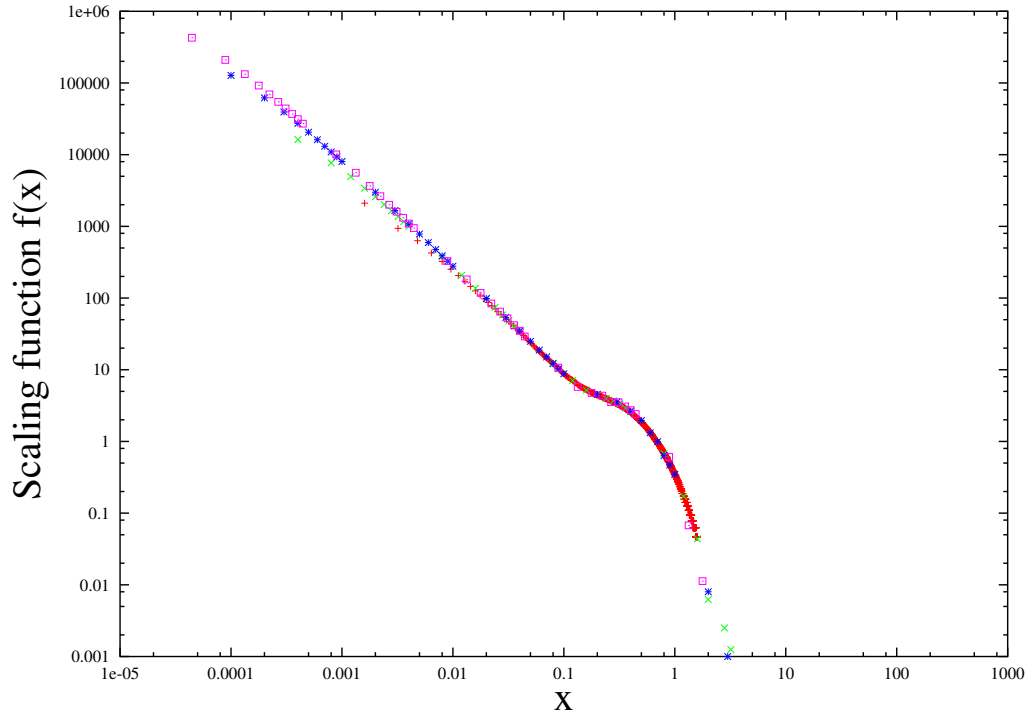


Fig 3.7: The plot of scaling function $L^3 Prob_L(T = t)$ against the scaled variable t/L^2 for different lattice sizes for the 1d BTW model driven at an end.

there is a toppling at the site. Two grains are thrown out from the unstable site, one grain of the three goes to right nearest neighbour site, one goes to the left nearest neighbour site and the other one stays put. It is decided at random which one goes to the right, which one goes to the left. The probability that a particular grain of the three going to the right or to the left, or staying there is $1/3$. The height of any site is either 1 or 2, when the system is stable. In the steady state, at most one site has height 1 and all the others have height 2. All configurations in the recurrent configuration space are equally probable. The number of recurrent configurations is same as before. The residence time distribution $Prob_L(T = t)$, for $1 \ll t \ll L$, is

$$\sum_{t'=0}^t \binom{t+t'}{t'} C_{2^{t'}} 3^{-(t-t')} \frac{2t!}{t!(t+1)!} 3^{-(2t+1)} \sim \frac{1}{t^{3/2}} \quad (3.5)$$

Here also we can extend this result for $1 \ll t \ll L^2$, just as we did in the case for $h_c = 1$. The probability distribution function has similar scaling form as in the case with $h_c = 1$. For $h_c = 2$, the mean residence time $\langle T \rangle$ is equal to $2L$ in the limit when L is large. So The scaling function $f(x)$ for $h_c = 1$ gets scaled by a factor 2 for $h_c = 2$, i.e., the scaling function becomes $\frac{1}{2}f(x/2)$.

To calculate the coefficient K_L , we can construct the transition probability matrix

exactly in the similar way for the previous case. In this case the number of basis states is L and K_L can be determined as before.

3.3.2 Scaling function of the distribution of residence times.

Consider a particular configuration $\mathcal{C}_{a,b}$ where the site a has height 0, and the marked grain is at site b . Now we add another (unmarked) grain at $i = L$. If $b < a$, then it is easily seen that the wave of toppling [76] does not reach the marked grain, and the final configuration is $\mathcal{C}_{a+1,b}$.

When $b > a$, the wave of toppling, started at the right end, reaches the site b and the site will topple. The marked grain will move one step to the left or right, with equal probabilities. If the marked grain moves to the left, it will move again due to toppling, unless that site has no grains. In this way, the marked grain can take zero, one or more consecutive steps to the left in one meso-step. It stops diffusing as soon as it takes a right step or if the marked grain falls on a . We thus see that on adding more grain, if $b > a$, the final configuration is $\mathcal{C}_{a+1,b+\Delta b}$, with Δb taking values $1, 0, -1, -2, \dots, a + 2 - b$ and $a - b$ with probabilities $2^{-1}, 2^{-2}, 2^{-3}, 2^{-4}, \dots, 2^{a-b}$ and 2^{a-b} respectively. For $b - a$ large, the mean square displacement $\langle(\Delta b)^2\rangle$ tends to 2.

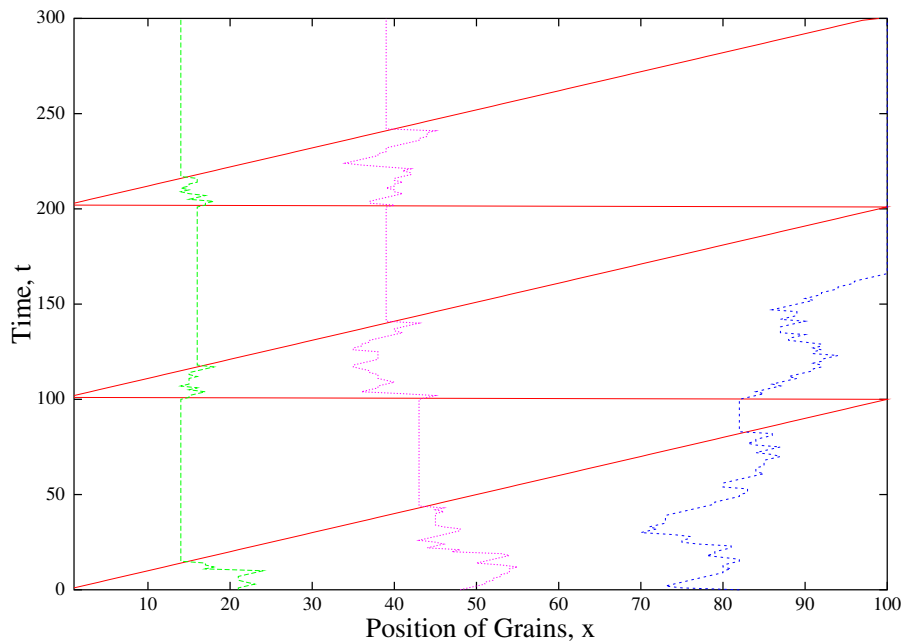


Fig 3.8: Motion of three grains starting from $x = 20, 50, 80$ in the $1d$ BTW sandpile of length $L = 100$ where sand grains are added only at the right end.

Consider a marked grain at b , at some time T , with $b = \alpha L$, $0 < \alpha < 1$, and L large. We consider the change in its position Δb after one cycle ($(L + 1)$ meso-steps). Fig.1 shows the motion of grains in a cycle in one realization. The grain diffuses for a while, and is stuck when the zero is to the right of the marked grain. The average fraction of time it moves is α . A grain at b is hit by b waves of toppling [76] in this interval. The net displacement Δb is sum of displacements due to these waves. Each wave causes a displacement with mean zero, and variance 2. Then by central limit theorem, the net displacement will be distributed normally with variance given by $2b$. Thus Δb is of order $\sqrt{2\alpha L}$, and is much smaller than L when L is very large. Then, for times $t \gg L$, we can average over the motion in a cycle, and say that if the marked grain is at i , it moves to the left or right neighbor with a rate (i/L) per unit time. If $P(i, t)$ is the probability that the marked grain is at i at time t , the evolution equation for $P(i, t)$ for times $t \gg 1$ is

$$\frac{d}{dt}P(i, t) = \frac{i+1}{L}P(i+1, t) + \frac{i-1}{L}P(i-1, t) - \frac{2i}{L}P(i, t). \quad (3.6)$$

At time $t = 0$, we can assume that the marked particle is at $i = L$, so that $P(i, t = 0) = \delta_{i,L}$. Integrating this equation, we determine the survival probability $S(t) = \sum_i P(i, t)$, and then the DRT is given by

$$Prob(t|L) = S(t) - S(t+1). \quad (3.7)$$

We introduce the reduced coordinate $\xi = i/L$, and $\tau = t/L^2$ and consider the Eq.(3.14) when L is large. In terms of these reduced variables, the evolution equation for the probability density $P(\xi, \tau)$ becomes, in the continuum limit,

$$\frac{\partial}{\partial \tau}P(\xi, \tau) = \frac{\partial^2}{\partial \xi^2}[\xi P(\xi, \tau)]. \quad (3.8)$$

We can integrate this equation numerically using the initial condition $P(\xi, t = 0) = \delta(\xi - 1 + 1/L)$. The scaling function $f(x)$ is given by,

$$f(x) = \left[\frac{d}{d\tau} \int_0^1 P(\xi, \tau) d\xi \right]_{\tau=x} \quad (3.9)$$

Let $\varphi_j(\xi)$ be solution to the eigenvalue equation corresponding to eigenvalue λ_j

$$\frac{d^2}{d\xi^2}[\xi \varphi_j(\xi)] = -\lambda_j \varphi_j(\xi), \quad (3.10)$$

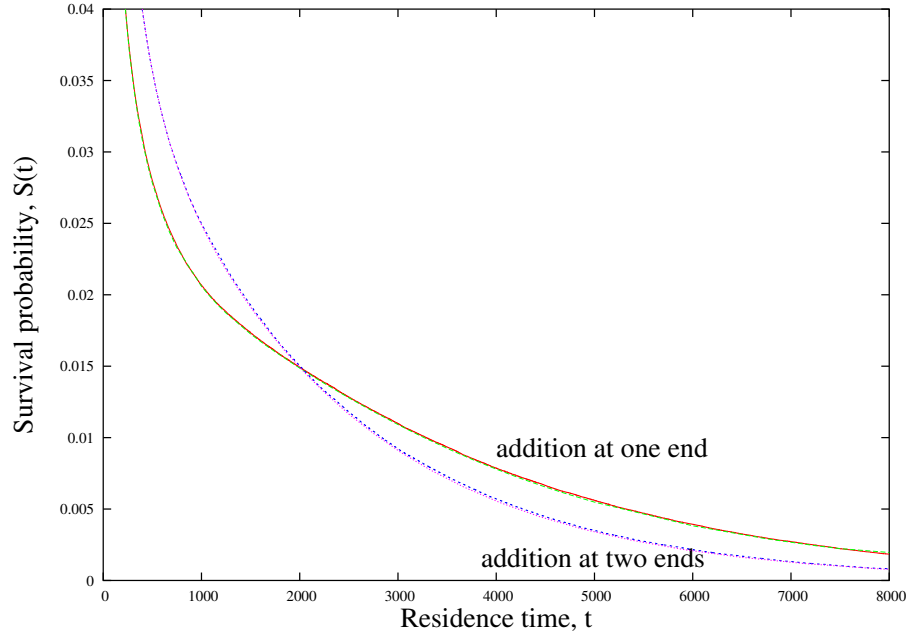


Fig 3.9: Survival probability versus residence time t for the $1d$ BTW model in two cases with grains added only at one or both ends. The theoretical result(full curve) and the simulation result(dotted line) match perfectly. $L = 100$ for both the cases.

where $\varphi_j(\xi = 1) = 0$ corresponding to an absorber being present at $i = L + 1$. At $\xi = 0$, we do not need to assume any special condition, as the absorber at $i = 0$ is automatically taken care of by the fact that rate of jump out of i is $2i/L$, which becomes zero at $i = 0$.

We look for a solution $\varphi_j(\xi)$ that does not diverge at $\xi = 0$. Expanding $\varphi_j(\xi)$ in a power series, and matching coefficients, we get

$$\varphi_j(\xi) = \sum_{n=0}^{\infty} \frac{(-\lambda_j \xi)^n}{n!(n+1)!} = I_1(2i\sqrt{\lambda_j \xi}) / (i\sqrt{\lambda_j \xi}),$$

where $I_1(x)$ is the modified Bessel function of order 1[77]. For details see Appendix A. The eigenvalues λ_j is obtained by imposing the condition $\varphi(\xi = 1) = 0$. Thus if the j -th zero $I_1(z)$ occurs at $\pm 2ik_j$, then $\lambda_j = k_j^2$. At large times t , $S(t)$ varies as $\exp(-Ct/L^2)$, where we get $C = k_1^2 = 3.6705$. This value is in good agreement with the value obtained by extrapolation of estimates obtained by measuring the coefficients of the exponential determined by exact diagonalization of the master equation for finite L (see section 3.2.2 and Fig.3.5).

3.4 Generalization to higher dimensions.

3.4.1 Distribution of residence times for isotropic models.

The generalization of these results to d dimensions is straight-forward. We consider a d -dimensional sandpile model on a lattice with number of sites V . We assume that when a new grain is added, the site \vec{x} is chosen with probability $r(\vec{x})$. Clearly, the sum of $r(\vec{x})$ over all sites is 1. In the steady state, $n(\vec{x})$, the average number of topplings at \vec{x} per added grain, satisfies the equation (using conservation of sand grains)

$$\nabla^2 n(\vec{x}) = -r(\vec{x}), \quad (3.11)$$

with $n(\vec{x}) = 0$ at the boundary. The solution of this equation is

$$n(\vec{x}) = \sum_{\vec{x}'} G(\vec{x}, \vec{x}') r(\vec{x}'), \quad (3.12)$$

where $G(\vec{x}, \vec{x}')$ is the average number of topplings at \vec{x} due to addition of a grain at \vec{x}' , and is equal to the inverse of the toppling matrix Δ [35].

The important point to realize is that while avalanches in sandpile can spread quite far, the typical distance traveled by one marked grain in an avalanche is much smaller than L . In fact, in many cases, we expect it to be of order 1. During its motion to the boundary, the marked grain would be involved in a large number of avalanches. At time-scales much larger than a meso-step, the motion is diffusive, with the jump-rate out of different sites being space-dependent because on the average some parts of the lattice have more avalanche activity than others.

Consider a grain at site \vec{x} at time t . Let its position be $\vec{x} + \Delta\vec{x}$ after Δt new grains have been added, where $L^d \gg \Delta t \gg 1$. As the path of the grain is an unbiased random walk, we have $\langle (\Delta\vec{x})^2 \rangle = s$, where s is the average number of jumps the grain makes in this interval. Assuming that $|\Delta\vec{x}| \ll L$, and that $n(\vec{x})$ is a slowly varying function of \vec{x} , we see that s has to be proportional to $n(\vec{x})\Delta t$, total no of toppling waves during time interval Δt . Let us say $s = Kn(\vec{x})\Delta t$, where K is some constant. Writing $\langle (\Delta\vec{x})^2 \rangle = \Gamma(\vec{x})\Delta t$, we get

$$\Gamma(\vec{x}) = Kn(\vec{x}), \quad (3.13)$$

where the constant K depends on the details of the model. For large times t , the probability-density $P(\vec{x}, t)$ satisfies the equation

$$\frac{\partial}{\partial t}P(\vec{x}, t) = \frac{1}{2}K\nabla^2[n(\vec{x})P(\vec{x}, t)] \quad (3.14)$$

with the initial condition is given by

$$P(\vec{x}, t = 0) = r(\vec{x}). \quad (3.15)$$

It may be noted that Eq.(3.14) is not the diffusion equation with space-dependent diffusion constant $D(\vec{x})$, where the right hand side would have been of the form $\nabla(D(\vec{x})\nabla P(\vec{x}))$. The net current between two sites depends on the difference in the product nP at the two sites, and can be non-zero even if ∇P is zero.

Solving this differential equation, with the condition that $P(\vec{x}, t)$ is zero at the boundary corresponding to the absorbing boundaries, we can determine $P(\vec{x}, t)$ at any time t . Integrating over \vec{x} determines the probability that marked particle remains in the system at time t , and the DRT is obtained from the survival probability using Eq.(3.7).

3.4.2 Exact solutions in some special cases.

Consider, as an example, the case of a linear chain with L sites, when we add particles at each step at either of the two ends with probability $1/2$. In this case, we get $n(x) = \frac{1}{2}$, independent of x , and $K = 2$. One can then solve the Eq.(3.14) analytically. We get a simple diffusion equation.

$$\frac{\partial}{\partial t}P(x, t) = \frac{1}{2}\frac{\partial^2 P(x, t)}{\partial x^2} \quad (3.16)$$

We solve this equation with boundary condition $P(x = 0, t) = 0$ and $P(x = L + 1, t) = 0$. Since grains are added at both ends with equal probability we choose initial condition to be $P(x, t = 0) = \frac{1}{2}\delta(x - 1) + \frac{1}{2}\delta(x - L)$. Eq. 3.16 can be solved following eigenfunction method as done previously in section 2.2.1. The general solution can be written in a sine series as given below.

$$P(x, t) = \sum_{n=1}^{\infty} a_n e^{-\frac{n^2\pi^2 t}{2(L+1)^2}} \sin\left(\frac{n\pi x}{L+1}\right) \quad (3.17)$$

where coefficient a_n can be obtained from the initial condition. We obtain a_n to be as given below.

$$a_n = \frac{1}{L+1} \sin\left(\frac{n\pi}{L+1}\right) [1 + (-1)^{n+1}]$$

The cumulative probability $Prob_L(T \geq t)$ of the residence time T being greater than or equal to t is $\int_0^{L+1} P(x, t) dx$ and can be written after integrating Eq. 3.17 as given below.

$$Prob_L(T \geq t) = \sum_{m=1}^{\infty} \frac{2\pi^2}{(L+1)^2} (2m-1)^2 e^{-\frac{(2m-1)^2 \pi^2 t}{2(L+1)^2}} \quad (3.18)$$

A straightforward calculation now gives $Prob_L(\tau) = \theta_3(0, \tau) - \theta_3(\pi/2, \tau)$, where $\tau = \pi^2 t / 2(L+1)^2$ and $\theta_3(z, \tau)$ is the Jacobi theta function [78] defined by

$$\theta_3(z, \tau) = 1 + 2 \sum_{n=1}^{\infty} \exp(-n^2 \tau) \cos(2nz).$$

In fig 2, we have plotted the analytically computed survival probability $S(t)$ versus t/L^2 for this case and compared with the results of simulation for $L = 100$ using 10^6 grains. We have also shown the result of the numerical integration of Eq.(3.6) to determine the scaling function in the case where the grains are added only at one end, and compared it with the simulation data obtained for $L = 100$ using 10^6 grains. Clearly, the agreement is excellent. This supports our arguments used to obtain Eq.(3.14).

The Eq.(3.14) is very easy to solve in the special case when sand grains are added randomly at any sites in the system. Clearly here $r(\vec{x}) = 1/V$ where V is the number of sites in the lattice. Then $n(\vec{x})$ is a solution to the equation

$$\nabla^2 n(\vec{x}) = 1/V, \quad (3.19)$$

The function $P(x, t) = T(t)$, for all x , satisfies Eq.(3.14) in any dimension if

$$\frac{dT(t)}{dt} = -\frac{K}{2V} T(t)$$

With the initial condition $P(x, t=0) = 1/V$, it is easy to see that the full solution is given by

$$P(\vec{x}, t) = \frac{1}{V} \exp(-Kt/2V). \quad (3.20)$$

The probability of survival upto time t is $VP(\vec{x}, t)$, and we see that it decays in time as a simple exponential. Using the fact that the mean residence time is the average

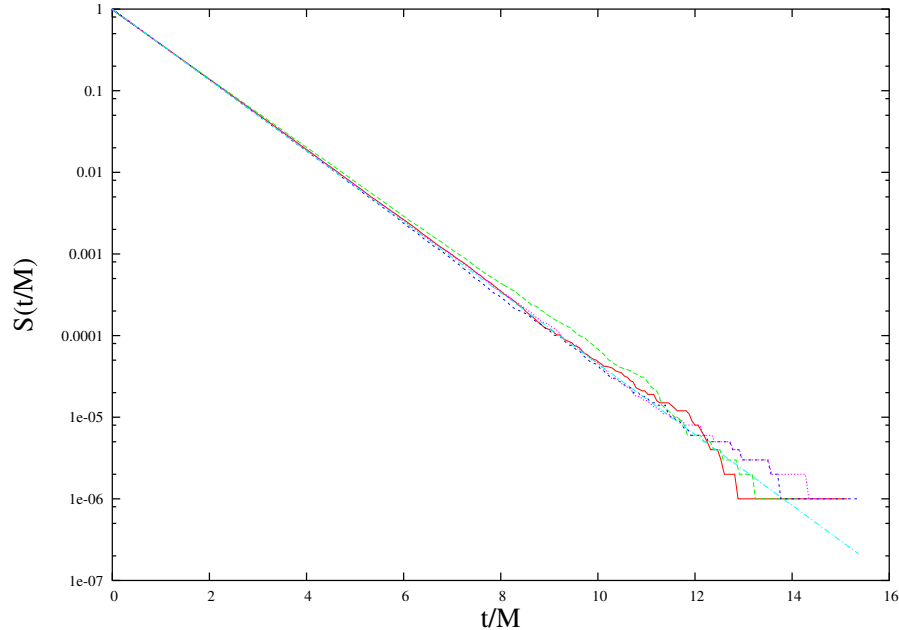


Fig 3.10: Semilog plot of the survival probability of a marked grain as a function of scaled residence time t/M for four different cases: (1) the 1d BTW model, (2) the 1d Manna model, (3) the 2d BTW model, (4) the 2d Manna model. We have chosen $L = 100$ in one dimension and 70×70 cylindrical square lattice in two dimensions.

mass \bar{M} in the pile, we see that $K/2V = 1/\bar{M}$. This then implies that

$$S(t) = \exp(-t/\bar{M}). \quad (3.21)$$

We note that our derivation depends only on Eq.(3.11) and Eq.(3.13). These two equations are valid under the conditions of local conservation of sand grains, transfer of fixed number of grains at each toppling and isotropy. Thus, the results would be equally applicable to models in which toppling conditions are different, or the transfer of particles is stochastic, as in the Manna model.

In Fig 3., we have shown the results of a MC simulation study of the DRT in four different models: (a) the 1-dimensional BTW model for $L=100$, (b) the 2-dimensional BTW model defined on a cylinder of size 50×50 , (c) the 1-dimensional Manna model with $L = 100$ with rule that if z_i exceeds 1, then 2 particles are transferred, each randomly to one of the neighboring sites, and (d) the 2-dimensional Manna model on 50×50 cylinder with two grains transferred at each toppling, each grain in randomly chosen direction. The number of particles used in each simulation was 10^6 . We plot the probability of survival of the marked grain as a function of time t/\bar{M} , where \bar{M} was

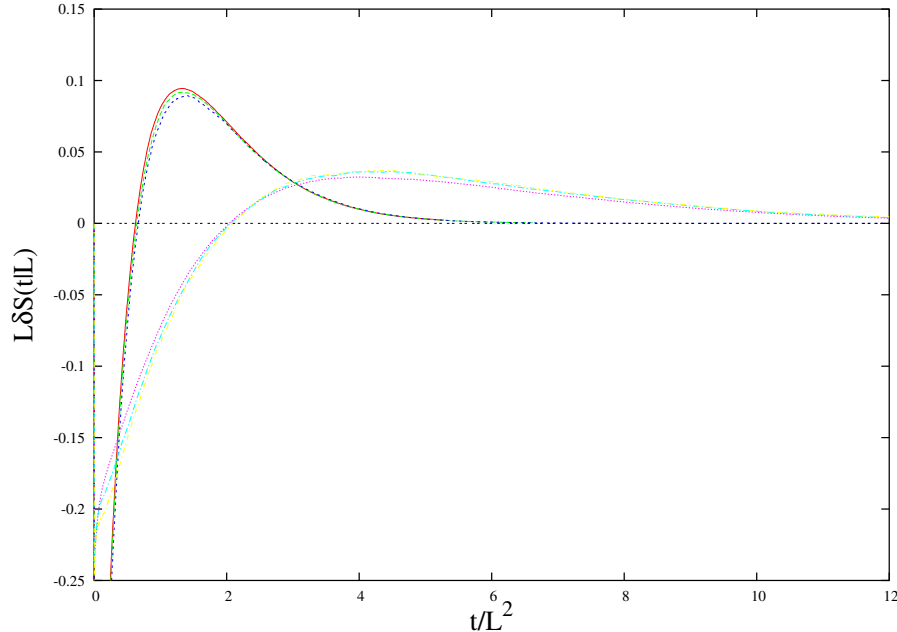


Fig 3.11: The scaled correction term $L\delta S(t|L)$ versus t/L^2 for the 2d BTW and Manna model for three different values of $L = 13, 20, 30$. The curve with higher peak is for the Manna model.

determined from the simulation directly. We see a very good collapse and agreement with the theoretical prediction that $\exp(-t/\bar{M})$ for $t \gg 1$.

3.5 Finite size corrections.

For small t , the probability distribution is determined by the grains which are added very near the boundary. Boundary avalanches are not properly taken care of by our analysis. In particular, it is easy to see that the probability of added grain coming out immediately is nonzero in d -dimensions, and varies as $1/L$ for large L (this being the ratio of surface to volume). But Eq.(3.20) would give this to be $\mathcal{O}(L^{-d})$. This comes from the fact that near the boundary the height distribution is modified, resulting in the effective K becoming different near the boundary. Eq.(3.20) is valid for $t \gg 1$.

In Fig 4., we have plotted the difference $\delta S(t|L)$ between the survival probability from MC simulation data and the scaling theory prediction [Eq. (3.21)], for a 2-dimensional BTW and the Manna models on an $L \times L$ square lattice for different values of L . We find that the curves for different L collapse onto each other if $L\delta S(t|L)$ is plotted versus t/L^2 , indicating that the correction $\delta S(t|L)$ to the Eq. (3.21) has the

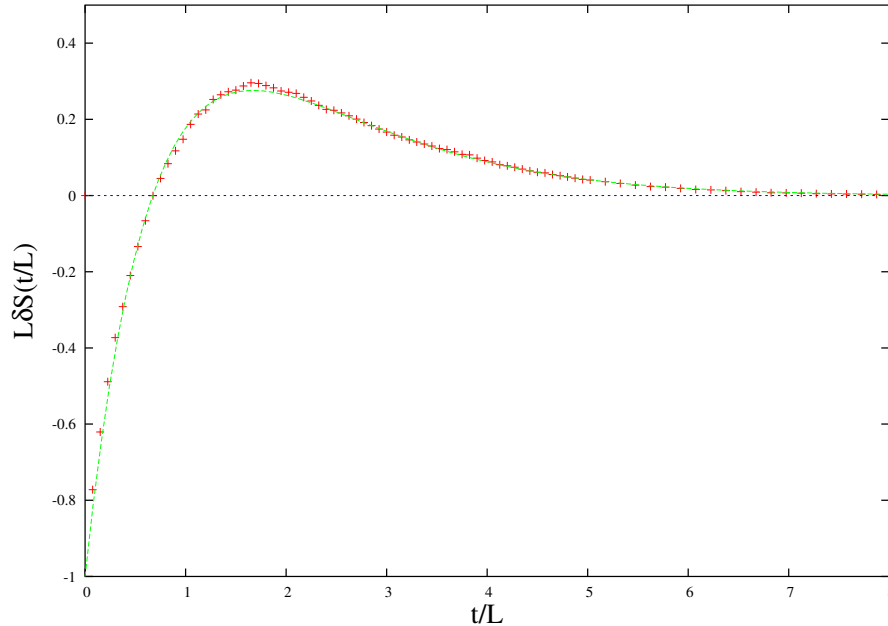


Fig 3.12: Finite size correction for the 1d BTW model with grains added everywhere for $L = 40$. Plotted is the scaled deviation of simulation data, $L\delta S(t/L)$, from the simple exponential scaling solution [Eq.(3.21)] and the full curve is the scaled deviation $L\delta S(t/L)$ from theory [Eq.(3.23)].

scaling form

$$\delta S(t|L) \sim \frac{1}{L}g(t/L^2), \quad (3.22)$$

where the correction-to-scaling function $g(x)$ is different for the two models.

For the one-dimensional BTW model, with grains added everywhere with equal probability, we can determine exactly the leading $\mathcal{O}(1/L)$ correction to the scaling solutions Eq.(3.21). Thus, from the scaling solution Eq.(3.20), we get $Prob(T = 0|L) = 1/L + \mathcal{O}(L^{-2})$. But a straightforward calculation shows that actually $Prob(T = 0|L) = 2/L + \mathcal{O}(L^{-2})$ (see Appendix A.1). However, $Prob(t|L)$ for $t = 1, 2, \dots$, is correctly given to the lowest order by $1/L$ (see Appendix A.2). Assuming that the remaining distribution is a simple exponential, we get

$$S_{1d BTW}(t) = \frac{1}{L}\delta_{t,0} + (1 - \frac{1}{L})\exp[-\frac{t}{L}(1 - \frac{a}{L})], \quad (3.23)$$

where we have used the normalization condition $S(0) = 1$, and added a $\mathcal{O}(1/L)$ correction term to the coefficient in the exponential. Using the condition that first moment

of this distribution is $\bar{M} = L^2/(L + 1)$, we get $a = 1/2$ (see Appendix A.3). In Fig. 5, we have shown the results of a Monte Carlo simulation of this case for $L = 40$ and number of grains = 10^6 , and compared with the theoretical prediction [Eq.(3.23)]. We see that the agreement is very good.

3.6 Concluding remarks.

It is interesting to note that the DRT [Eq.(3.20)] has a simple universal form, and does not depend on the critical exponents for the distribution of avalanches, which differ for BTW and Manna models, and also depend on dimension in a nontrivial way. In contrast for the Oslo ricepile model, Christensen et al [62] and Boguna and Coral [63] found that the DRT for the 1-dimension ricepile of size L , with $L \gg 1$, does involve nontrivial exponents, and has the form

$$Prob(T|L) = \frac{1}{L^\nu} f(T/L^\nu). \quad (3.24)$$

The exponent $\nu \simeq 1.3$ is related to the roughness of the ricepile surface. The function $f(x)$ takes a constant value for x small, and varies as x^{-b} for large x , with $b \simeq 2.4$.

For the Oslo ricepile model, if we consider only grains those are not permanently stuck in the pile as constituting “active mass” of the ricepile, all mass above the minimum slope of the pile is active. The configuration with the minimum slope is recurrent, and will recur infinitely often in the steady state as grains are added to the pile. Therefore, all the grains added after the pile has reached the minimum slope have a finite residence-time in the pile. Then the argument given earlier in this paper implies that mean active mass of the ricepile should vary as L^2 . But the result, obtained in [62] and [63], shows that it varies as $L^{1.3}$. The reason for the discrepancy in the estimate of mean mass in [62, 63] is presumably due to the very long residence of the grains which happen to get deeply embedded, making the estimate of the first moment of the DRT unreliable from short simulations.

The distribution of residence times in ricepile models.

In this chapter we consider the probability distribution of residence times of grains at a site, and of their total residence times in the pile, in critical slope type slowly-driven sandpile (equivalently ricepile) models. We define the residence time T_i at a site i is the time spent by a grain at the site, measured in units of the time interval between successive addition of grains. The total residence time T is defined similarly.

Granular materials have drawn a lot of attention due to their complex flow behaviour under different driving conditions [80]. Slowly driven pile of sand grains serve as a prototype for self-organized criticality (SOC) [25]. Although SOC was not seen in experiments on piles of sand [81], but experiments on piles of long grained rice have shown evidence of power law distribution of avalanche sizes [43, 82, 83]. Studies of sandpiles [32] have generally focused on the distribution of avalanche sizes. There are only a few theoretical studies of other interesting quantities such as the distribution of total residence times of grains in piles, even though the experimental studies by the Oslo group [43, 82] using coloured tracer grains are now almost a decade old.

In the earlier chapter, we studied the total residence time distribution in the critical height type sandpile models with both deterministic and stochastic toppling rules. We reduced the problem to a diffusion problem of a single particle in a medium with space dependent jump rates and showed that the distribution of the total residence time does not have any power law tail.

In the slope type sandpile models, the residence time distributions are qualitatively different from the critical height type models. In critical height models, the distribution decays exponentially with average total residence time equal to average active mass in the pile. In critical slope models, there is a possibility that the grain gets buried very

deep in the pile, and then takes a long time to come out. We shall show that this makes the cumulative probability distribution of these residence times to have a characteristic $1/t$ decay for large times t . We show that the probability of the residence time at a site or the total residence time in the pile, being greater than or equal to t , decays as $1/t(\ln t)^\delta$ for a very wide range of t . The upper cutoff in both the distributions scales with system size L as $\exp(\kappa L^\gamma)$ where γ is an exponent ≥ 1 and κ is a positive constant.

For the Oslo ricepile model, we describe an unexpected behaviour in the cumulative probability that a grain staying at a site i at least upto time t , is not a monotonically increasing function of system size L . We will argue that this implies the cumulative probability distribution function $Prob_L(T_1 \geq t)$ cannot have a simple finite size scaling form and show that $\gamma = d + 2$ in d dimensions for this model.

Plan of the chapter is as follows. In section 4.1 we define four models studied in this paper. In section 4.2 we present the simulation results for the residence time T_1 at site 1 for the $1d$ Oslo ricepile model and explain the non-monotonic behaviour of the cumulative distribution $Prob_L(T_1 \geq t)$ with L by relating the residence times of grains at the site 1 to the statistical properties of height fluctuation at that site. We also explain the origin of multiplicative logarithmic correction factor appearing in the $1/t$ decay of $Prob_L(T_1 \geq t)$. In section 4.3 we argue that the probability of minimum slope configuration occurring in the steady state of the $1d$ Oslo ricepile model, scales with system size L as $\exp(-\kappa L^3)$ where κ is some positive constant. In section 4.4 we discuss the $1/t$ power law form of $Prob_L(T \geq t)$, where T is the total residence times, for large t in the $1d$ Oslo model and show that this also has a multiplicative logarithmic correction. In section 4.5 we present our simulation results for other models and show that in all cases the cumulative distributions is qualitatively similar to the $1d$ Oslo ricepile model. The last section contains some concluding remarks.

4.1 Definition of the Models

We consider general critical slope type sandpile models where the configurations are specified by integer height variables $h(\vec{x})$, *i.e.*, number of grains, at any site \vec{x} of a finite d -dimensional lattice. Whenever height difference between two adjacent sites is greater than a threshold value, some specified number of grains are transferred to the neighbouring sites. Piles are driven by adding grains, one at a time, at a fixed, or at a

randomly chosen site. Grains are added only when there are no unstable sites left in the system, and can leave the pile from the boundary. We update all unstable sites in parallel. We have studied four different models both in one and two dimensions : the Oslo ricepile model and it's $2d$ generalization, local limited model and it's variation. We now define the precise rules of these four models.

4.1.1 Model-A: The Oslo ricepile model.

The Oslo ricepile model [43] is defined as follows. We consider a one dimensional ricepile, which is specified by an integer height variable h_i at each site i of a one-dimensional lattice, with $1 \leq i \leq L$. The slope z_i at site i is defined to be $h_i - h_{i+1}$. Whenever the slope z_i at any site i is higher than a critical value $z_{c,i}$, the site becomes unstable and one grain from the unstable site goes to the right neighbour, *i.e.*, $h_i \rightarrow h_i - 1$ and $h_{i+1} \rightarrow h_{i+1} + 1$. Whenever there is a toppling at site i , $z_{c,i}$ is randomly, independent of the history, reset to one of the two values, 1 and 2, with probability q and p respectively, where $p + q = 1$. Whenever there is a toppling at site $i = L$ (rightmost end), one grain goes out of the system. Grains are added only at site 1.

The $1d$ Oslo ricepile model has an Abelian property [44]. The final height configuration does not depend on the order we topple the unstable sites. After addition of total $L(L + 1)$ grains, the pile reaches the critical steady state [44]. Since we have chosen the values of z_c to be 1 or 2, height profile, in the steady state, fluctuates between slope 1 and 2. For number of sites L , the number of possible configurations in the critical states are exponentially large, approximately $\frac{1+\sqrt{5}}{2\sqrt{5}}(\frac{3+\sqrt{5}}{2})^L$, for large L [84]. The probabilities of various configurations in the steady state differ from one another by many orders of magnitude unlike the BTW model

4.1.2 Model-B : $2d$ generalization of the Oslo model.

We note that the $1d$ Oslo model defined above can easily be generalized to two dimensions. We take a triangular region of a square lattice, the sites of which are indexed by (i, j) with $i, j \geq 1$ and $i + j \leq L + 1$. The height of the pile at site (i, j) is denoted by $h(i, j)$. Whenever the height difference between site (i, j) and any of it's neighbouring sites exceeds a critical value $z_c(i, j)$, assigned to the site (i, j) , there is a toppling at site (i, j) and one grain is transferred from this site to the lower neighbouring site towards the unstable direction. If there are more than one unstable directions, grain

is transferred towards the greatest slope. If the two directions have equal slope values, one grain is transferred randomly towards any one of these two directions. Whenever there is a toppling at a site (i, j) , $z_c(i, j)$ is reset randomly, independent of the history, to either 2 or 1 with probability p or q respectively, where $p + q = 1$. One grain is lost, whenever there is a toppling at the boundary sites *i.e.*, along $i + j = L + 1$ line. The model defined above in two dimensions is not Abelian because final stable configuration depends on the order we topple the unstable sites. Grains are added only at the corner site $(1, 1)$.

4.1.3 Model-C : The local limited model.

The local limited model [41] is a one dimensional model defined as follows. The slope z_i is defined as *i.e.*, $z_i = h_i - h_{i+1}$. Whenever value of the slope z_i at any site i is higher than a critical value z_c , which we choose to be 2, the site becomes unstable and two grains from the unstable site go to the right neighbour, *i.e.*, $h_i \rightarrow h_i - 2$ and $h_{i+1} \rightarrow h_{i+1} + 2$. Slope at any site may be negative in the local limited model. Whenever there is a toppling at site $i = L$ (rightmost end), two grains go out of the system simultaneously.

Grains are added uniformly everywhere. This model is also not Abelian. It is easy to see that in this case the maximum and the minimum slopes are 2 and 1 respectively. Total number of recurrent configurations in the steady state can be determined exactly, and varies as $\frac{4^L}{L^{3/2}}$ for large L [86]. It is known that the probabilities of occurrence of various configurations in the steady state is not equal, and may differ from one another by many orders of magnitude.

4.1.4 Model-D : Model with non-nearest neighbour transfer of grains.

Model-D is a variation of the model-C [41]. Whenever value of the slope $z_i > 2$ at any site i , the site becomes unstable and two grains from the unstable site are transferred to the right, one grain transferred to site $i + 1$ and the other one transferred to site $i + 2$, *i.e.*, $h_i \rightarrow h_i - 2$, $h_{i+1} \rightarrow h_{i+1} + 1$ and $h_{i+2} \rightarrow h_{i+2} + 1$. If there is a toppling near the right boundary, grain goes out of the pile. The order we relax unstable sites matters. The grains are added uniformly everywhere. The local slope can be negative as in model-C. The minimum and maximum slope in this model are also 1 and 2 respectively.

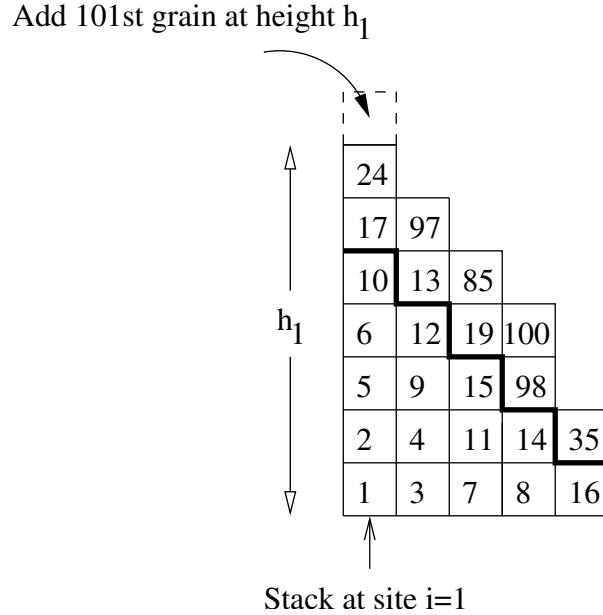


Fig 4.1: Rice pile of size $L = 5$ after addition of 100 grains. All grains are numbered by the time they were added to the pile. Minimum slope is denoted by the thick line.

The pile in all four cases is driven slowly, by adding one grain per unit time, starting with the initial configuration of height zero at all sites. We assume that the time interval between addition of two grains is chosen long enough so that all avalanche activity has died before a new grain is added. The grain added at time n will be labeled by the number n . We think of the grains at a particular site as stacked vertically, one above the other (Fig. 4.1). Whenever a grain is added at a site, it sits on the top of the stack. When one unstable grain leaves the stack, it is taken from the top of the stack. In model-C, when two grains leave a site, we first take out the topmost grain from the site and put it on the top of right nearest neighbour stack, then we take the second unstable grain and put it on the top of the first grain at right nearest stack. In model-D, we transfer the unstable grain, second from the top, to the right nearest neighbour and transfer the topmost one to next to the right nearest neighbour.

If a particular grain n enters a site i at time $t_{in}(i, n)$ and leaves the site at time $t_{out}(i, n)$, its residence time $T_i(n)$ at site i is defined as the time spent by the grain at the site i , *i.e.*, $T_i(n) = t_{out}(i, n) - t_{in}(i, n)$. The residence time of the n^{th} grain, $T(n)$, is the total time spent by the grain inside the pile. For a directed ricepiles in one dimension where grains move only in one direction and by one step in each toppling,

the residence time $T(n)$ equals to $\sum_{i=1}^L T_i(n)$ (e.g. in model-A and model-C). We define the function $Prob_L(T_j \geq t)$ as the probability that a new grain added in the steady state of the pile will have a residence time at site j is greater than or equal to t , and $Prob_L(T \geq t)$ as the probability that its total residence time in the pile is greater than or equal to t . Clearly, we have $Prob_L(T_j \geq 0) = Prob_L(T \geq 0) = 1$.

4.2 Relation between residence times at a site and height fluctuations.

We can understand the residence time distribution of grains at any site in terms of the fluctuation of height at that site. The $h_i(t)$ be the height of the pile at a site i just after the t^{th} grain has been added. The height $h_i(t)$ as a function of time t is a stochastic process and, in the steady state, it fluctuates in time between a upper bound, h_{max} , and a lower bound, h_{min} . In case of the height fluctuation at site 1, $h_{max} = 2L$ and $h_{min} = L$. The height $h_1(t)$ at the site 1 has a stationary probability distribution which is sharply peaked near its average value \bar{h}_1 , and has the width σ_{h_1} which is standard deviation of the fluctuation of height h_1 . In the steady state, the average value of h_1 varies as L , and the width σ_{h_1} varies as L^{ω_1} , where exponent $\omega_1 < 1$. For large L , the probability distribution of h_1 has a scaling form as given below.

$$Prob_L(h_1) = L^{-\omega_1} g\left(\frac{h_1 - \bar{h}_1}{L^{\omega_1}}\right) \quad (4.1)$$

In Fig. 4.1 we have shown a scaling collapse of various probability distribution of height at site 1, $Prob_L(\Delta h_1)$, where $\Delta h_1 = h_1 - \bar{h}_1$, for various values of system sizes, $L = 100, 200$ and 400 in the 1d Oslo ricepile model. We get a good collapse using the scaled variable $\Delta h/L^{\omega_1}$ where $\omega_1 \approx 0.25$. Here the scaling function $g(x)$ is nearly Gaussian for x near zero. But very large deviations of h_1 from the mean value are not well-described in the Gaussian approximation. Later we shall argue that in the Oslo model scaling function $g(x)$ varies as $\exp(-|x|^{\frac{1}{1-\omega_1}})$ for $x \gg 1$ and it varies as $\exp(-|x|^{\frac{3}{1-\omega_1}})$ for $x \ll -1$.

Let us consider variation of height h_1 at the first site with time t shown schematically in Fig. 4.2. Note that $h_1(t)$ is piecewise constant line segments, with possible jumps at the integer time t . Since the value of $h_1(t)$ is discontinuous at integer times, it is not immediately obvious that which value of height is assigned against the integer

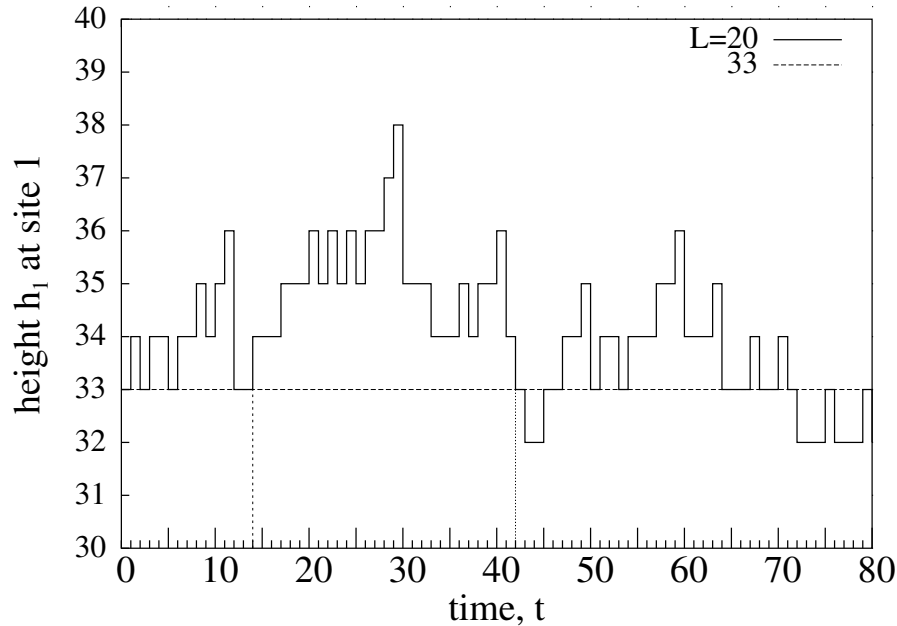


Fig 4.2: Fluctuation of height at first site with time plotted for the $1d$ Oslo ricepile model for $L = 20$. The horizontal line is at $h_1 = 33$ which is the most probable height. The first and second vertical lines are at $t = 14$ and $t = 42$ respectively.

time variable t . We shall use the following convention. The value of $h_1(t)$ at time t is denoted by the line segment which is just at the right of the coordinate t , *e.g.*, $h_1(0) = 33$, $h_1(1) = 34$, *etc.* A grain added at time t , when the height at the first site is $h_1(t-1)$, leaves the site at time t' , we must have $h_1(t') \leq h_1(t)$, and $h_1(t'') > h_1(t)$, for all t'' satisfying $t < t'' < t'$. As an example, for the time series of $h_1(t)$ shown in Fig. 4.2, the grain added at $t = 14$ stays at site 1 upto time $t = 41$ and then goes out of the site 1 at $t = 42$ (*i.e.*, just after addition of the $42nd$ grain), and so $T_1(14) = 28$. As $h_1(13) = h_1(12)$, the grain added at $t = 12$ comes out immediately, and hence $T_1(12) = 0$.

Let $Prob_L(T_1 \geq t|h_1)$ be the conditional probability that a grain stays at site 1 for time greater than t , given that it was added when the height was h_1 . Since $Prob_L(h_1)$ is the probability that height was h_1 when the grain was added, we have the following, summing over all possible values of h_1 .

$$Prob_L(T_1 \geq t) = \sum_{h_1=h_{min}}^{h_{max}} Prob_L(h_1) Prob_L(T_1 \geq t|h_1) \quad (4.2)$$

But $Prob_L(T_1 > t|h_1)$ can also be written as the conditional probability that the

height of the pile at site 1 would remain above h_1 for an interval $\geq t$, given that the height is h_1 in the steady state. This probability can be calculated from the general theory of Markov chains as the probability of first return to a height less than or equal to h_1 , given that we start with height h_1 in the steady state, and add one grain per unit time. The probability that no return has occurred up to time t decreases as $\exp[-\lambda(h_1)t]$ for large t , where $\lambda(h_1)$ is the largest eigenvalue of the reduced Markov matrix, with rows and columns corresponding to configurations with heights at site 1, below or equal to h_1 , removed [87, 88]. While it is not very easy to calculate $\lambda(h_1)$ exactly, clearly it decreases as h_1 decreases. For $h_1 = h_{max}$, it is $+\infty$ as the height at the site cannot be higher than h_{max} and T_1 must always be zero. Also it is very small for h_1 near h_{min} , as the pile returns to very low values of h_1 only rarely.

For large t , in the sum in r.h.s. of Eq.(4.2), only terms with h_1 near h_{min} make a significant contribution. In this case, it is a reasonable approximation to replace the function $Prob_L(T_1 > t|h_1)$ by a simple exponential, with $\lambda(h_1) = \langle T_1 \rangle_{h_1}$. Thus we write, for large t ,

$$Prob_L(T_1 > t|h_1) \simeq \exp(-t/\langle T_1 \rangle_{h_1}) \quad (4.3)$$

It is easy to write the conditional expectation value of the residence time at the first site, $\langle T_1 \rangle_{h_1}$, given that the grain was added at the height h_1 in terms of the stationary probability distribution $Prob_L(h_1)$ exactly as

$$\langle T_1 \rangle_{h_1} = \frac{Prob_L(\text{height} > h_1)}{p_1 Prob_L(h_1)} \quad (4.4)$$

where p_1 is the probability of adding a grain at site $i = 1$. When we add grains only at first site, $p_1 = 1$ and when we add grains uniformly everywhere, $p_1 = 1/L$.

Proof : Define an indicator function $\eta_{n,t} = 1$, if the n^{th} grain is at height h_1 at time t , and zero otherwise. Clearly, the sum of $\eta_{n,t}$ over t is the residence time of n^{th} grain at height h_1 . Then, averaging over n we get the mean residence time. But the sum of $\eta_{n,t}$ over n and t both gives a contribution whenever there is a grain at height h_1 , and hence is equal to $N Prob_L(\text{height} \geq h_1)$ where N is total number of grains added and N is very large. Dividing this sum by average number of grains added at height h_1 , which is equal to $p_1 N Prob_L(h_1)$, we get $\langle T_1 \rangle_{h_1}$. Hence, Eq.(4.4) follows.

We substitute this estimate of $\langle T_1 \rangle_{h_1}$ in Eq. (4.3). We note that for large t , the

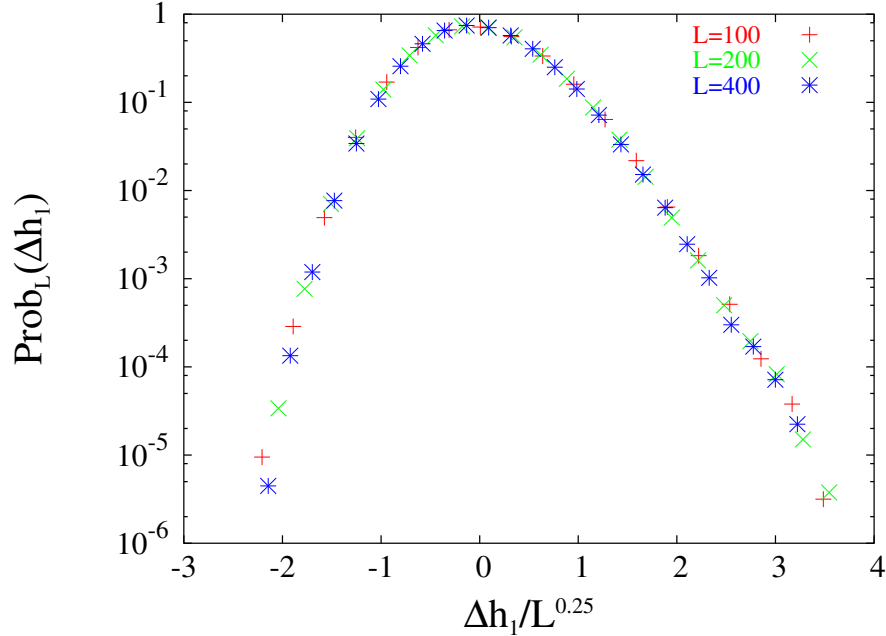


Fig 4.3: Scaling collapse of various probability distributions $Prob_L(\Delta h_1)$ where Δh_1 is the deviation of height at site 1 from its average value, for different system sizes, $L = 100, 200$ and 400 for the $1d$ Oslo ricepile model.

terms in the summation that contribute significantly correspond to h_1 near h_{min} . For these values of h_1 , $Prob(\text{height} > h_1)$ is nearly 1, and $\langle T_1 \rangle_{h_1}$ may be replaced, with small error, by $1/Prob_L(h_1)$ (see Eq. 4.4). Then Eq. (4.2) can be approximately written as given below.

$$Prob_L(T_1 \geq t) \simeq \sum_{h_1=h_{min}}^{h_{max}} Prob_L(h_1) e^{-t Prob_L(h_1)} \quad (4.5)$$

Thus, the distribution of residence times T_1 can be expressed in terms of the probability distribution $Prob_L(h_1)$ of height h_1 .

4.3 Probability of minimum slope configuration in the Oslo ricepile model

4.3.1 Explicit calculation of $Prob_L(h_1)$ small L .

The probability of slope of the pile being 1 in the steady state can be exactly calculated numerically for small L using the operator algebra satisfied by addition operators [44].

We denote any stable configuration by specifying slope values at all sites from $i = 1$ to $i = L$ by a string of 0's, 1's and 2's, *e.g.*, $|1202\dots212\rangle$. Whenever slope z_i becomes 2 after additions or toppling at site i , we denote such slope by $\bar{2}$, *i.e.*, $|\dots\bar{2}\dots\rangle$. Overbar denotes that the site may topple or become stable with probability q or p respectively, *i.e.*, $|\dots1\bar{2}1\dots\rangle \rightarrow p|\dots121\dots\rangle + q|\dots\bar{2}0\bar{2}\dots\rangle$, etc. Using these two toppling rules repeatedly and the Abelian property of the $1d$ Oslo ricepile model, we can relax any unstable configurations.

Let us now consider the state $|\bar{2}\bar{2}\dots\bar{2}\bar{2}\rangle$ where all the sites have slope values 2 and not stable. If we add one more grain at site $i = 1$ in this state, we get the same state back (toppling the site with $z_i = 3$ repeatedly) which implies that it is the steady state. So if we relax this configuration fully, we get probabilities of all the configuration in the steady state. For example, if we relax $|\bar{2}\bar{2}\rangle$ for $L = 2$, we get the following sequence,

$$\begin{aligned} |\bar{2}\bar{2}\rangle &\rightarrow p|2\bar{2}\rangle + q|1\bar{2}\rangle \rightarrow \\ &p^2|22\rangle + pq|12\rangle + pq|1\bar{2}\rangle + q^2|\bar{2}1\rangle \rightarrow \dots \rightarrow \\ &p^2|22\rangle + (p + p^2)q|12\rangle + (p + p^2)q^2|21\rangle + (p + p^2)q^3|02\rangle + (1 + p)q^4|11\rangle. \end{aligned}$$

Below we make a table of explicit formulas for probability of the minimum slope for smaller values of system sizes $L = 2, 3, 4$.

System size L	Probability of the minimum slope
$L = 2$	$(1 + p)q^4$.
$L = 3$	$(1 + 4p + 6p^2 + 5p^3 + 2p^4)q^{10}$.
$L = 4$	$(1 + 10p + 45p^2 + 125p^3 + 241p^4 + 341p^5 +$ $369p^6 + 307p^7 + 190p^8 + 81p^9 + 18p^{10})q^{20}$.

4.3.2 Asymptotic behaviour of $Prob_L(h_1)$ for large L .

The probability of maximum slope configuration (*i.e.*, when $h_1 = 2L$) can be easily calculated. We start with the unstable configuration $|\bar{2}\bar{2}\dots\bar{2}\bar{2}\rangle$. The probability that no site topples in this unstable configuration is p^L and this is the probability of the maximum slope configuration (*i.e.* $h_1 = 2L$) in the steady state. That this probability varies as exponentially with L can be incorporated in the scaling hypothesis by assuming that the scaling function $g(x)$ in Eq. (4.1) varies as $\exp(-ax^{\frac{1}{1-\omega_1}})$ for $x \gg 1$ where a is a constant.

The probability of the minimum slope configuration cannot be calculated so easily. However we argue below that this probability asymptotically varies as $\exp(-\kappa L^3)$ where κ is a constant.

Firstly, the above calculation for $L = 2$ showed that, in the steady state, the probability of the minimum slope configuration is $\mathcal{O}(q^4)$. For $L = 3$, we calculated this probability explicitly (see the table in section 4.3.1) which is $\mathcal{O}(q^{10})$. Similar analysis, for other values of $L = 1$ to 20, shows that the probability of minimum configuration is $\mathcal{O}(q^{m_L})$, where m_L is exactly given by the formula $L(L+1)(L+2)/6$. The coefficient of q^{m_L} in the probability is harder to compute explicitly for large L . We conjecture that this simple formula holds true for all L . Then for sufficiently small q , the probability of minimum height configuration in the 1d Oslo model varies as $\exp[-\kappa(q)L^3]$, where $\kappa(q)$ is a q -dependent function. Then, as there is no change in the behaviour of the Oslo ricepile expected, as a function of q , this behavior should persist for all non-zero q . For the scaling function, this would imply that $g(x)$ varies as $\exp[-\kappa(q)|x|^{\frac{3}{1-\omega_1}}]$ for $x \gg 1$.

We have calculated, $Prob_L(\text{slope} = 1)$, i.e., the probability of the minimum slope configuration, exactly numerically for $q = 0.50, 0.60, 0.75$ for $L = 1$ to 12 and the $\log_e[Prob_L(\text{slope} = 1)]$ has been plotted versus $\frac{L(L+1)(L+2)}{6}$ in Fig. 4.4.

More specifically, consider a very low-slope unstable configuration $|11\dots 1\bar{2}\rangle$ which has total L number of grains with slopes 1 at all sites except at the last site with slope 2 and estimate the probability to go to the minimum slope from this configuration. To do this, we have to remove L grains, and each grain has to be moved a distance of $\mathcal{O}(L)$ on the average. Thus we need $\mathcal{O}(L^2)$ steps for large L , and each step requires a factor q in probability. Actually the probability of transition from this configuration with height $h_{min} + 1$ to the minimum slope configuration (with height h_{min}) is $\mathcal{O}(q^{\frac{L(L+1)}{2}})$ and the coefficient of $q^{\frac{L(L+1)}{2}}$ in this case is exactly 1. Now the probability of minimum slope can be written in a general form as given below.

$$Prob(\text{slope} = 1) \sim \exp[-\kappa(q).L^3] \quad (4.6)$$

where $\kappa(0) = \infty$ and $\kappa(1) = 0$. The different asymptotic behaviour of large deviations in $g(x)$ is somewhat unexpected, but has been seen in other problems, such as distribution of the large deviation of current in the asymmetric exclusion process in a ring [89].

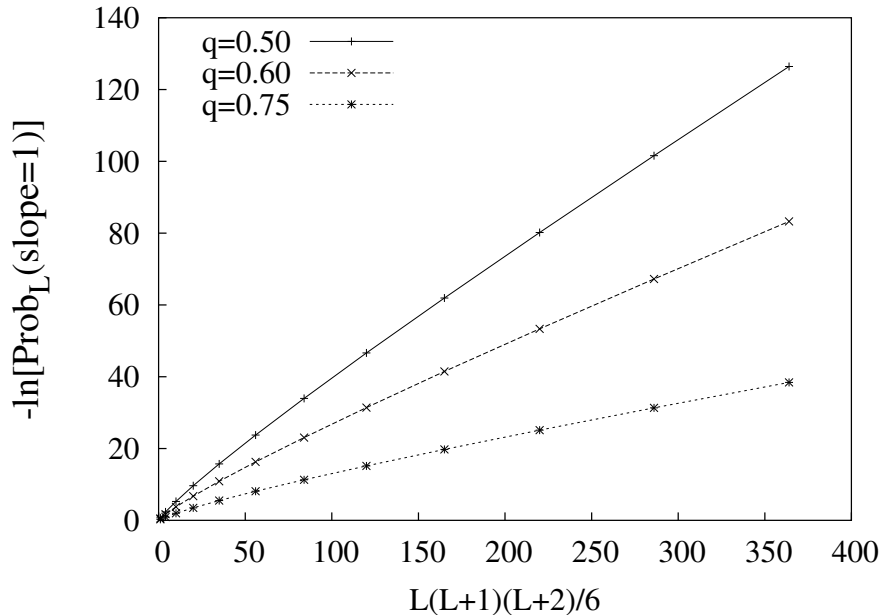


Fig 4.4: Logarithm of the probability of occurrence of minimum slope configuration (calculated exactly) is plotted versus $L(L+1)(L+2)/6$ for the 1d Oslo ricepile model for $L = 1$ to 12.

Large deviations of fluctuation in a system have been studied extensively [91, 92] and especially recently it has attracted much attention for systems in non-equilibrium steady state [89, 93, 94, 95, 96, 97]. In the previous section, we have studied the probability distribution of residence times of grains at a site in the 1d Oslo ricepile model. We will discuss this in detail in later sections and show that tail of the distribution is determined by the deeply buried grains which come out only in rare height fluctuations.

4.3.3 Verification by Monte Carlo simulation.

In this subsection, we numerically study the probability of large deviations of steady state height fluctuation of the pile in the one dimensional Oslo ricepile model and test our analytic arguments given in the previous subsection. We use a Monte Carlo algorithm with importance sampling (IS). We show that the probability of minimum slope configuration of the pile varies as $\exp(-\kappa L^3)$ for large L where κ is a constant. We also calculate the probability distribution function $P(\Delta h|L)$ where Δh is the deviation of the height of the pile from its average value and get a scaling collapse of data for various system sizes.

The probability distribution function $Prob(h_1|L)$ decays sharply and the event when the $h_1 \approx L$ happens very rarely. Now we give an estimate of how small are the probabilities of occurrences of these rare events. We have calculated probability of minimum slope configuration in the steady state exactly numerically in the Oslo ricepile model for $L \leq 12$ using a simple code written in *C*. The number of topplings required to get to the final stable configuration from $|\bar{2}\bar{2}\dots\bar{2}\bar{2}\rangle$ increases L^3 , and hence complete traversal of all possible branches of the different possibilities takes a computer time that varies as $\exp(L^3)$. For example for $L \geq 13$, the computer CPU time is so large that it will take years for the code to be over and one certainly cannot calculate this probability using this simple enumeration algorithm.

Even for system size as small as $L = 6$ and $L = 7$, the probabilities of minimum slope are 4.81×10^{-11} and 1.76×10^{-15} respectively. For $L = 12$, this probability is much smaller, 1.23×10^{-55} . In Fig. 4.4 we have plotted Logarithm of the probability of occurrence of minimum slope configuration versus $L(L+1)(L+2)$. In the table below we give exact (upto five significant digits) numerical values of probabilities of the minimum slope configuration for $L \leq 12$ calculated using the relaxation rules mentioned in section 4.3.1. We can see that $L \geq 6$, it is almost impossible to get this rare event in a simple Monte Carlo simulation.

<u>System size L</u>	<u>Probability of the minimum slope for $p = q = 1/2$</u>
$L = 2$	9.3750×10^{-2}
$L = 3$	5.1269×10^{-3}
$L = 4$	6.4540×10^{-5}
$L = 5$	1.4746×10^{-7}
$L = 6$	4.8163×10^{-11}
$L = 7$	1.7660×10^{-15}
$L = 8$	5.6961×10^{-21}
$L = 9$	1.2640×10^{-27}
$L = 10$	1.5074×10^{-35}
$L = 11$	7.5371×10^{-45}
$L = 12$	1.2317×10^{-55}

To get probabilities of various steady state configurations, one can relax the unstable configuration $|\bar{2}\bar{2}\dots\bar{2}\bar{2}\rangle$ fully. To do this, a random number is assigned to each of the L sites using a pseudo random number generator which generates number between 0 and

1 uniformly. When $z_i = \bar{2}$ at site i , the random number at that site is checked and one makes the site stable if the random number is less than or equal to p and topple the site i if it is greater than p . After each toppling at a site, a new random number is generated at the site, independent of any history. When the slope value at a site increases from $z_i = 1$ to $z_i = 2$, one assigns a new random number to the site. The site i with $z_i = 3$ is toppled with probability 1. One has to keep on relaxing $|\bar{2}\bar{2} \dots \bar{2}\bar{2}\rangle$ until slopes at all the sites are less than or equal to 2 and the random numbers at all the sites are less than or equal to p and one gets a stable steady state configuration. So one starts with N number of initial configurations, all with $|\bar{2}\bar{2} \dots \bar{2}\bar{2}\rangle$, simultaneously topple all the unstable sites of each configuration until a stable configuration is reached. At the end, one gets N_{min} configurations with $|11..11\rangle$, out of total N number of steady state configurations. Now $\frac{N_{min}}{N}$ is the required probability of the minimum slope configuration in the steady state.

Clearly simple Monte Carlo algorithm given above cannot sample the low slope configurations at all when L is large. Because the number $\frac{N_{min}}{N}$ is very small for large L and therefore, after fully relaxing N initial configurations, one almost always get $N_{min} = 0$, unless N is too large. Now we explain the idea of importance sampling for getting the steady state weight of the minimum slope configuration. We use an important fact in our algorithm that the Oslo ricepile model is Abelian and the order of toppling the unstable sites does not matter. Since we are not interested in the probabilities of other stable configurations, we like to topple in such a way that we do not get trapped in any one of the other stable configurations and at the end, we get only the minimum slope configuration.

To explain this, let us start with an unstable configuration C_0 where there are some sites with $z_i = \bar{2}$ and other sites are stable. Now random numbers are assigned to the sites with $z_i = \bar{2}$. Consequently some of these sites become stable with $z_i = 2$ and some become unstable. At the next step, after toppling all the unstable sites with $z_i = 2$ once and then toppling the resultant unstable sites with $z_i = 3$, we can get a set \mathcal{S} of stable configurations, say S_1, S_2, S_3 , with cumulative probability $P(\mathcal{S})$ and a set \mathcal{U} of unstable configurations (where $z_i = 0, 1, 2$ or $\bar{2}$), say U_1, U_2, U_3, U_4 , with probability of each unstable configuration U_i is $P(U_i)$. This is schematically shown in Fig.4.5. If we reject these stable configurations and directly go to the space of unstable configurations, then the probability of each unstable configuration $P(U_i)$ is normalized to be $P'(U_i) = \frac{P(C_i)}{1-P(\mathcal{S})}$. At each step of toppling, we take this factor $[1 - P(\mathcal{S})]$ out and keep on multiplying the factors at various steps until we reach the minimum slope

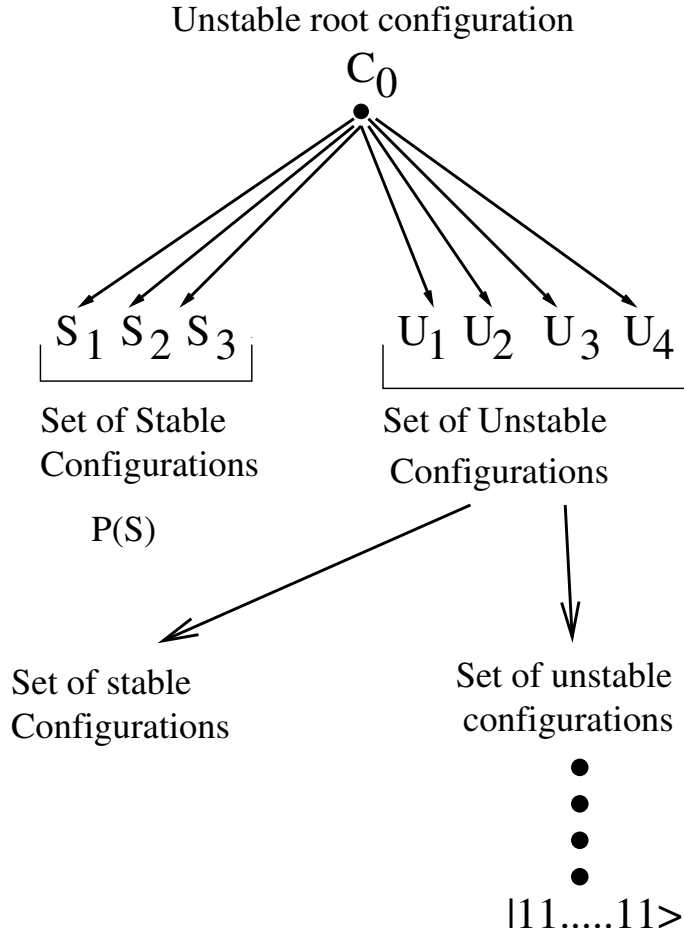


Fig 4.5: Schematic diagram illustrating our algorithm. If we start with unstable configuration C_0 , at the next step after toppling the unstable sites, we get a set \mathcal{S} of stable configurations S_1, S_2, S_3 and a set \mathcal{U} of unstable configurations U_1, U_2, U_3, U_4 . The probability of getting any stable configuration is $P(\mathcal{S}) = Prob(S_1) + Prob(S_2) + Prob(S_3)$.

configuration $|11\dots 11\rangle$.

For example, if we relax $|\bar{2}\bar{2}\bar{2}\dots\bar{2}\rangle$, using the relaxation rules explained in section 4.3.1, we get the following.

$$\begin{aligned}
 |\bar{2}\bar{2}\bar{2}\dots\bar{2}\rangle &\rightarrow p^L|222\dots 2\rangle + (p^{L-1} + p^{L-2} + \dots + p + 1)q|1\bar{2}\dots\bar{2}\bar{2}\rangle \\
 &\rightarrow p^L|222\dots 2\rangle + (1 - p^L)|\bar{1}\bar{2}\dots\bar{2}\bar{2}\rangle
 \end{aligned}$$

We see that if we start with the configuration $|\bar{2}\bar{2}\bar{2}\dots\bar{2}\rangle$ (C_0), at the first step there are two possibilities, (1) all the sites becomes stable or (2) at least one site becomes unstable and topple. In the case of second possibility, after toppling the unstable sites with $z_i = 2$ once and then toppling all the resultant unstable sites with $z_i = 3$, we

get an unstable configuration U_1 with $|1\bar{2}\bar{2}\dots\bar{2}\rangle$ with probability $(1 - p^L)$. We get the stable configuration $|22\dots 2\rangle$ with probability p^L . Now we reject the stable configuration $|222\dots 2\rangle$ from our list and can directly go to the configuration $|1\bar{2}\dots\bar{2}\rangle$ but with a multiplicative weight factor $(1 - p^L)$ to the unstable configuration.

Therefore in the simplest strategy, one thinks of different possible configurations in the course of evolution at each step t as a branching tree. If we reach a configuration \mathcal{C}_t at a node at the t -th step, the probability of the process dying is say $a(\mathcal{C}_t)$, we do not allow the process to die, and select one of the remaining branches with probability equal to their original probability, divided by the factor $[1 - a(\mathcal{C}_t)]$, and the final survival probability is estimated by product of such factors. This procedure is not satisfactory for our problem, as there are some nodes have first-generation descendants, but these descendants do not have any descendants. For example let us consider a case for $L = 5$. We start with, say a configuration $|\bar{2}110\bar{2}\rangle$. Now the first generation descendants will eventually die if the last site $i = 5$ gets stable at the next time step. If one reaches such a node, the process will die after one more generation, but it is difficult to identify these directly and avoid them, without a computationally expensive depth-search. Thus, the resulting process still has a nonzero probability of reaching such a node at the next step, and the overall probability of survival still decreases exponentially with the depth of the tree.

In the following we describe a technique that does manage to estimate the small survival probabilities, but at the cost of having to define and update one additional random real variable at each site of the lattice.

Algorithm for sampling rare events

We start with a configuration with all sites unstable, and all $z_i = \bar{2}$. Let $x(i, t)$ be the random number at site i at the end of the update-step t . Initially, at $t = 0$, all $x(i, 0)$ are independent random variables lying between 0 and 1.

The Abelian property of the Oslo model implies that it does not matter in which order we topple the unstable sites. We choose the following rule: At any time step, we first topple any unstable sites with $z_i = 3$. When all the unstable sites are with slope $z = \bar{2}$, we topple the site having the largest random number, if the random number is greater than p . If the number is less than p , the avalanche stops. After the toppling, the random number at the site is reset to a new value, independent of the previous

history. This constitutes the end of one update step. Note that one update step may involve more than one topplings at sites with $z = 3$, but there is exactly one toppling at a site with $z = \bar{2}$ in each update step.

The toppling history can be specified by giving the site with $z = \bar{2}$ selected for toppling at each update step, and the random number at that site at the time of toppling. Let $j(t)$ be the site selected for toppling at the t -th update step, and $y(t)$ be the value of the random number at $j(t)$ at the time, i.e., $y(t) = x(j(t), t)$ which is the largest among the random numbers associated with slopes $z = \bar{2}$. We shall denote the toppling history as a sequence upto time t by $\mathcal{T}_t = \{[j(t'), y(t)]; t' = 1 \text{ to } t\}$. It is straight forward to determine the conditional joint probability distribution of $[j(t+1), y(t+1)]$, given only the toppling history \mathcal{T}_t . Firstly, given the sites that have been toppled, one can determine the set of unstable sites $\mathbf{u}(t)$ with $z = \bar{2}$, out of which the site with the maximum random number has to be selected at update-step $t+1$. Since we know that $x(j, t)$ for any site $j \in \mathbf{u}$ has not been selected for toppling earlier since it was reset, it must be smaller than all the corresponding y 's selected since then. If it was reset at update step $t_{prev}(j, t)$, we must have

$$x(j, t) \leq x_{max}(j, t) \quad (4.7)$$

where $x_{max}(j, t)$ is the maximum value of $x(j, t)$ allowed by these constraints

$$x_{max}(j, t) = \text{Min}\{y(t') : t_{prev}(j, t) \leq t' \leq t\}. \quad (4.8)$$

Let us now define a function $g(\xi)$ as $g(\xi) = \xi$, for $0 \leq \xi \leq 1$, and $g(\xi) = 1$ for $\xi > 1$. Then, the conditional probability distribution of $x(j, t)$, for $j \in \mathbf{u}(t)$, given the toppling sequence \mathcal{T}_t , is

$$\text{Prob}(x(j, t) \leq x | \mathcal{S}_t) = g\left(\frac{x}{x_{max}(j, t)}\right) \quad (4.9)$$

In addition, there is no further correlation between the values $x(j, t)$ for $j \in \mathbf{u}(t)$, beyond that implied by the conditions that $x(j, t) \leq x_{max}(j, t)$, we must have

$$\text{Prob}[y(t+1) \leq y | \mathcal{T}_t] = \Phi_t(y) = \prod_{j \in \mathbf{u}(t)} g\left(\frac{y}{x_{max}(j, t)}\right) \quad (4.10)$$

If we put an additional condition that $y(t+1) > p$, the corresponding conditional

distribution is given by

$$\text{Prob}[y(t+1) \leq y | \{\mathcal{T}_t, y(t+1) \geq p\}] = \frac{\Phi_t(y) - \Phi_t(p)}{1 - \Phi_t(p)} \quad (4.11)$$

Let $F(t+1)$ be the probability that $y(t+1) \geq p$. Clearly, we have

$$F(t+1) = 1 - \prod_{j \in \mathbf{u}(t)} g\left(\frac{p}{x_{\max}(j, t)}\right) \quad (4.12)$$

Also the relative weight of a particular history \mathcal{T}_t being realized without the avalanche getting stopped is $\prod_{t'=1}^t F(t')$.

We implement this procedure in the algorithm as follows: As time evolves, we update the configuration variables $z_i(t)$ and also keep an array $\{x_{\max}(i, t)\}$, which is regularly updated to store what is known about the largest allowed value of the random number stored at that point.

At $t = 0$, $z_i(0) = \bar{2}$ for all i , and $x_{\max}(i, 0) = 1$. At any later update step t , we first topple any sites with $z = 3$. Once this is done, using the toppling process, we determine the set of unstable sites $\mathbf{u}(t)$ where $z = \bar{2}$. We randomly select which of the \mathbf{u} has the largest $x(j, t)$ and its value $y(t+1)$ having the distribution given by 4.11. We generate the largest $x(j, t)$ using the algorithm given in the next paragraph below.

For example, consider independent random variables x_1, x_2, x_3, x_4, x_5 , which are known to be uniformly distributed between the respective intervals as given below,

1. $x_1 \in [0, 1]$
2. $x_2 \in [0, u]$
3. $x_3 \in [0, u]$
4. $x_4 \in [0, v]$
5. $x_5 \in [0, v]$

where we take $1 \geq u \geq v$ without loss of generality. Then the cumulative probability distribution of y , the largest among these random numbers, is given by

$$\begin{aligned} \text{Prob}(y \leq x) &= x, \text{ for } u \leq x \leq 1 \\ &= x^3/u^2, \text{ for } v \leq x \leq u; \\ &= x^5/(u^2v^2), \text{ for } 0 \leq x \leq v. \end{aligned} \quad (4.13)$$

To generate a variable y with this distribution, we use the following algorithm: generate a number z randomly between 0 and 1. Then following cases are possible.

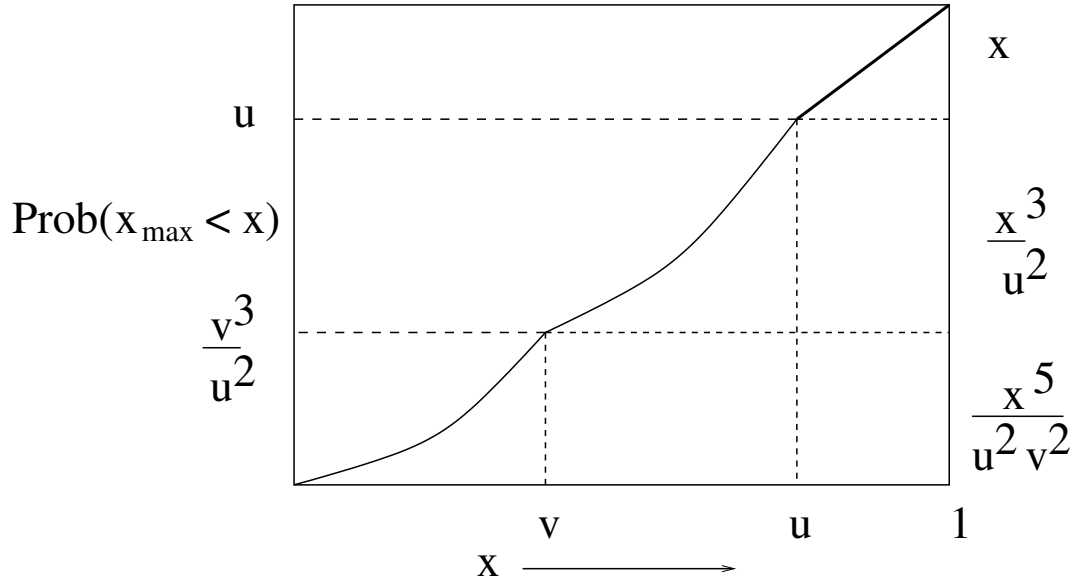


Fig 4.6: Plot of the probability $Prob(x_{max} < x)$ versus x .

1. If $u < z \leq 1$ we choose the largest random number to be $y = z$ and the maximum is surely x_5 .
2. If $v^3/u^2 < z \leq u$, we choose the largest random number to be $y = (zu^2)^{1/3}$ and the maximum is chosen between x_3, x_4 and x_5 with probability $1/3$ each.
3. If $0 \leq z \leq v^3/u^2$, we choose the largest random number to be $y = (zu^2v^2)^{1/5}$ and the maximum is chosen between x_1, x_2, x_3, x_4 and x_5 with probability $1/5$ each.

If the resulting value of y is less than p , the value is rejected, and the whole procedure is implemented afresh. Probability distributions for the maximum of more variables can be obtained similarly.

We calculate the attrition factor $F(t + 1)$ using Eq.(4.12). We then topple at the selected site $j(t + 1)$, and update the values of $x_{max}(j(t + 1)) = 1$, and set $x_{max}(j') = y(t + 1)$ for $j' \neq j$. And iterate this process. Clearly this process will not die until the minimum slope configuration is reached. The estimate of probability of the minimum configuration is obtained by calculating the weight function

$$W_{min} = \prod_{\tau} F(\tau) \tag{4.14}$$

where the product is over all update steps τ required to reach the minimum config-

uration. For different realizations, we get different values of W_{min} . We average over different values by taking many realizations.

We illustrate this procedure by a simple example. Consider a rice pile with $L = 6$. At $t = 0$, we have $\mathbf{u}(0) = \{1, 2, 3, 4, 5, 6\}$, as all sites are unstable. Also, at this stage $x_{max}(i, 0) = 1$ for all sites. In this case, the probability distribution of $y(0)$ is given by

$$\text{Prob}(y(0) \leq y | y(0) > p) = y^6 / (1 - p^6), \text{ for } p \leq y \leq 1. \quad (4.15)$$

This can be generated as follows: Select a random number z uniformly distributed between 0 and 1. If $z^{1/6} > p$, put $y(0) = z^{1/6}$. If not, discard this value, and choose again. In this case, we get $F(1) = (1 - p^6)$. Then, we choose $j(0)$ as one of the sites from $\mathbf{u}(0)$ at random, with equal probability. Say, we get $j(0) = 2$. Then, we topple at this site. This makes sites 1 and 3 unstable, and we topple there as well. Toppling at all unstable sites with $z = 3$, we finally get the configuration with $\mathbf{u}(1) = \{2, 3, 4, 5, 6\}$, and because of forced topplings, $x_{max}(i, 1)$ at all these sites is set to 1. So, now

$$\text{Prob}(y(1) \leq y | y(0) > p) = y^5 / (1 - p^5), \text{ for } p \leq y \leq 1, \quad (4.16)$$

and $F(2) = (1 - p^5)$. Now we choose $j(1)$ at random from $\mathbf{u}(1)$, say $j(1) = 4$. Toppling at this site induces toppling at other sites, and finally we get the configuration of unstable sites $\mathbf{u}(2) = \{1, 3, 4, 5, 6\}$, and we have $x_{max} = 1$ at all these sites. We now generate the variable $y(2)$, which turns out to have the same distribution as $y(1)$. Then we have $F(3) = (1 - p^5)$ again. Now we choose a site from $\mathbf{u}(2)$ and so on.

Results.

Since the final product of all the factors in each realization is a very small number, we keep track of logarithm of these factors and final product. We do the above procedure for many realizations and take the average of the logarithm of the final weight W_{min} . For a random variable X , we know $\langle \ln X \rangle \leq \ln \langle X \rangle$ and therefore the estimated logarithm of the probability W_{min} is the lower bound of probability of minimum slope. In Fig.4.7 we have plotted negative of logarithm of the probability of the minimum slope configuration in the steady state with $L(L + 1)(L + 2)$ and fit it with a straight line. We have compared our results obtained from two procedures, *i.e.*, exact numerical calculation and the Monte Carlo simulation and plotted negative of logarithm of the probabilities against $L(L + 1)(L + 2)$ in Fig.4.8 for L upto 12. In Fig.4.9, we have

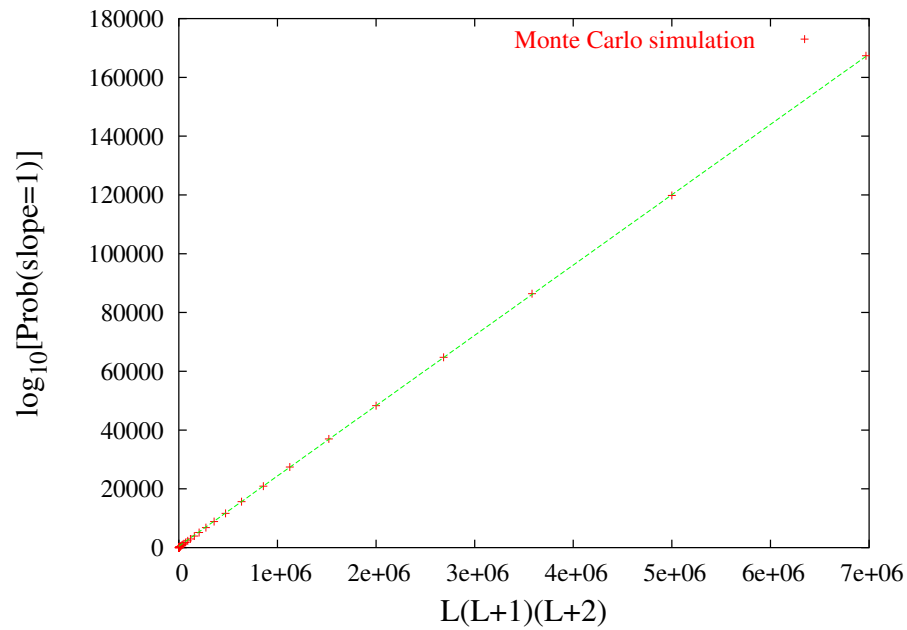


Fig 4.7: Monte Carlo simulation: Logarithm of probability of the minimum slope configuration plotted against the system size L for the 1d Oslo ricepile model. The data is averaged over 10^3 realizations.

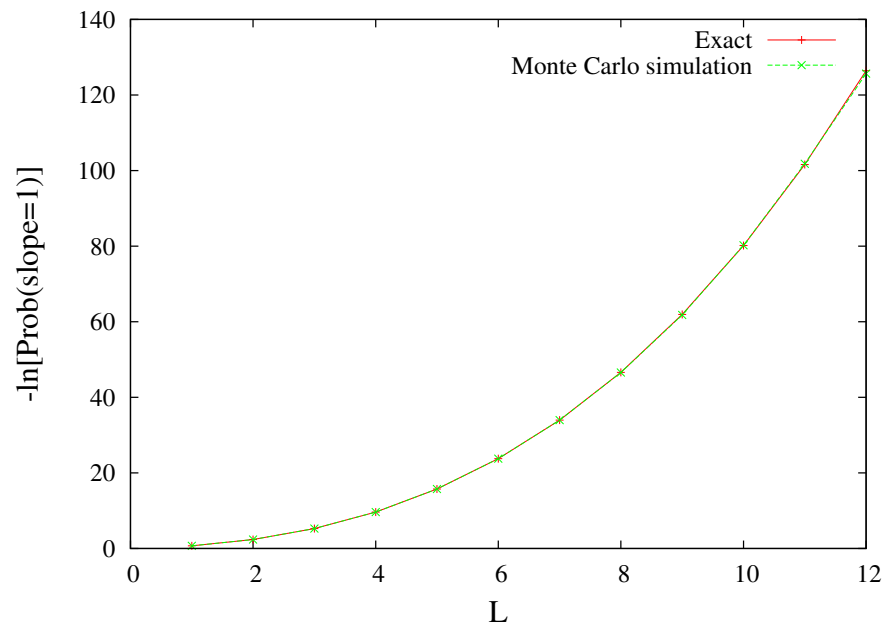


Fig 4.8: Exact numerical calculation and the Monte Carlo simulation for $L \leq 12$: Logarithm of the probability of the minimum slope configuration is plotted against the system size L for the 1d Oslo ricepile model. The data is averaged over 10^5 realizations.

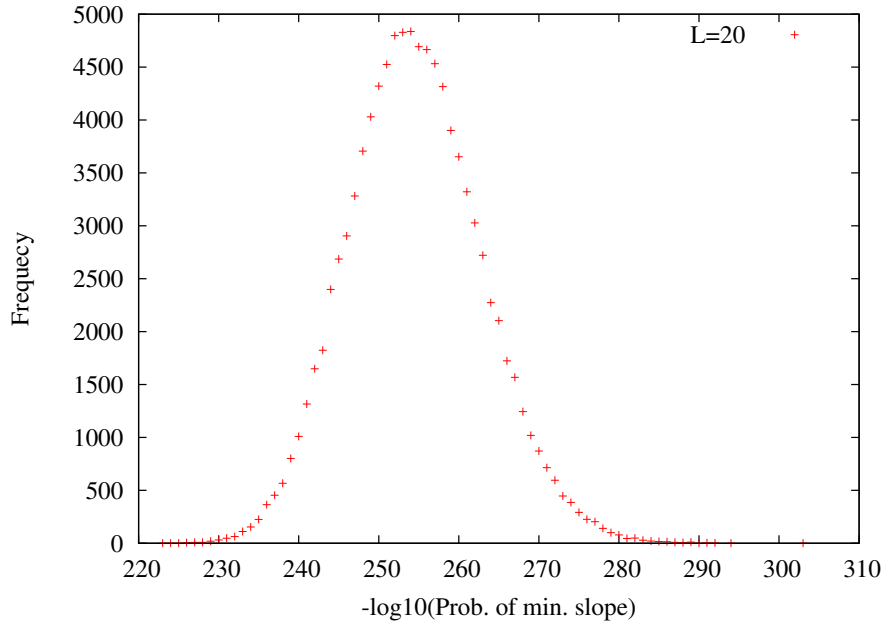


Fig 4.9: The frequency distribution of $\log_{10}(\text{Prob. of min. slope})$ taking bin size = 1 and for $L = 20$ for the 1D Oslo ricepile model. The data is averaged over 10^5 initial realizations.

plotted frequency distribution of the final product at each realization. The total number of realizations we have taken for the frequency distribution is 10^5 . Although we cannot estimate $\langle \log_{10}(W_{min}) \rangle$ for large L , we can calculate $\log_{10}(\langle W_{min} \rangle)$ and show from the numerical analysis that $-\log_{10}(\langle W_{min} \rangle)$ varies as L^3 for large L . We report, in the table below, values of $\log_{10}(\langle W_{min} \rangle)$, $\langle \log_{10} W_{min} \rangle$ and estimate of spread (standard deviation) in $\langle \log_{10}(W_{min}) \rangle$ for various system sizes.

L	$\log_{10}(\langle W_{min} \rangle)$	$\langle \log_{10}(W_{min}) \rangle$	Spread in $\langle \log_{10}(W_{min}) \rangle$
10	-35.4	-40.7	± 2.9
11	-45.0	-52.0	± 3.4
12	-55.6	-65.2	± 3.9
13	-69.9	-80.4	± 4.4
14	-85.8	-97.8	± 4.9
15	-102.0	-117.4	± 5.4
16	-123.4	-139.4	± 6.0
17	-164.2	-164.2	± 6.6
18	-171.4	-191.7	± 7.2

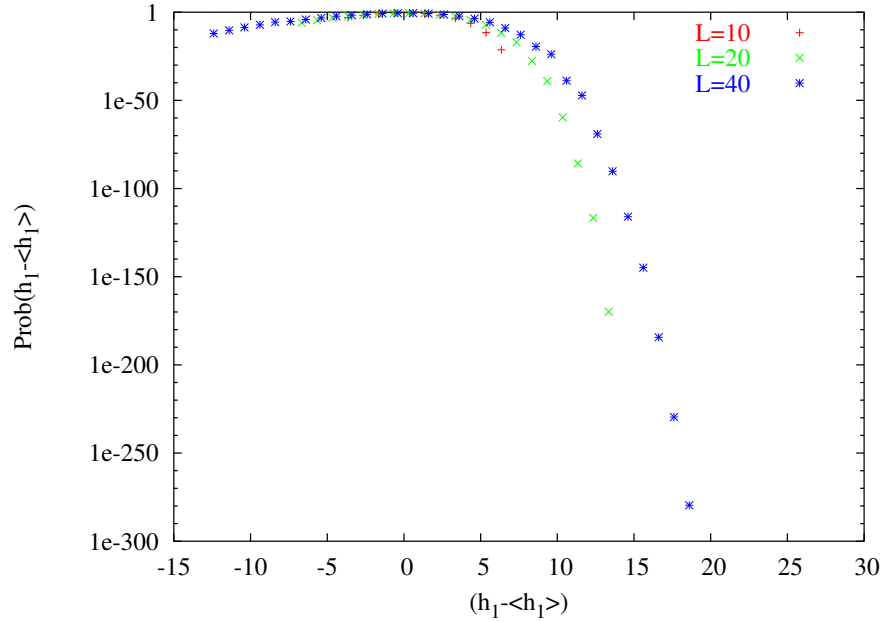


Fig 4.10: Probability distribution of height at site 1 $Prob_L(h_1 - \langle h_1 \rangle)$ versus $(h_1 - \langle h_1 \rangle)$ is plotted for system sizes $L = 10, 20, 40$ for the 1d Oslo ricepile model. The data is averaged over 10^5 initial realizations.

19	-198.0	-221.9	± 7.8
20	-230.0	-255.1	± 8.3

We can also calculate the full probability distribution $Prob_L(h_1)$ of height h_1 at site 1. After we start relaxing the unstable configuration $|\bar{2}\bar{2}\bar{2}\dots\dots\bar{2}\rangle$, the height at site 1 gradually decreases. At some step of relaxation, the height at first site becomes $h_1 \leq h$ for the first time in the course of relaxation. We multiply all the previous factors, $F(t)$'s, upto this step and this product gives the probability of height at the first site being less than or equal to h , i.e., $Prob_L(h_1 \leq h)$.

$$Prob_L(h_1 \leq h) = \prod_{\{C_t: h_1 > h\}} F(t) \tag{4.17}$$

We take the average of this product over many realizations. In Fig.4.10, we have plotted $Prob_L(h_1 \leq h)$ for $L = 10, 20, 40$. The data is averaged over 10^5 initial realizations. In Fig.4.11, we get a good scaling collapse by plotting $L^{\omega_1} Prob_L(h_1 = h)$ against the scaling variable $(h_1 - \bar{h}_1)/L^{\omega_1}$ where $\omega_1 \approx 0.25$. We see from the scaling plot the scaling function is highly asymmetric about the origin.

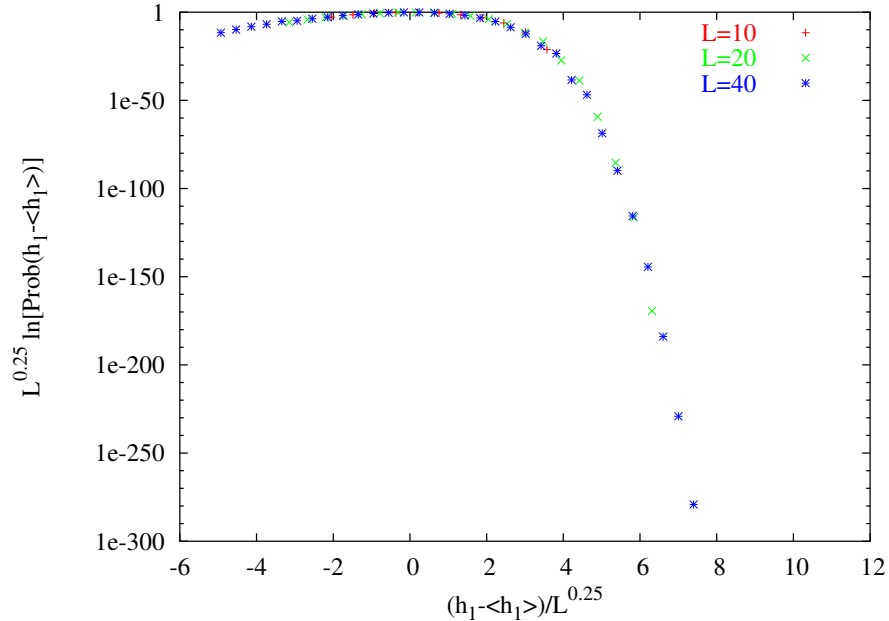


Fig 4.11: Scaling collapse: $L^{0.25} Prob_L(h_1 - \langle h_1 \rangle)$ has been plotted against the scaling variable $(h_1 - \langle h_1 \rangle)/L^{0.25}$ for the 1d Oslo ricepile model. The scaling function is highly asymmetric in the tails.

4.4 Residence times in the Oslo ricepile model

4.4.1 Distribution of residence times at site 1

The qualitative behaviour of distributions $Prob_L(T_i \geq t)$ for $i = 1$ can be seen in the simulation results shown in Fig. 4.12 and Fig. 4.13. We have done our simulations for $p = q = \frac{1}{2}$ and different system sizes, $L = 20, 25, 35$ and 50 . We averaged the data for a total 10^9 grains added in the pile for each L . Fig. 4.12 shows the plot of $Prob_L(T_1 \geq t)$ versus time t for different values of L . Interestingly, various curves for different L have steps like structures. The curves for different values of L cross each other many times. The unusual non-monotonic behaviour is not an artifact of statistical fluctuations. The statistical errors in the data are much smaller than the step sizes except in the tail region (*i.e.*, $t \gg 10^6$). The crossing of the curves for the cumulative probabilities persists for quite large system sizes also. In Fig. 4.12, we have plotted $Prob_L(T_1 \geq t)$ versus t for two much bigger system sizes, $L = 100$ and $L = 200$. We see that in this case also the probability that a grain remains in the pile of size $L = 100$, for time greater than or equal to 6×10^5 , is higher by a factor 1.8 than for a pile, two times larger size $L = 200$. Steps like structures are not log periodic as the

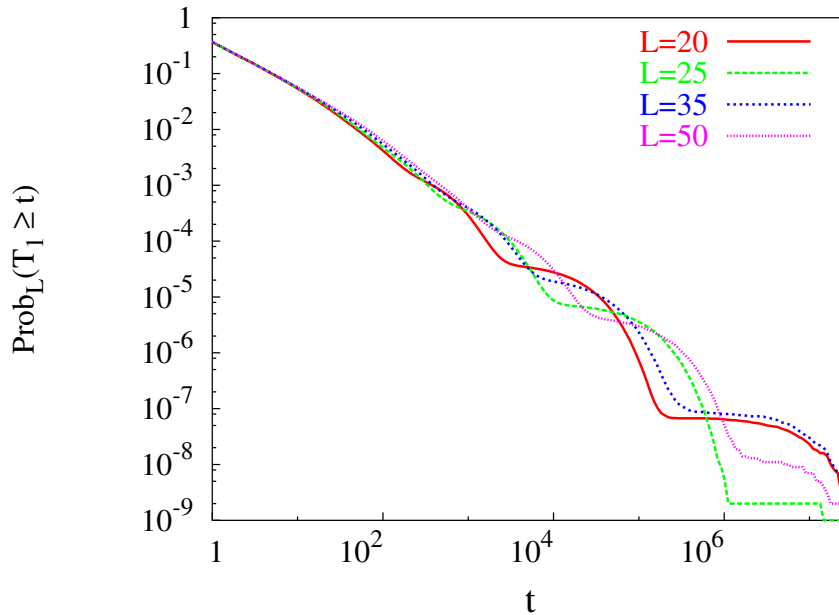


Fig 4.12: The cumulative probability $\text{Prob}_L(T_1 \geq t)$ versus time t for lattice sizes $L = 20, 25, 35$ and 50 for the $1d$ Oslo ricepile model. A total of 10^9 grains were added.

height and width of a step in each curve increases when going down the curve even on the log scale. The existence of several steps, whose positions and logarithmic widths are different for different L 's, implies that simple finite size scaling cannot hold in this case.

Now we shall use the knowledge of the behaviour of $\text{Prob}_L(h_1)$ to explain the step-like structures in the distribution function $\text{Prob}_L(T_1 \geq t)$.

For $h_1 \ll \bar{h}_1$, the probability distribution of height $\text{Prob}_L(h_1)$ falls very rapidly. Actually, it will be argued in section 5 that for $h_1 \ll \bar{h}_1$ the ratio $\text{Prob}_L(h_1 - 1)/\text{Prob}_L(h_1)$ is of order $\exp(-aL^2)$ where a is a constant and hence is very much less than 1. The values of $\text{Prob}_L(h_1)$ for different h_1 's could differ by several orders of magnitude from each other, if h_1 is sufficiently near h_{min} . Now in the interval of $1/\text{Prob}_L(h_1 - 1) \gg t \gg 1/\text{Prob}_L(h_1)$, only a single term corresponding to h_1 contributes significantly to the summation, and then the summation is nearly independent of t . It is clearly seen from Fig. 4.14, where $\text{Prob}_L(T_1 \geq t)$ is plotted versus t for $L = 20$ in the $1d$ Oslo model. We can identify three steps in the plot. Each step in the curve can be associated with a unique value of h_1 ($h_1 = 28, 29$ and 30) and steps appear at the corresponding value of $\text{Prob}_L(h_1)$ along the y -axis.

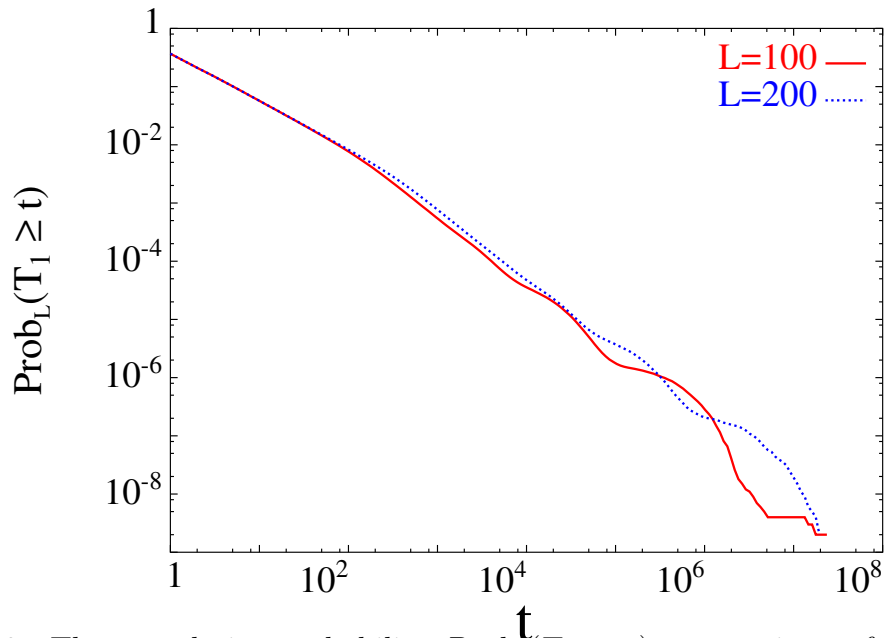


Fig 4.13: The cumulative probability $\text{Prob}_L(T_1 \geq t)$ versus time t for lattice sizes $L = 100$ and $L = 200$ for the 1d Oslo ricepile model.

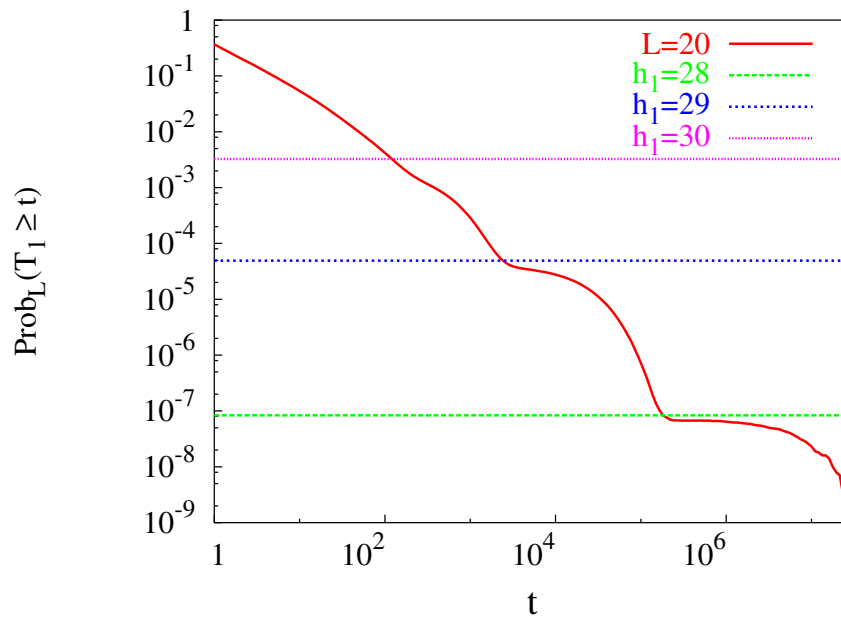


Fig 4.14: The cumulative probability $\text{Prob}_L(T_1 \geq t)$ versus time t for lattice size $L = 20$ for the 1d Oslo model.

This explains the steps like structure of $Prob_L(T_1 \geq t)$ as a function of t . Also, the function decays roughly as $1/t$ since we must have $Prob_L(h_1) \sim 1/t$ for the term to contribute in Eq. (4.5). If $h_1^*(t)$ is the value of h_1 that contributes most in Eq. (4.5), the value of $h_1^*(t)$ is given by the condition $Prob_L(h_1^*(t)) \approx 1/t$. Substituting this condition in Eq. (4.1), we get

$$g\left(\frac{h_1^*(t) - \bar{h}}{L^{\omega_1}}\right) \approx L^{\omega_1}/t \quad (4.18)$$

Thus the t dependence of $h_1^*(t)$ comes through the scaling variable $tL^{-\omega_1} = \tau$ (say). Then for τ large the argument establishing the $1/t$ dependence of $Prob_L(t_1 > t)$ given above is quite robust. However, a more careful analysis of Eq. (4.5) shows that there is also a logarithmic multiplicative correction factor with the $1/t$ decay of $Prob_L(T_1 \geq t)$.

For large L and t , the terms, which contribute to $Prob_L(T_1 \geq t)$ in Eq. (4.5), correspond to the values of h_1 for which $h_1 \ll \bar{h}_1$. Substituting the scaling form of $Prob_L(h) = \frac{1}{L^{\omega_1}} g\left(\frac{h - \bar{h}_1}{L^{\omega_1}}\right)$ (see Eq. (4.1)) in Eq (4.5) and putting $x = (h - \bar{h}_1)/L^{\omega_1}$, we get the following.

$$Prob_L(T_1 \geq \tau L^{\omega_1}) \sim \int dx g(x) \exp[-g(x)\tau] \quad (4.19)$$

where $\tau = t/L^{\omega_1}$. We have assumed that the probability distribution $Prob_L(h_1) \ll 1$, but is not rapidly decaying so that $Prob_L(h_1 - 1)/Prob_L(h_1) \approx 1$, and then the summation of Eq. (4.5) can be replaced by an integral over the scaled variable x . Actually in the real simulation (or experiment) for large L , this is the region of t we explore, we cannot go too far down the tail of $Prob_L(T_1 \geq t)$.

Now it is easy to see the origin of logarithmic correction if we choose a particular form of the scaling function $g(x)$ as $\exp(-|x|^\alpha)$ for $x \ll 1$, with $\alpha > 0$, and try to find out the large t behaviour of the above equation in terms of the scaling variable $\tau = t/L^{\omega_1}$. We first substitute $s = \exp(-|x|^\alpha)$ in Eq (4.19) and get,

$$Prob_L(T_1 \geq \tau L^{\omega_1}) \sim \frac{1}{\alpha} \int \frac{ds}{[-\ln(s)]^{\frac{\alpha-1}{\alpha}}} \exp(-s\tau) \quad (4.20)$$

The asymptotic behaviour of the of the above integral for τ large is easy to evaluate, giving

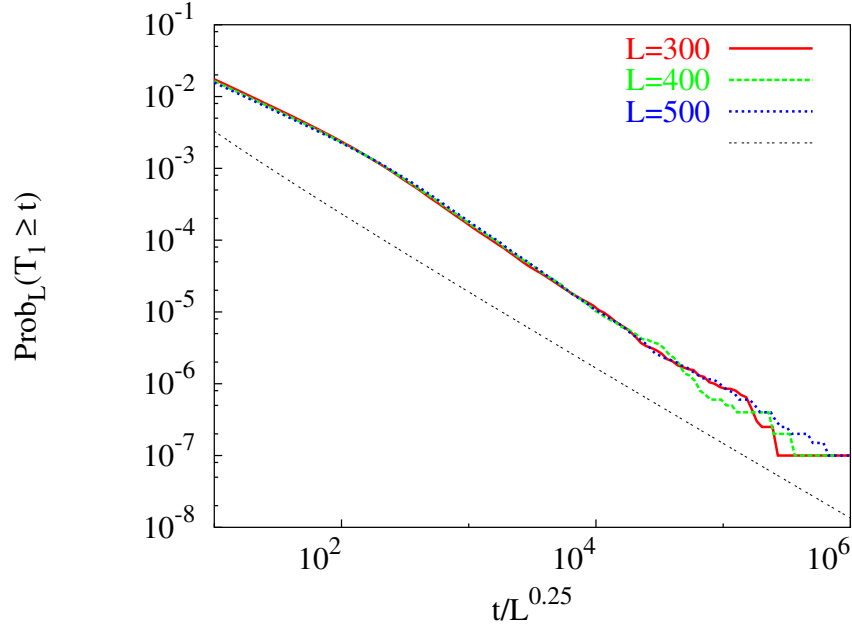


Fig 4.15: The cumulative probability $Prob_L(T_1 \geq t)$ for residence time at the first site plotted against the scaled residence time $t/L^{0.25}$ for lattice sizes $L = 300, 400$ and 500 for the $1d$ Oslo ricepile model. A total of 10^7 grains were added. The scaling function is fitted with $0.05/(x[\ln x]^{0.5})$.

$$Prob_L(T_1 \geq \tau L^{\omega_1}) \sim 1/[\tau(\ln \tau)^{\frac{\alpha-1}{\alpha}}] \quad (4.21)$$

In Fig. 4.15 we have plotted $Prob_L(T_1 \geq t)$ against scaled variable t/L^{ω_1} with $\omega_1 = 0.25$ for large values of system sizes $L = 300, 400$ and 500 in the $1d$ Oslo model. We fit the scaled curves with a functional form given in Eq. (4.21) with $\alpha = 2$ since the scaling function $g(x)$ is Gaussian near $x = 0$.

Now it is clear that there is a logarithmic multiplicative factor in $1/t$ decay and we take account of this logarithmic multiplicative correction by writing the cumulative probability as given below.

$$Prob_L(T_1 \geq t) \simeq L^{\omega_1} [t \ln^{\delta_1}(tL^{-\omega_1})]^{-1} \quad (4.22)$$

where we have used the fact that the answer is function of the scaling combination $tL^{-\omega_1}$ and $\delta_1 = (\alpha - 1)/\alpha$. As a check we calculate the average residence time at site 1 as given below.

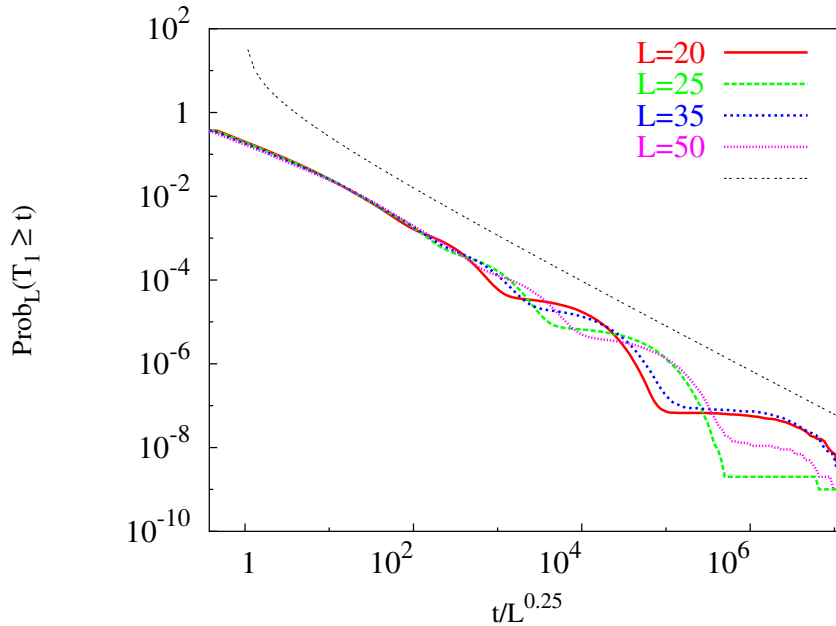


Fig 4.16: The cumulative probability $Prob_L(T_1 \geq t)$ for residence time at the first site has been plotted against the scaled time $t/L^{0.25}$ for lattice sizes $L = 20, 25, 35$ and 50 for the $1d$ Oslo ricepile model. A total of 10^9 grains were added. The envelop is fitted with $5/(x[\ln x]^{0.75})$.

$$\langle T_1 \rangle \simeq \int_1^{T_{1,max}} Prob_L(T_1 \geq t) dt \sim L^{\omega_1} \ln(T_{1,max})^{1-\delta_1} \quad (4.23)$$

The upper cutoff on the timescale is provided by $1/Prob_L(h = h_{min})$, which is the average time interval between successive returns to the minimum height. Assuming the scaling function $g(x)$ varies as $\exp(-|x|^\alpha)$ for $x \ll -1$ and then putting $T_{1,max} = \exp[kL^{\alpha(1-\omega_1)}]$ in the above equation, we see that $\langle T_1 \rangle$ is proportional to L .

For the $1d$ Oslo model, numerical estimate from the simulation gives $\omega_1 \approx 0.25$. Assuming the value $\alpha \approx 4$ (argued in section 5), we get $\delta_1 \approx 0.75$. In Fig. 4.16 we have plotted $Prob_L(T_1 \geq t)$ versus a scaled variable t/L^{ω_1} where $\omega_1 = 0.25$ for $L = 20, 25, 35$ and 50 and fitted the envelop formed by steps in the curves with a function $1/x(\ln x)^{\delta_1}$ where $\delta_1 = 0.75$. We see that we get a reasonable fit to the data. We note that the multiplying logarithmic factor is necessary to get a good fit to $1/t$ dependence.

4.4.2 Total residence times T in the pile.

The arguments given in the previous section are easily extended to distribution of the residence times T_i with $i \neq 1$, and we conclude that they would also have a similar $1/t$ distribution with same logarithmic correction factor which is for T_1 , so long as i is not near the right end. Hence the distribution of their sum $T = \sum_i T_i$ would also be of same form.

Even though the cumulative distribution of residence times T_i at any site i has steps like structure, the step-structure may be washed out in the sum $\sum_i T_i$.

Results of the numerical simulation for distribution of the total residence times using a total 5×10^7 grains are shown in Fig. 4.17. We see that the steps are not seen in the distribution $Prob_L(T \geq t)$ for different values of L for the range of the total residence times reached in the simulation ($T \leq 10^8$). The function $Prob_L(T \geq t)$ is much smoother than the function $Prob_L(T_1 \geq t)$. However for small values of L (say for $L \leq 20$), various curves of $Prob_L(T \geq t)$ still cross each other at large times. But for larger values of L , we don't see any inter-crossing of the curves in the times reached in our simulation (except at the tail where the data is less reliable due to the statistical fluctuations).

In analogy with results for the the distribution of T_1 , We can expect the behaviour of the cumulative distribution $Prob_L(T \geq t)$ to be a scaling function of t/L^ω , where the exponent ω is different from ω_1 defined earlier. So we write

$$Prob_L(T \geq t) = f\left(\frac{t}{L^\omega}\right) \quad (4.24)$$

where the scaling function $f(x)$ varies as $1/[x(\ln x)^\delta]$ for large x , and the exponent δ would also be different from δ_1 defined earlier. Using the condition that the mean residence time in the pile is equal to the mean active mass in the pile, and hence scales as L^2 , can be used to determine δ in terms of ω and γ by integrating $Prob_L(T \geq t)$ over t upto the cut-off time scale $\exp(\kappa L^\gamma)$. Now we get,

$$\delta = 1 - (2 - \omega)/\gamma \quad (4.25)$$

In Fig. 4.18 we have plotted $Prob_L(T \geq t)$ versus scaled variable t/L^ω where $\omega \approx 1.25$ [63]. We get the value of δ approximately equal to 0.75 from Eq. (4.25), assuming $\gamma = 3$ (argued in section 5). The fit is seen to be very good. In the numerical analysis

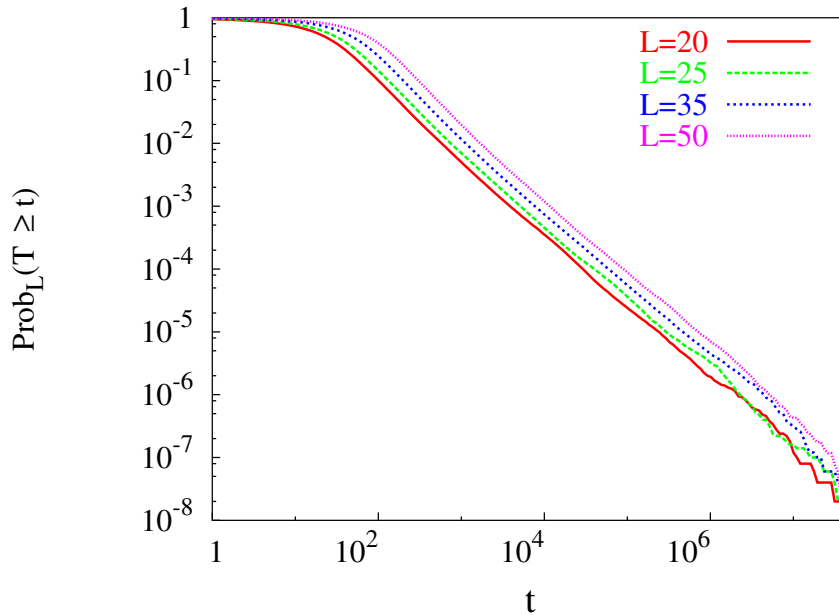


Fig 4.17: The cumulative probability $Prob_L(T \geq t)$ versus time t for lattice sizes $L = 20, 25, 35$ and 50 for the $1d$ Oslo ricepile model. A total of 5×10^7 grains were added.

of Christensen *et. al.* [43], no logarithmic factor was used, and the data was fitted with a larger effective exponent, i.e., $1/t^{1.22}$ decay.

4.5 Generalization to other slope type models

In this section we present the simulation results in other models and show that the cumulative distributions $Prob_L(T_1 \geq t)$ and $Prob_L(T \geq t)$ have same $1/t$ power law behaviour for large t , but with different logarithmic corrections.

4.5.1 Distribution of residence times at site 1 in model-B, C, D.

Model-B: Now we present the simulation results for $2d$ ricepile model. We add marked grains at the corner site, i.e., at $(1, 1)$. We simulated this model choosing $p = 0.75$ and $q = 0.25$, and study the residence time distribution of grains at the corner site $(1, 1)$. The standard deviation $\sigma_{h_{1,1}}$ of height $h_{1,1}$ at the corner site about the mean varies as L^{ω_1} where we estimated $\omega_1 \approx 0.2$ from the simulation. We added total 10^6 grains.

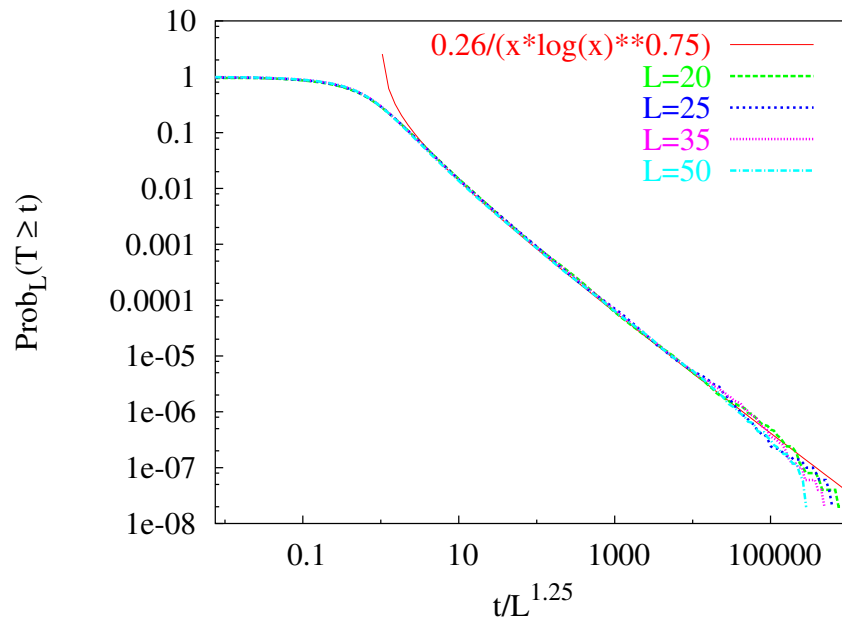


Fig 4.18: Scaling collapse of $Prob_L(T \geq t)$ versus scaled residence time $t/L^{1.25}$ for the 1d Oslo ricepile model for lattice sizes $L = 20, 25, 35$ and 50 . A total of 5×10^7 grains were added. Scaling function is fitted with $0.26/(x[\ln x]^{0.75})$.

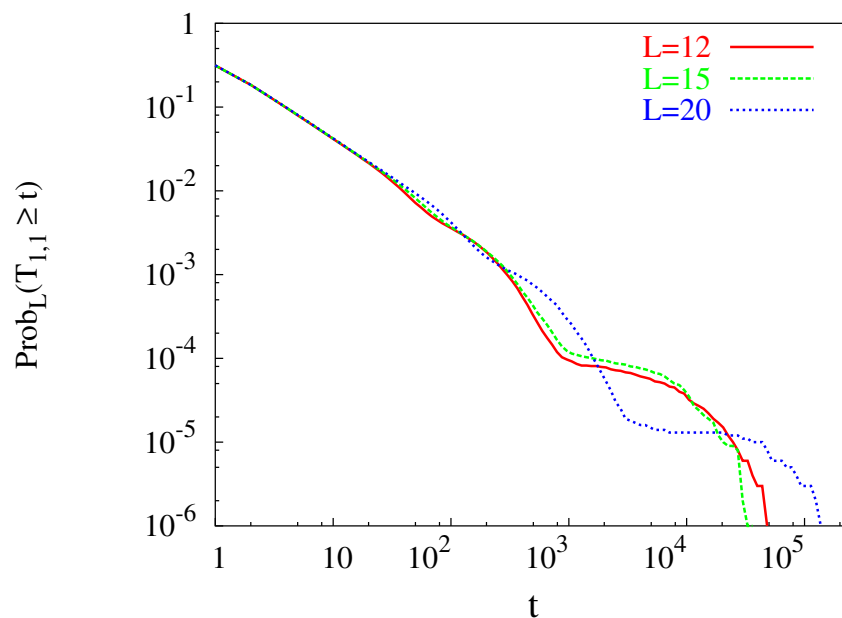


Fig 4.19: The residence time distribution $Prob_L(T_{1,1} \geq t)$ of grains at the corner site versus time t for model-B for lattice sizes $L = 12, 15$ and 20 . A total of 10^6 grains were added.

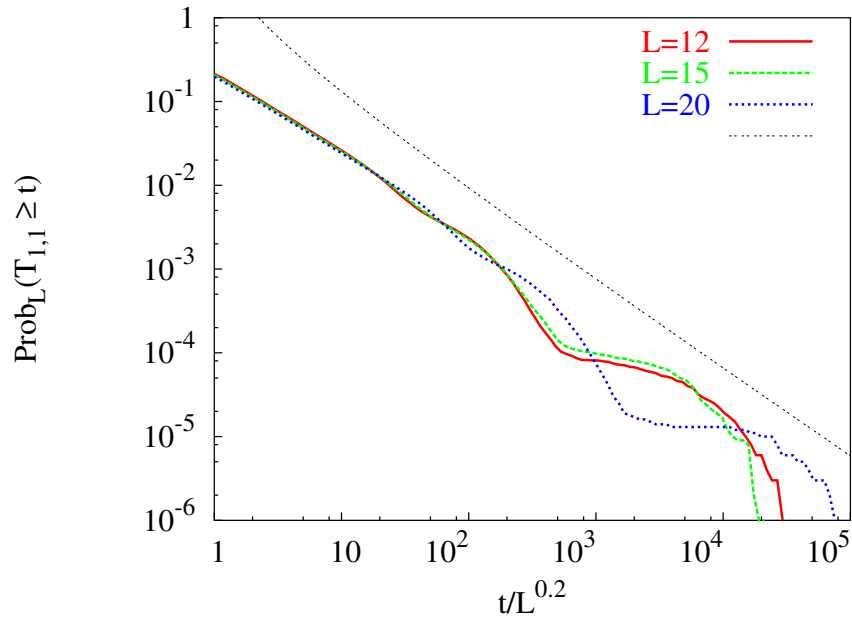


Fig 4.20: The cumulative probability distribution function $Prob_L(T_{1,1} \geq t)$ versus scaled scaled residence time $t/L^{0.2}$ for model-B for lattice sizes $L = 12, 15$ and 20 . A total of 10^6 grains were added. The envelop formed by the steps is fitted with $2.0/(x[\ln x]^{0.5})$.

We have plotted various curves for cumulative distribution function $Prob_L(T_{1,1} \geq t)$ of residence time $T_{1,1}$ at the corner site versus times t for $L = 12, 15$ and 20 in Fig. 4.19 and we see steps like structure appearing for $t \geq 50$. Various curves for different L inter-cross each other many times as seen in the $1d$ Oslo ricepile model. In this case also, steps like structures are not log periodic as the step-length in each curve increases on log scale when going down the curve. Any simple finite size scaling in the whole range of t ($t \gg 1$) does not work as in the case of the $1d$ Oslo ricepile model. The probability distribution of height at the corner site has a scaling form as given in Eq. (4.1) for the $1d$ Oslo ricepile model. From the simulation we determined the exponent $\omega_1 \approx 0.2$ which is very small. Since, for $t \ll L^{\omega_1}$, $Prob_L(T_{1,1} \geq t)$ scales with t/L^{ω_1} for large L (see Eq. (4.19)), we plotted various cumulative distributions $Prob_L(T_{1,1} \geq t)$ versus a scaled time t/L^{ω_1} with $\omega_1 = 0.2$ in the Fig. 4.20. We see that decay of the envelop formed by various steps in different curves fit well with the function $2/[x(\ln x)^{0.5}]$ where the logarithmic correction factor is according to Eq. (4.21).

Model-C : Since in model-C, grains are added randomly everywhere in the pile, average residence time $\langle T_1 \rangle_{h_1}$ of a grain added at height h_1 varies as $1/[p_1 Prob_L(h_1)]$

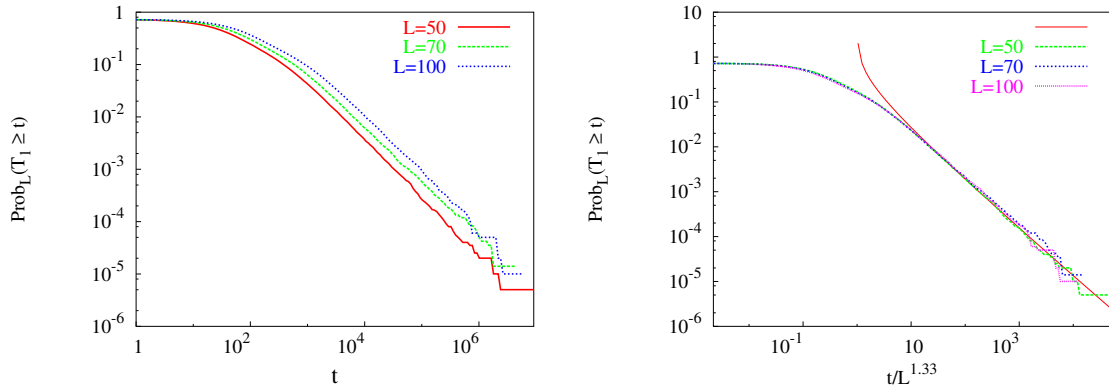


Fig 4.21: Model-C for lattice sizes $L = 50, 70$ and 100 . A total of 10^5 grains were added at the first site. **Left panel:** The cumulative probability $Prob_L(T_1 \geq t)$ versus time T_1 . **Right panel:** Scaling collapse of $Prob_L(T_1 \geq t)$. The scaling function is fitted with $0.41/(x[\ln x]^{0.5})$.

according to Eq. (4.4). Now there will be an extra $1/L$ factor inside the exponential in the Eq. (4.19). Consequently the scaling variable $\tau = \frac{t}{L^{\omega_1}}$ in Eq. (4.19) is replaced by $\tau = \frac{t}{L^{1+\omega_1}}$ and Eq. (4.19) is modified to

$$Prob_L(T_1 \geq \tau L^{1+\omega_1}) \sim 1/[\tau(\ln \tau)^{\frac{\alpha-1}{\alpha}}] \quad (4.26)$$

Similarly average residence time at the first site equals to $\langle h_1 \rangle / p_1$ (proof is similar as for $\langle T_1 \rangle_{h_1}$ in Eq. 4.4) which, in this case, varies as L^2 . This can be checked directly by integrating the above equation upto the cutoff time scale as done in Eq. (4.23).

Total number of grains added in the pile are different for different L so that 10^5 grains are added at the first site. The standard deviation σ_{h_1} of height fluctuations at the first site varies as L^{ω_1} with system size L , where $\omega_1 \approx 1/3$ [90]. We have plotted $Prob_L(T_1 \geq t)$ for different values of L in the log scale in the left panel of Fig. 4.21. We note that, unlike in the $1d$ Oslo ricepile model, the cumulative probability here is smooth (except at the tail due to statistical fluctuations) and monotonic function of L for a fixed t . This is due to the fact that the probability distribution $Prob_L(h_1)$ of height at first site is not as sharply decaying function for $h_1 \ll \bar{h}_1$ as it was in the $1d$ Oslo model. In fact, in the right panel of Fig. 4.21 we get a good scaling collapse of various $Prob_L(T_1 \geq t)$ for different L using the scaled residence time $t/L^{1+\omega_1}$ where $\omega_1 \approx 1/3$. The scaling function is fitted well with the function $1/[x(\ln x)^{(\alpha-1)/\alpha}]$ for $x \gg 1$, taking $\alpha = 2$ (see Eq. (4.21)).

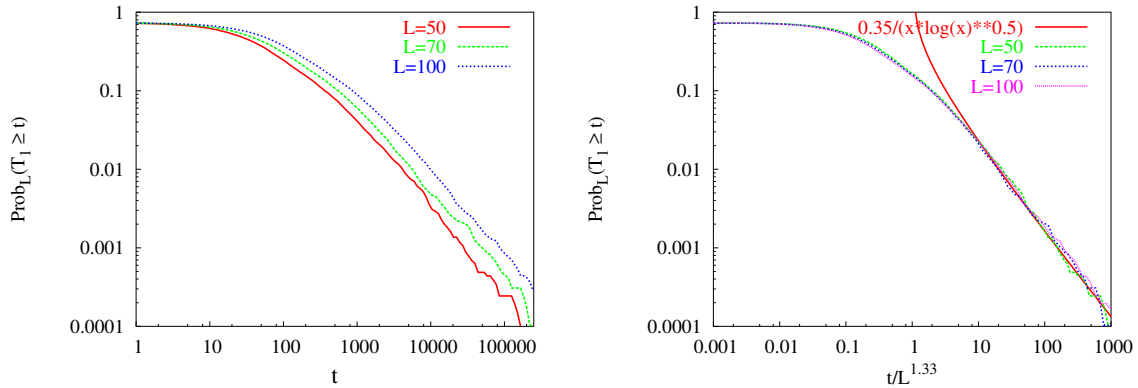


Fig 4.22: Model-D for lattice sizes $L = 50, 70$ and 100 . A total of 10^4 grains were added at the first site. **Left panel:** The cumulative probability $Prob_L(T_1 \geq t)$ versus time t . **Right panel:** Scaling collapse of $Prob_L(T_1 \geq t)$. The scaling function is fitted with $0.8/(2x[\ln 2x]^{0.5})$.

Model-D: In the model-D, the standard deviation σ_{h_1} of the high fluctuation at site 1 scales with L as L^{ω_1} where we found $\omega_1 \approx 0.33$ [90]. In the left panel of Fig. 4.22 we have plotted various $Prob_L(T_1 \geq t)$ against the residence time t at the first site for $L = 50, 70$ and 100 . We added 10^4 grains at the first site. In the right panel of Fig. 4.22 we have plotted $Prob_L(T_1 \geq t)$ versus scaled time $t/L^{1+\omega_1}$ with $\omega_1 \approx 0.33$ and get a good scaling collapse of all the curves for various L . We fit the scaling function with $0.8/[2x(\ln 2x)^{(\alpha-1)/\alpha}]$, using Eq. (4.21) and putting $\alpha = 2$, as done in the model-C.

4.5.2 Distribution of total residence times in the pile in model-B, C, D.

Model-B: Using a similar argument to the $1d$ Oslo model, in this case, we must have $\gamma = 4$. To get to the minimum slope configuration, we will have to topple $\mathcal{O}(L^3)$ grains and each grain $\mathcal{O}(L)$ times. As the average mass of the pile, in this case, varies as L^3 , Eq. (4.25) is modified as given below.

$$\delta = 1 - (3 - \omega)/\gamma.$$

In the left panel of Fig. 4.23 we have plotted various distribution of the total residence time, $Prob_L(T \geq t)$, versus time t for different $L = 12, 15$ and 20 . In the right panel of Fig. 4.23 we have plotted $Prob_L(T \geq t)$ for different L against the scaling variable t/L^ω where $\omega \approx 2.0$. Now we can estimate δ to be approximately 0.75 from

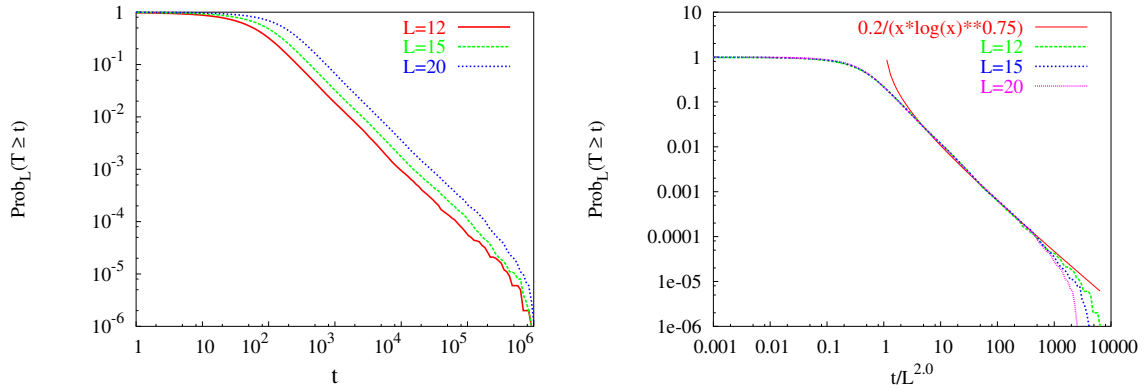


Fig 4.23: Model-B for lattice sizes $L = 12, 15$ and 20 . A total of 10^6 grains were added. **Left panel:** The residence time distribution $Prob_L(T \geq t)$. **Right panel:** Scaling collapse of various $Prob_L(T \geq t)$ versus scaled variable $t/L^{2.0}$. The scaling function is fitted with $0.2/(x[\ln x]^{0.75})$.

the above equation. In the right panel of Fig. 4.23 we fit the scaling function for $Prob_L(T \geq t)$ with $0.2/[x(\ln x)^{0.75}]$ which seems to be a reasonable fit.

Model-C : In the left panel of Fig. 4.24 we have plotted various $Prob_L(T \geq t)$ versus residence time t for lattice sizes $L = 50, 70$ and 100 . Total 10^6 grains were added in this case. In the right panel of Fig. 4.24 we have collapsed various $Prob_L(T \geq t)$ for different L using the scaled variable t/L^ω where $\omega \approx 1.33$. We fit the scaling function of the cumulative distribution with $0.3/x[\ln(x)]^\delta$ for $x \gg 1$ where $\delta \approx 0.5$.

Model-D: In the left panel of Fig. 4.25 we have plotted various $Prob_L(T \geq t)$ for the total residence time versus t for lattice sizes $L = 50, 70$ and 100 . Total 10^5 grains were added in this case. In the right panel of Fig. 4.25 we have plotted $Prob_L(T \geq t)$ versus scaled time t/L^ω where $\omega \approx 1.33$ and we get a good collapse for the scaling function which fits reasonably well with the function $0.63/(2x[\ln(2x)]^\delta)$ for $\delta \approx 0.55$.

4.6 Concluding remarks.

To summarize, in this chapter, we studied distribution of the residence times of grains in various ricepile models. We reduced the problem of finding the residence time distribution of grains at a particular site to that of determining the distribution of first return time of height at the site to the same value. The result that the probability of the residence times T_i at site i or the total residence time T in the pile, being greater than

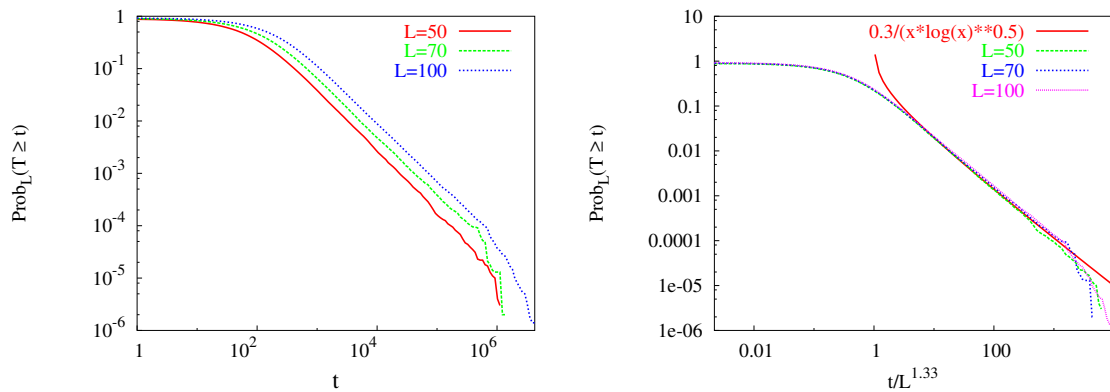


Fig 4.24: Model-C for lattice sizes $L = 50, 70$ and 100 . A total of 10^6 grains were added. **Left panel:** The distribution function $Prob_L(T \geq t)$ versus time t . **Right panel:** Scaling collapse of $Prob_L(T \geq t)$ versus scaled time $t/L^{1.33}$. The scaling function is fitted with $0.3/(x[\ln(x)]^{0.5})$.

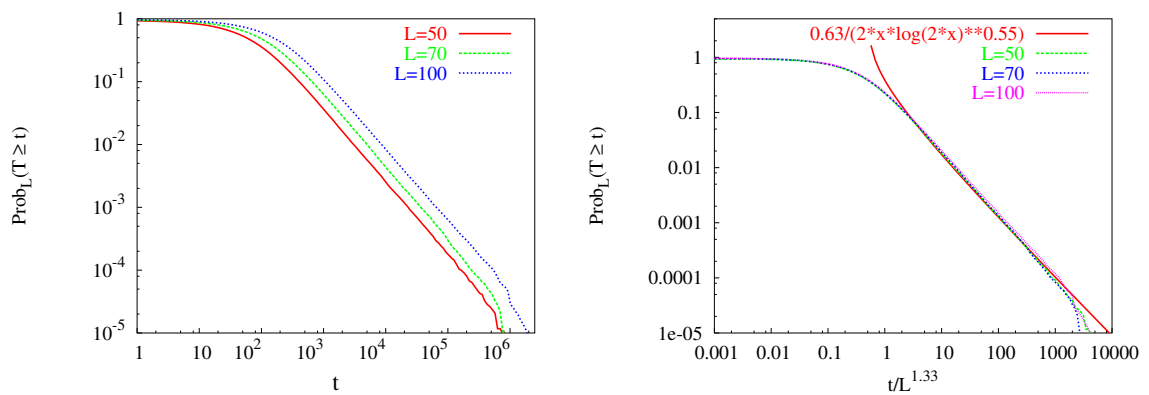


Fig 4.25: Model-D for lattice sizes $L = 50, 70$ and 100 . A total of 10^5 grains were added. **Left panel:** The cumulative probability $Prob_L(T \geq t)$ versus time t . **Right panel:** Scaling collapse of $Prob_L(T \geq t)$ against the scaled variable $t/L^{1.33}$. The scaling function is fitted with $0.63/(2x[\ln(2x)]^{0.55})$.

or equal to t , decay as power law $1/t$ is valid for a large class of sandpile models, where height fluctuation at a particular site grows with the system sizes, and is independent of dimensions. It depends only on the fact that there are some deeply buried grains which come out only in rare fluctuations, i.e., slope of the pile becomes very close to the minimum slope. It is important to note that, since the total residence time T is sum of T_i 's, the probability of $T = 0$ decreases with system size, and clearly our analysis cannot predict the small t behaviour of the cumulative probability $Prob_L(T \geq t)$, i.e., for $t < L^\omega$.

We also found that cumulative probability $Prob_L(T_1 \geq t)$, for a fixed t , is non-monotonic with system size L for some of the ricepile models. The non-monotonic behaviour of the cumulative probability distribution $Prob_L(T_i \geq t)$ of residence times at site i with system size L is possible when the probability distribution function $Prob_L(h_i)$, where h_i is the height at site i , sharply decays for $h_i < \bar{h}_i$. However this non-monotonicity is seen only for $t \gg t^*(L)$ where $t^*(L)$ increases with increasing values of L , and hence may be harder to observe in real experiments.

It is important to note that if we change the transfer rule of grains, the distribution of residence times may change completely. The rule, chosen in this chapter, is called first-in-last-out rule. We may employ some other rules. For example, a different rule could be the first-in-first-out rule. In this case we add grains at the top of the stack but take out grains from the bottom of the stack. Another rule would be to add and take out grain from a stack in random order. In these cases, there are no sites with deeply buried grains and the residence time distribution will be similar to that in the critical height models studied earlier by us.

Summary

We list the main new results obtained in this thesis as given below.

1. We have studied the first passage time distribution of a particle obeying simple diffusion equation with absorbing boundary. We explicitly calculated the scaling function, for the following geometries of the boundaries - a box in one dimension, circular, square and triangular boundaries in two dimensions and cubical box and sphere in three dimensions.
2. The DRT of sand grains in height type models, in the scaling limit, can be expressed in terms of the survival probability of a single diffusing particle in a medium with absorbing boundaries and space-dependent jump rates. This is valid under the conditions of local conservation of sand grains, transfer of fixed number of grains at each toppling and isotropy, and equally applicable to deterministic and stochastic models.
3. For height type models, the DRT has scaling form $L^{-d}f(t/L^d)$. The scaling function $f(x)$ is non-universal, and depends on the probability distribution according to which grains are added at different sites. However, the DRT does not have any long time tail and $f(x)$ decays exponentially for $x \gg 1$.
4. For ricepile models, the tail in the DRT at a site, and the DRT of grains inside a pile, are dominated by the grains that get deeply buried in the pile. We show that, for a pile of size L , the probabilities that the residence time at a site or the total residence time is greater than t , both decay as $1/t(\ln t)^x$ for $L^\omega \ll t \ll \exp(\kappa L^\gamma)$ where γ is an exponent ≥ 1 , and values of x and ω in the two cases are different. This power law tail is independent of details of the toppling rules, and of the dimensionality of the systems.

-
- 5.** For stochastic ricepile models, we find that the probability of the residence time T_i at a site i , being greater than or equal to t , is a non-monotonic function of L for a fixed t and does not obey simple finite size scaling.
- 6.** For these models, we show that probability of the minimum slope configuration in steady state of a d -dimensional pile, for large L , varies as $\exp(-\kappa L^{d+2})$ where κ is a constant.

Calculation of eigenfunctions of Eq. 3.10

Here we solve the eigenvalue equation $\frac{d^2}{dx^2}[x\varphi(x)] = -\lambda\varphi(x)$, which can be written as below.

$$x\frac{d^2\varphi}{dx^2} + 2\frac{d\varphi}{dx} + \lambda\varphi = 0, \quad (\text{A.1})$$

where $\varphi(x=1) = 0$. We don't put any particular boundary condition at $x=0$, we only demand that the solution is well behaved and does not diverge at $x=0$. We use Frobenius power series method [79]. It should be noted $x=0$ is a singular point of the Eq. A.1, however it is a regular singular point. So we expect we get at least can a solution of the form

$$\varphi(x) = \sum_{i=0}^{\infty} a_i x^{i+\alpha} \quad (\text{A.2})$$

where α may take negative values. Putting Eq. A.2 in the Eq. A.1 and equating the coefficient of lowest power of x to zero, we get the indicial equation [79]

$$\alpha(\alpha+1) = 0 \Rightarrow \alpha = 0 \quad \text{or} \quad \alpha = -1.$$

For two values of α , we get two independent solution of Eq. A.1. If we take $\alpha = -1$, the solution in Eq. A.2 has a singularity of $1/x$ at $x=0$. Since the solution diverges at $x=0$ and cannot be normalized in the region $[0, 1]$, we therefore do not consider solution in Eq. A.2 with $\alpha = -1$. We take $\alpha = 0$ when the solution is well behaved in the region $[0, 1]$ and so can be expanded into Taylor series around $x=0$.

Now putting Eq. A.2 in Eq. A.1 and equating coefficient of x^i for each i independently to zero we get following recurrence relation.

$$a_i = \frac{-\lambda}{i(i+1)} a_{i-1} \Rightarrow a_i = \frac{(-\lambda)^i}{i!(i+1)!} \quad (\text{A.3})$$

So we get the solution to be

$$\varphi(x) = \sum_{i=0}^{\infty} \frac{(-\lambda)^i}{i!(i+1)!} x^i \quad (\text{A.4})$$

The modified Bessel function of order 1 $I_1(z)$ is defined to be

$$I_1(z) = \left(\frac{1}{2}z\right) \sum_{i=0}^{\infty} \frac{\left(\frac{1}{4}z^2\right)^i}{i!(i+1)!} \quad (\text{A.5})$$

Now writing $\frac{1}{4}z^2 = -\lambda x$, we can easily express $\varphi(x)$ in terms of modified Bessel function of order 1 as

$$\varphi(x) = I_1(2i\sqrt{\lambda x}) / (i\sqrt{\lambda x})$$

Finite size corrections

B.1 Calculation for $Prob_L(T = 0)$

In this appendix, we calculate the leading order term of $\mathcal{O}(1/L)$ for probability $Prob_L(T = 0)$ of the residence time $T = 0$ for a given system size L in the one dimensional BTW model when grains are added randomly everywhere. First let us consider the case when a grain is ejected out of the system from the right end just after addition of the grain. Now let us make a list of all possible configuration when a grain is added at any site at right side of the site with height zero.

Configuration	Probability of ejection from the right
$ 0111\dots11\rangle$	$\frac{1}{(L+1)L} \left[\frac{1}{2^{L-1}} + \frac{1}{2^{L-2}} + \dots + \frac{1}{2} \right] = \frac{1}{(L+1)L} \left(1 - \frac{1}{2^{L-1}} \right)$
$ 1011\dots11\rangle$	$\frac{1}{(L+1)L} \left[\frac{1}{2^{L-2}} + \frac{1}{2^{L-3}} + \dots + \frac{1}{2} \right] = \frac{1}{(L+1)L} \left(1 - \frac{1}{2^{L-2}} \right)$
$ 1101\dots11\rangle$	$\frac{1}{(L+1)L} \left[\frac{1}{2^{L-3}} + \frac{1}{2^{L-4}} + \dots + \frac{1}{2} \right] = \frac{1}{(L+1)L} \left(1 - \frac{1}{2^{L-3}} \right)$
...	
$ 11\dots011\rangle$	$\frac{1}{(L+1)L} \left[\frac{1}{2^2} + \frac{1}{2} \right] = \frac{1}{(L+1)L} \left(1 - \frac{1}{2^2} \right)$
$ 11\dots101\rangle$	$\frac{1}{(L+1)L} \cdot \frac{1}{2}$
$ 11\dots110\rangle$	$\frac{1}{(L+1)L} \cdot 0$
$ 11\dots111\rangle$	$\frac{1}{(L+1)L} \left[\frac{1}{2^L} + \frac{1}{2^{L-1}} + \dots + \frac{1}{2} \right] = \frac{1}{(L+1)L} \left(1 - \frac{1}{2^L} \right)$

At the right, for each configuration we write probability of a grain being ejected from the right side where each term in the series is for the addition at respective site. For example first term in the first series is for when grains is added at site 2, next term is for when grains is added at site 3, etc. The factor $\frac{1}{(L+1)L}$ comes because the probability of choosing a particular configuration is $\frac{1}{L+1}$ and then we add grain at a particular site with probability $\frac{1}{L}$. Collecting all the terms written above and summing them up, we get the probability of grain being ejected from the right end at the same time

step when the grain is added to the system. This probability is $\frac{1}{(L+1)L}[L-1+2^{1-L}]$. Since the probability of a grain being ejected from the left end is also same, we get $Prob_L(T=0)$ by multiplying this probability by a factor 2, i.e.,

$$Prob_L(T=0) = \frac{2}{(L+1)L}[L-1+2^{1-L}]. \quad (\text{B.1})$$

Now expanding Eq. B.1 in power series of $1/L$ for large L , we get

$$Prob_L(T=0) = \frac{2}{L} + \frac{4}{L^2} + \mathcal{O}(1/L^3). \quad (\text{B.2})$$

B.2 Calculation for $Prob_L(T=1)$

Now we calculate the leading order term, $\mathcal{O}(1/L)$, for probability $Prob_L(T=1)$ of the residence time $T=1$ for a given system size L in the one dimensional BTW model when grains are added randomly everywhere. This calculation is similar as in the previous case although more tedious. We calculate $Prob_L(T=1)$ in the limit of large system size L . When L is large, the site with height zero is likely to be far away from origin. So the $\mathcal{O}(1/L)$ terms come from these configuration when we add grains near the end, with probability $1/L$. Let us consider such an configuration and add a marked grain to the left of the site with zero height. In a particular case we see what are possible positions of the marked grain (denoted by star symbol in the figure) added in the pile after one time step shown in Fig. B.1 when we add grain at site $x=x_a$ where $x_a=3$. We can easily count the number of all possible ways the marked grain can stay put at any site after starting from $x=3$ in one time step. In general we define $N(x_a, x_f)$ as the number of ways the marked grain can come to rest at a site $x=x_f$ in one time step after starting at $x=x_a$. At the next step when we add another grain, the marked grain has to come out of the system so that the residence time $T=1$.

For example in Fig. B.1, the probability $Prob(x_a=3, x_f=1)$ of marked grain, added at site $x=3$, will reach site $x=1$ is $3/2^4$. Now the probability that it will come out of the system from the left end is $\frac{1}{2} \cdot \frac{3}{2^4}$ (it cannot come out from the right end unless all sites have height 1 and then the probability of the grain coming through the right end is exponentially small). The numbers $N(x_a, x_f)$ for various values of x_a and x_f can be shown to be generated from the algorithm shown in Fig. B.2. We start from topmost row, add two consecutive numbers and write in the next row in the specified position shown in the Fig. B.2, go on to next row and repeat this, etc. Now

$N(x_a, x_f)$ can be expressed in terms of coefficients B_x of y^x in the binomial expansion of $(1+y)^{x_a+x_f-1} = \sum_{x=0}^{x_a+x_f-1} B_x y^x$, i.e., $N(x_a, x_f) = \frac{(x_a+x_f-1)!}{(x_a-1)!x_f!}$.

The probability $Prob_L(T=1)$ is equal to $(\frac{1}{2}P_R + \frac{1}{2}P_L)$ where P_R and P_L are the probabilities of the marked grain being ejected from the right end or left end respectively. From symmetry of the problem, we obviously get $P_R = P_L$, i.e., $Prob_L(T=1) = P_L$. Now we can express the leading order term ($\mathcal{O}(1/L)$) of $Prob_L(T=1)$ in the limit of large L as given below,

$$Prob_L(T=1) = P_L = \frac{1}{L} \sum_{x_a=1}^{\infty} \sum_{x_f=1}^{\infty} N(x_a, x_f) \frac{1}{2^{x_a+2x_f}} + \mathcal{O}\left(\frac{1}{L^2}\right) \quad (\text{B.3})$$

Changing the summation index to $n' = x_a - 1$ and $n = x_f$, and substituting the expression for $N(x_a, x_f)$ in the above equation, we get

$$\begin{aligned} Prob_L(T=1) &= \frac{1}{L} \sum_{n=1}^{\infty} \sum_{n'=0}^{\infty} \frac{(n+n')!}{n!n'} \frac{1}{4^n} \frac{1}{2^{n'}} + \mathcal{O}\left(\frac{1}{L^2}\right) \\ &= \frac{1}{2L} \sum_{N=1}^{\infty} \sum_{n'=0}^{N-1} \frac{N!}{(N-n')!n'} \frac{1}{4^{N-n'}} \frac{1}{2^{n'}} + \mathcal{O}\left(\frac{1}{L^2}\right) \\ &= \frac{1}{2L} \sum_{N=1}^{\infty} \left[\left(\frac{3}{4}\right)^N - \left(\frac{1}{2}\right)^N \right] + \mathcal{O}\left(\frac{1}{L^2}\right) \\ &= \frac{1}{L} + \mathcal{O}\left(\frac{1}{L^2}\right). \end{aligned} \quad (\text{B.4})$$

B.3 Correction in the cumulative distribution

The cumulative distribution $S_{1d \text{ BTW}}(t)$ is written upto $\mathcal{O}(1/L)$ as $\frac{1}{L}\delta_{t,0} + (1 - \frac{1}{L})\exp[-\frac{t}{L}(1 - \frac{a}{L})]$. The mean residence time $\langle T \rangle = \sum_{t=1}^{\infty} S_{1d \text{ BTW}}(t)$ is given by

$$\begin{aligned} \langle T \rangle &= \sum_{t=1}^{\infty} \left(1 - \frac{1}{L}\right) \exp\left[-\frac{t}{L}\left(1 - \frac{a}{L}\right)\right] \\ &= \left(1 - \frac{1}{L}\right) \frac{e^{-\lambda}}{1 - e^{-\lambda}} \quad \text{where } \lambda = \frac{1}{L}\left(1 - \frac{a}{L}\right). \\ &= \left(1 - \frac{1}{L}\right) \frac{1 - \lambda + \mathcal{O}(\lambda^2)}{\lambda - \frac{\lambda^2}{2} + \mathcal{O}(\lambda^3)} \\ &= \left(1 - \frac{1}{L}\right) \frac{L}{1 - \frac{a}{L}} \frac{1 - \frac{1}{L}\left(1 - \frac{a}{L}\right) + \mathcal{O}(1/L^2)}{1 - \frac{1}{2L}\left(1 - \frac{a}{L}\right) + \mathcal{O}(1/L^2)} \end{aligned}$$

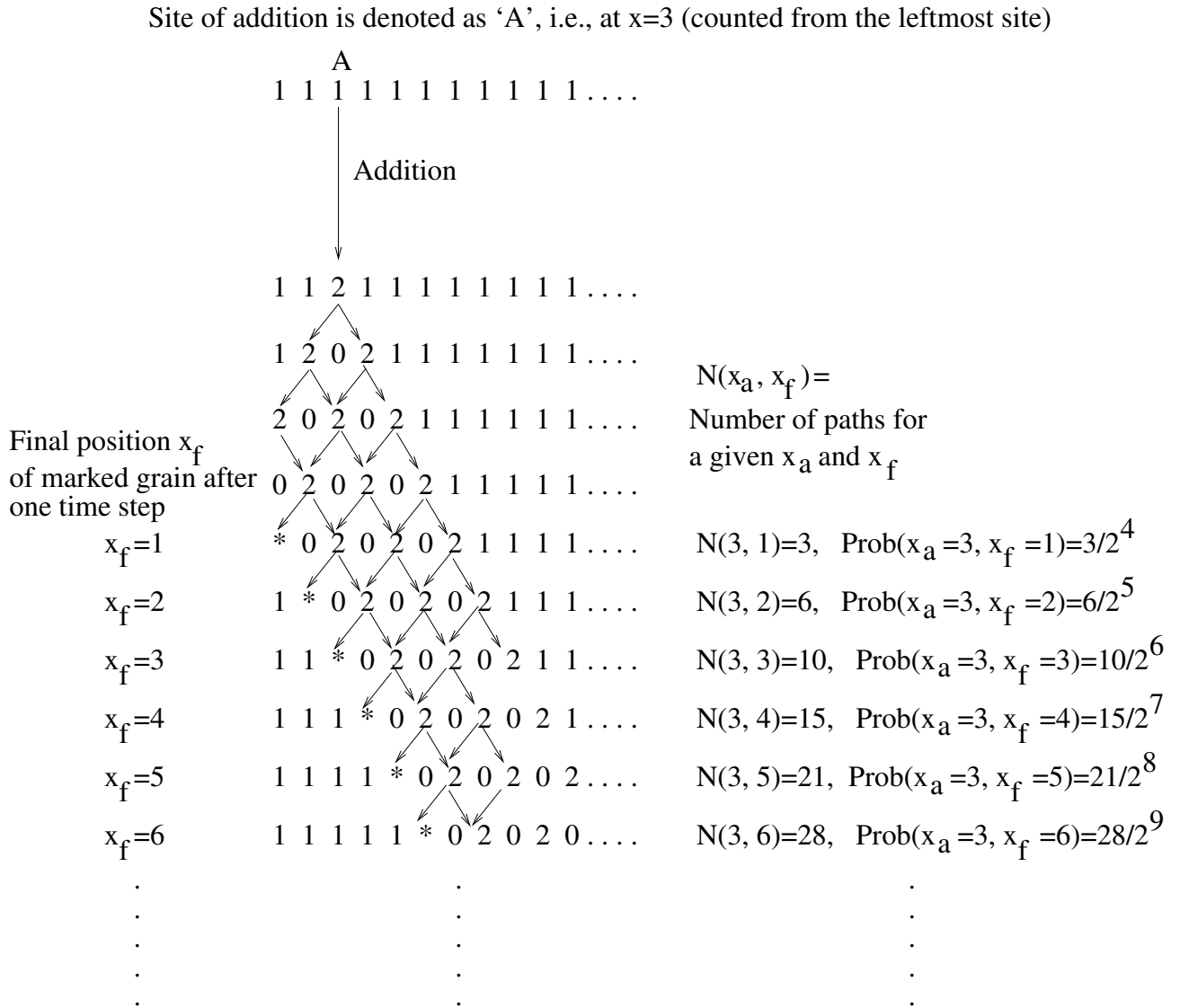


Fig B.1: The marked grain is added at the site denoted as 'A', i.e., at the site $x = 3$ from the left. The site with height zero is at the left but far away from the site where marked grain is added. The star symbol indicates the possible final positions of the marked grain added at 'A'.

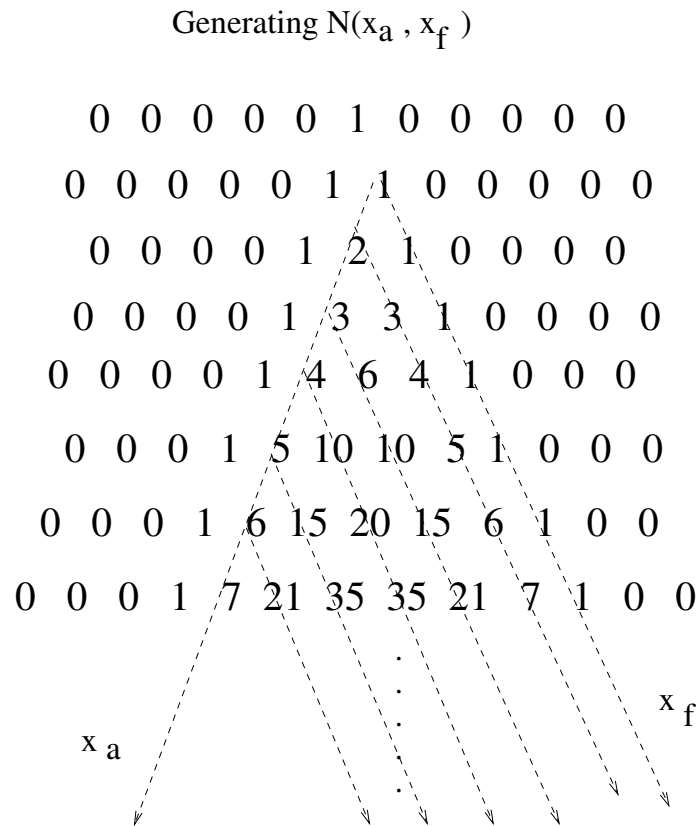


Fig B.2: To generate $N(x_a, x_f)$, we add two numbers diagonally one step above the number $N(x_a, x_f)$. Therefore $N(x_a, x_f) = N(x_a - 1, x_f) + N(x_a, x_f - 1)$.

Now collecting terms only upto leading order, we get

$$\begin{aligned}\langle T \rangle &= L[(1 - \frac{1}{L})(1 + \frac{a}{L})(1 - \frac{1}{L})(1 + \frac{1}{2L}) + \mathcal{O}(1/L^2)] \\ &= L[(1 + \frac{a}{L} - \frac{3}{2L}) + \mathcal{O}(1/L^2)]\end{aligned}\tag{B.5}$$

We know that the average residence time is equal to the mean number of grains in the pile, i.e.,

$$\begin{aligned}\langle T \rangle &= \langle M \rangle = \frac{L^2}{L+1} \\ &= L[(1 - \frac{1}{L}) + \mathcal{O}(1/L^2)]\end{aligned}\tag{B.6}$$

Comparing leading order terms in Eq. B.5 and Eq. B.6, we obtain $a = 1/2$.

Bibliography

- [1] R. Metzler and J Klafter, Phys. Rep. **339**, 1-77 (2000). R. Metzler and J Klafter, J. Phys. A: Math Gen., **37**, R161 (2004).
- [2] W. Feller, *An Introduction to Probability Theory*, John Wiley and Sons, New York, 3rd edition, 1967, Vol. 1.
- [3] S. Redner, *A Guide to First-Passage Processes*, (Cambridge University Press, 2001)
- [4] R. Metzler and J. Klafter, Physica A, **278**, 107 (2000).
- [5] S. Anderson, Math. Scand., **1**, 263 (1953). S. Anderson, Math. Scand., **2**, 195 (1954).
- [6] U. Frisch and H. Frisch, *Levy Flight and Related Topics in Physics* (edited by M. F. Shlesinger, G. M. Zaslavsky and U. Frisch, Berlin: Springer, 1995).
- [7] G Zumofen and J Klafter, Phys. Rev. E, **51**, 2805 (1995).
- [8] E. W. Montroll and B. J. West, *Fluctuation Phenomena* (edited by E. W. Motroll and J. L. Lebowitz, Amsterdam: Noth Holland, 1976).
- [9] M. Gitterman, Phys. Rev. E, **62**, 6065 (2000).
- [10] S. V. Buldyrev, M. Gitterman, S. Havlin, Y. A. Kazakov, M. G. E. da Luz, E. P. Raposo, H. E. Stanley and G. M. Viswanathan, Physica A, **302**, 148 (2001).
- [11] C. Godreche and J. M. Luck, J. Stat. Phys., **104**, 489 (2001).
- [12] S. N. Majumdar and A. Comtet, Phys. Rev. Lett., **89**, 060601 (2002).
- [13] S. N Majumdar, Cur. Sci., **77**, 370 (1999).

- [14] D. Slepian, Bell Syst. Tech. J., **41**, 463 (1962).
- [15] Y. G. Sinai, Theor. Math. Phys., **90**, 219 (1992).
- [16] G. Wilemski and M. Fixman, J. Chemical Phys., **58**, 4009 (1972).
- [17] M. Doi, J. Chem. Phys., **11**, 107 (1975).
- [18] A. Szabo, K. Schulten and Z. Schulten, J. Chem. Phys., **72**, 4350 (1980).
- [19] S. E. Fienberg, Biometrics, **30**, 399 (1974).
- [20] H. C. Tuckwell, *Introduction to Theoretical Neurobiology*, Vol. 2 (Cambridge University Press, Cambridge, 1988).
- [21] W Bialek, F Rieke, R. R. de Ruyter van Steveninck, D. Warland, Science, **252**, 1854 (1991).
- [22] J. J. Hopfield, Nature, **376**, 33 (1995).
- [23] G. L. Gerstein and B. B. Mandelbrot, Biophys. J., **4**, 41, 1964.
- [24] J. E. Fletcher, S. Havlin and G. H. Weiss, J. Stat. Phys., **51**, 215, 1988.
- [25] P. Bak, C. Tang, and K. Wiesenfeld, Phys. Rev. Lett. **59**, 381 (1987); Phys. Rev. A **38**, 364 (1988).
- [26] P. H. Dodds and D. H. Rothman, Phys. Rev. E, **59**, 4865 (1999).
- [27] C. H. Scholz, *The Mechanics of Earthquakes and Faulting* (Cambridge Univ. Press, 1990).
- [28] B. Gutenberg and C. F. Richter, Ann. Geophys., **9**, 1 (1956).
- [29] H. E. Hurst, Nature, **180**, 494 (1957). H. E. Hurst, *Long-term Storage: An experimental Study* (Constable and Co. Ltd., London, 1965).
- [30] MRR-2, Physical Basis, page no. 21 (1998).
- [31] O. Peters, C. Hertlein and C. Christensen, Phys. Rev. Lett., **88**, 018701 (2002).
- [32] D. L. Turcotte, Rep. Prog. Phys., **62**, 1377(1999).
- [33] E. V. Ivashkevich and V. B. Priezzhev, Physica A **254**, 97 (1998).

-
- [34] D. Dhar, *Physica A* **263**, 4 (1999).
- [35] D. Dhar, *Phys. Rev. Lett.*, **64**, 1613, 1990.
- [36] S. S. Manna, *J. Stat. Phys.*, **59**, 509 (1990). S. S. Manna, *Physica A* **179**, 249 (1991).
- [37] S. S. Manna, *J. Phys. A: Math. and Gen.*, **24**, L363 (1991).
- [38] S. S. Manna, *J. Phys. A: Math. Gen.*, **24**, L363 (1991).
- [39] Y. C. Zhang, *Phys. Rev. Lett.*, **63**, 470 (1989).
- [40] D. Dhar and R. Ramaswamy, *Phys. Rev. Lett.*, **63**, 1659 (1989).
- [41] L. P. Kadanoff, S. R. Nagel, L. Wu, and S. Zhou, *Phys. Rev. A*, **39**, 6524, 1989.
- [42] V. Frette, *Phys. Rev. Lett.* **70**, 2762 (1993).
- [43] K. Christensen, A. Corral, V. Frette, J. Feder, and T. Jøssang, *Phys. Rev. Lett.*, **77**, 107 (1996).
- [44] D. Dhar, *Physica A*, **340**, 535 (2004).
- [45] A. Ben-Hur and O. Biham, *Phys. Rev. E*, **53**, R1317 (1996). E. Milshtein, O. Biham, and S. Solomon, *Phys. Rev. E*, **58**, 303 (1998).
- [46] S. Lubeck and K. D. Usadel, *Phys. Rev. E*, **55**, 4095 (1997).
- [47] L. Pietronero, A. Vespignani and S. Zapperi, *Phys. Rev. Lett.*, **72**, 1690 (1994).
- [48] J. Kertesz and L. B. Kiss, *J. Phys. A: Math. Gen.*, **23**, L433 (1990).
- [49] H. J. Jensen, K. Christensen and H. C. Fogedby, *Phys. Rev. B*, **40**, R7425 (1989).
- [50] M. P. Kuntz and J. P. Sethna, *Phys. Rev. B*, **62**, 11699 (2000).
- [51] L. Laurson, M. J. Alava and S. Zapperi, *J. Stat. Mech.: Theo. and Expt.*, L11001 (2005).
- [52] A. A. Ali, *Phys. Rev. E*, **52**, R4595 (1995). S. Maslov, C. Tang and Y. Zhang, *Phys. Rev. Lett.*, **83**, 2449 (1999).

- [53] S. Maslov, C. Tang and Y. C. Zhang, Phys. Rev. Lett., **83**, 2449 (1999).
- [54] J. Davidsen and M. Paczuski, Phys. Rev. E, **66**, 050101(R) (2002).
- [55] M. de Sousa Vieira, Phys. Rev. E, **61**, 6056 (2000).
- [56] M. Paczuski and S. Boettcher, Phys. Rev. Lett., **77**, 111 (1996).
- [57] R. Sanchez, D. E. Newman and B. A. Carreras, Phys. Rev. Lett., **88**, 068302 (2002).
- [58] T. Hawa and M. Kardar, Phys. Rev. A, **45**, 7002 (1992).
- [59] H. M. Jaeger, C. Liu and S. R. Nagel, Phys. Rev. Letts., **62**, 40 (1989).
- [60] V. Frette, K. Christensen, A. Malthe-Sorensen, J. Feder and T. Jossang and P. Meakin, Nature (London) **379**, 49 (1996).
- [61] V. Frette, Phys. Rev. Lett. **70**, 2762 (1993).
- [62] K. Christensen, A. Corral, V. Frette, J. Feder, and T. Jossang, Phys. Rev. Lett., **77**, 107 (1996).
- [63] M. Boguna and A. Corral, Phys. Rev. Lett., **78**, 4950, 1997.
- [64] B. A. Carreras *et. al.*, Phys. Plasmas, **6**, 1885 (1999). B. A. Carreras *et. al.*, Phys. Plasmas, **3**, 2903 (1996). S. Garbet and R. E. Waltz, Phys. Plasmas, **5**, 2836 (1998).
- [65] B. A. Carreras, V. E. Lynch, D. E. Newman and G. M. Zaslavsky, Phys. Rev. E, **60**, 4770, 1999.
- [66] E. W. Montroll and J. L. Lebowitz (editors), *Fluctuation Phenomena*, (Elsevier Science Publishing Company, Inc., 1987), page nos. 61-206.
- [67] S. S. Manna and A. L. Stella, cond-mat/0206481
- [68] M. Khantha and V. Balakrishnan, Pramana **21**, 111 (1983)
V. Balakrishnan and M. Khantha, Pramana **21**, 187 (1983)
- [69] E. W. Montroll and H. Scher, J. Stat. Phys. **9**, 101 (1973).

- [70] M. Abramowitz and I. A. Stegun, *Hand Book of Mathematical Functions* (Dover Publications, Inc., New York, 1972).
- [71] M. Kac, *American Math. Monthly* **73**, 1 (1966)
- [72] The precise question has been answered in the negative. see
C. Gordon, D. L. Webb and S. Wolpert, *Bull. Amer. Math. Soc.* **27**, 134 (1992)
- [73] M. Abramowitz and I. A. Stegun, *Hand Book of Mathematical Functions*, (Dover Publications, Inc., New York, 1972). For convenience we give definition of $\vartheta_3(z, q)$ here: $\vartheta_3(z, q) = 1 + 2 \sum_{n=1}^{\infty} q^{n^2} \cos 2nz$ ($|q| < 1$).
- [74] S. S. Manna, *J. Phys. A: Math. and Gen.*, **24**, L363, 1991.
- [75] J. D. C. Little, *Operations Research*, **9**, 383, 1961.
- [76] E. V. Ivashkevich, D. V. Ktitarev, and V. B. Priezhev, *Physica A* **209**, 347(1998).
- [77] M. Abramowitz and I. A. Stegun (Editors), *Hand Book of Mathematical Functions* (Dover, New York, 1970) p. 375.
- [78] *ibid.* p. 576 (put $q = \exp(-\tau)$).
- [79] G. Arfken, *Mathematical methods for physicists*, 3rd ed. (Academic Press, New York, 1983).
- [80] A. Mehta and G. C. Barker, *Rep. Prog. Phys.*, **57**, 383-416 (1994). H. M. Jaeger and S. R. Nagel, *Rev. Mod. Phys.*, **68**, 1259 (1996). S. R. Nagel, *Rev. Mod. Phys.*, **64**, 321 (1992).
- [81] H. M. Jaeger, C. Liu and S. R. Nagel, *Phys. Rev. Letts.*, **62**, 40 (1989). G. A. Held, D. H. Solina, H. Solina, D. T. Keane, W. J. Haag, P. M. Horn and G. Grinstein, *Phys. Rev. Letts.*, **65**, 1120 (1990). J. Rosendahl, M. Vekic and J. Kelley, *Phys. Rev. E*, **47**, 1401 (1993). P. Evesque, D. Fargeix, P. Habib, M. P. Luong and P. Porion, *Phys. Rev E*, **47**, 2326 (1993). E. Altshuler, O. Ramos, C. Martinez, L. E. Flores and C. Noda, *Phys. Rev. Letts.*, **86**, 5490 (2001).
- [82] V. Frette, K. Christensen, A. Malthé-Sørensen, J. Feder, and T. Jøssang and P. Meakin, *Nature (London)* **379**, 49 (1996). M. Kardar, *Nature (London)* **379**, 22 (1996).

- [83] C. M. Aegerter, R. Gunther and R. J. Wijngaarden, Phys. Rev. E, **67**, 051306 (2003).
- [84] A. Chua and K. Christensen, **cond-mat/0203260**.
- [85] L. P. Kadanoff, S. R. Nagel, L. Wu, and S. Zhou, Phys. Rev. A, **39**, 6524, 1989.
- [86] A. B. Chhabra, M. J. Feigenbaum, L. P. Kadanoff, A. J. Kolan and I. Procaccia, Phys. Rev. E, **47**, 3099 (1993).
- [87] W. Feller, *Introduction to Probability Theory*, John Wiley and Sons, New York, 3rd edition, 1967, Vol. 1, Chapter XV, XVI.
- [88] J. G. Kemeny and J. L. Snell, *Finite Markov Chains*, D. Van Nostrand Company, Inc., Princeton, New Jersey, 1970, Chapter IV.
- [89] B. Derrida and J. L. Lebowitz, Phys. Rev. Letts., **80**, 209 (1992).
- [90] J. Krug, J. E. S. Socolar and G. Grinstein, Phys. Rev. A, **46**, R4479 (1992).
- [91] L. Onsager and S. Machlup, Phys. Rev., **91**, 1505 (1953). L. Onsager and S. Machlup, Phys. Rev., **91**, 1512 (1953).
- [92] D. J. Evans and D. J. Searles, Adv. Phys., **51**, 1529 (2002).
- [93] L. Bertini, A. De Sole, D. Gabrielli, G. Jona-Lasinio and C. Landim, Phys. Rev. Lett., **87**, 040601 (2001).
- [94] M. Depken and R. Stinchcombe, Phys. Rev. Letts., **93**, 040602 (2004). M. Depken and R. Stinchcombe, Phys. Rev. E, **71**, 036120 (2005).
- [95] L. Bertini, A. De Sole, D. Gabrielli, G. Jona-Lasinio and C. Landim, Phys. Rev. Lett., **94**, 030601 (2005).
- [96] L. Bertini, A. De Sole, D. Gabrielli, G. Jona-Lasinio and C. Landim, **cond-mat/0506664**.
- [97] C. Giardinà, J. Kurchan and L. Peliti, **cond-mat/0511248**.